

# Diagnostic of sensors, transfer pipes, filters, transfer- and feed- pumps

ANDRÉ ELLNEFJÄRD



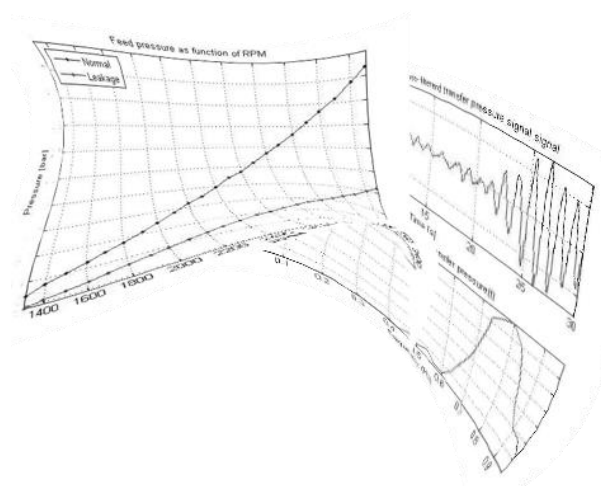
**KTH Industrial Engineering  
and Management**

Master of Science Thesis  
Stockholm, Sweden 2014



# DIAGNOSTIC OF SENSORS, TRANSFER PIPES, FILTERS, TRANSFER- AND FEED- PUMPS

André Ellnefjård



Master of Science Thesis MMK 2014:51 MDA 489

KTH Industrial Engineering and Management

Machine Design

SE-100 44 STOCKHOLM





KTH Industriell teknik  
och management

## Diagnostik för sensorer, överföringsledningar, filter, överförings- och matarpumpar.

André Ellnefjärd

Godkänt	Examinator	Handledare
2014-06-25	Lei Feng	Mikael Hellgren
	Uppdragsgivare	Kontaktperson
	Scania CV AB	Ola Stenlåås

### SAMMANFATTNING

Under de senaste åren så har kraven på olika systems körtid och tillförlitlighet ökat inom industriella applikationer. Diagnossystem har därför blivit alltmer viktiga för att se till att systemen körs normalt och säkert, för att förhindra eventuella systemfel. Ett nytt systemkoncept har nyligen tagits fram för lågtryckdelen av bränslesystemet på tunga motorer och detta system är i behov av ett diagnossystem.

I detta examensarbete så har man undersökt hur systemets utformning och diagnosalgoritmer skall se ut för att man ska kunna upptäcka felaktigt fungerande systemnivåer och kunna isolera felaktiga komponenter. Med systemets utformning menas antalet sensorer, deras placering och nödvändig upplösning.

Fyra systemutformningar har föreslagits och testats i en rigg som tagits fram i detta examensarbete. Utifrån dessa data så har det normala och det felaktiga beteendet definierats och utvärderats. Fel detektering- och isolerings- metoderna som tagits fram utnyttjar teori såsom fysikalisk redundans, filtrering av signaler, FFT, kombinationer av detektionsgränser, insvängningstid/stigtid samt enklare residualer. Dessa metoder har sedan kombinerats till ett diagnossystem för respektive system utformning. En jämförelse mellan de olika systemutformningarna med avseende på diagnosprestanda och systemkostnad har sedan utförts.

Resultaten visade att två av de framtagna systemutformningarna med motsvarande diagnosalgoritmer var överlägsna de andra två systemutformningarna när det gäller prestanda och enkelhet för diagnosen. De olika givarnas upplösningar har visat sig ha ett stort inflytande på vilken felstorlek som kan och inte kan upptäckas, därför har också krav på nya sensorer föreslagits och diskuterats. Den slutliga och valda systemutformningen påvisar att det är teoretiskt möjligt att kunna detektera och isolera alla systemfel som definierats. De föreslagna lösningarna behöver implementeras och verifieras innan diagnosen kan anses slutgiltigt verifierad.





KTH Industrial Engineering  
and Management

## Diagnostic of sensors, transfer pipes, filters, transfer- and feed- pumps

André Ellnefjård

Approved	Examiner	Supervisor
2014-06-25	Lei Feng	Mikael Hellgren
	Commissioner	Contact person
	Scania CV AB	Ola Stenlås

### ABSTRACT

During the later years, demands on the requirements such as system up-time and system reliability have been increased in industrial applications. Diagnostic systems have therefore become of importance to ensure that the system runs normal and safe in order to prevent possible system failures. A new system concept for the low pressure fuel circuit in heavy duty engines has recently been developed and it is in the need of a diagnostic system.

This master thesis investigates how the system layout and diagnostic algorithms of the new system concept shall be designed to be able to detect a faulty functioning system level and isolate failing components. The system layout is referring to the amount of sensors, their locations and their needed resolutions.

Four system layouts has been suggested and tested in a developed experimental rig where normal and faulty system behavior has been defined and evaluated. Fault detection and isolation methods that utilizes physical redundancy, filters, FFT, combinations of detection limits, settling time/rise time and residuals, has been developed and combined into a diagnostic system for each system layout. A comparison between the system layouts with respect to diagnostic performance and system cost was in turn performed.

The results showed that two of the system layouts with corresponding diagnostic algorithms were superior to the two other layouts in terms of diagnostic simplicity and diagnostic performance. The sensor resolutions were proven to have a big influence on what fault sizes are detectable or not which is why new sensor requirements has been suggested and discussed. The final system layout with corresponding diagnostic algorithm is theoretically capable of detecting and isolating all of the defined system faults. It is however in the need of implementation and verification to be considered validated.





# PREFACE

This master thesis work was performed at Scania CV AB in Södertälje at the department for engine combustion control software (NESC).

I would especially like to thank my supervisors at Scania, **Ola Stenlåås** and **Susanna Jacobsson** for keeping my project progress on schedule and providing good feedback throughout the whole project.

I also would like to thank the following people for answering project related questions and for providing guidance in the experimental rig development.

- **Andreas Jonsson**, NMCL
- **Patrik Fogelberg**, NMCL
- **Dan Cedfors**, NMCL
- **Daniel Ringström**, NMCT
- **Jan Österman**, NMA

I would finally like to thank my supervisor from KTH, **Mikael Hellgren**.

André Ellnefjärd

Södertälje, June 2014

# NOMENCLATURE

*In this master thesis several abbreviations related to the thesis work have been used. This chapter provides a list of the used abbreviations.*

## ***Abbreviations***

---

<i>OBD</i>	On-Board Diagnostics
<i>FDI</i>	Fault Detection and Isolation
<i>FDD</i>	Fault Detection and Diagnosis
<i>FTA</i>	Fault Tree Analysis
<i>SDG</i>	Sign Directed Graphs
<i>PCA</i>	Principal Component Analysis
<i>FFT</i>	Fast Fourier Transform
<i>ECU</i>	Electrical Control Unit
<i>IMV</i>	Inlet Metering Valve
<i>HPP</i>	High Pressure Pump
<i>SCR</i>	Selective Catalytic Reduction
<i>CAN</i>	Controller Area Network

---

# TABLE OF CONTENTS

## CONTENTS

- 1. INTRODUCTION ..... 1
  - 1.1 Background..... 1
  - 1.2 Purpose ..... 1
  - 1.3 Delimitations..... 2
  - 1.4 Method..... 2
- 2. FRAME OF REFERENCE ..... 3
  - 2.1 Fault detection and diagnostic strategies ..... 3
  - 2.2 Evaluation and conclusion of theory and research ..... 13
- 3. IMPLEMENTATION ..... 15
  - 3.1 System layouts..... 15
  - 3.2 Experimental rig ..... 21
  - 3.3 Development of the diagnostic system ..... 27
- 4. RESULTS AND ANALYSIS FOR NORMAL SYSTEM BEHAVIOR..... 29
  - 4.1 Determining the flow for different RPM levels ..... 30
  - 4.2 Definition of normal behavior ..... 32
  - 4.3 Data from normal system behavior ..... 33
- 5. RESULTS AND ANALYSIS FOR FAULTY SYSTEM BEHAVIOR..... 43
  - 5.1 Leak in pipe between feed pumps and fuel filter ..... 44
  - 5.2 Leak in pipe between transfer pumps and pre-filter ..... 50
  - 5.3 Leakage on suction line to feed-pump ..... 54
  - 5.4 Leakage on suction line to transfer-pump..... 59
  - 5.5 Open pre-filter ..... 65
  - 5.6 Open fuel filter ..... 69
  - 5.7 Clogged pre-filter ..... 72
  - 5.8 Clogged fuel filter ..... 74
  - 5.9 Stop in line between transfer pumps and pre-filter ..... 76
  - 5.10 Stop in line between fuel filter and high pressure circuit..... 78
  - 5.11 Stop in line between feed pumps and fuel filter ..... 80
  - 5.12 Non-operating pump ..... 81
  - 5.13 Stuck level sensor in main fuel tank..... 85
  - 5.14 Stuck level sensor in tech-tank..... 86
  - 5.15 Transfer or feed pumps are not shutting off when demanded ..... 87

5.16 Temperature sensor in main-tank broken.....	87
5.17 Temperature sensor in tech-tank broken .....	89
5.18 Pressure indicating the wrong pressure .....	90
5.19 Comparison between step responses .....	92
6. RESULTING DIAGNOSTIC SYSTEMS.....	97
6.1 Explanation procedure of the diagnostic systems.....	97
6.2 Algorithms for system layout C.....	98
6.3 Algorithms for system layout B .....	102
6.4 Algorithms for system layout D .....	105
6.5 Algorithms for system layout A .....	107
6.6 Comparison of system layouts .....	109
6.7 Detectable leakage sizes .....	111
6.8 Sampling frequency .....	112
7. DISCUSSION AND CONCLUSIONS.....	113
7.1 Discussion .....	113
7.2 Conclusions.....	116
8. RECOMMENDATIONS AND FUTURE WORK.....	119
8.1 Recommendations .....	119
8.2 Future work.....	119
9. REFERENCES.....	120
APPENDIX A.....	122
APPENDIX B.....	123
APPENDIX C.....	126

# 1. INTRODUCTION

*This chapter will introduce the subject of this thesis work by describing the background and purpose for this thesis followed by the delimitations and method.*

## 1.1 BACKGROUND

In all of the industrial and systems, maintenance has always been important to avoid system failures. During the later years, demands on the requirements such as system up-time and system reliability have increased. It is therefore more important to ensure that the systems runs normally and safe in order to prevent possible system failures. Since the sensors and microcontrollers came along, on-line condition monitoring systems became realistic for industrial applications such as airplanes, chemical plants, trains and automotives. Needed maintenance can today, therefore be predicted by using fault detection and diagnosis (FDD).

On today's diesel engines the mechanical fuel feed pump, which transports fuel to the high pressure circuit (HPP), is mounted on the engine and driven by the flywheel. This pump is oversized with respect to the system needs, resulting in operating losses. A new concept has therefore been investigated for vehicles with special needs, where the mechanical pump shall be replaced with electrical pumps. The concept includes a main fuel tank, a catch tank (tech-tank), two electrical transfer pumps, two feed pumps, two filters, two level sensors and at least one pressure sensor.

This concept is now in the stage where the final system layout and diagnostic algorithms needs to be defined and developed. The system layout is referring to the number of needed sensors and their positions in the system, in order to develop the diagnostic algorithms and define the level of error they can detect. The final system layout shall consider system price, diagnostic performance and control performance. The needed resolution of the sensors shall also be investigated as a fault free system should be avoided to be diagnosed as faulty.

## 1.2 PURPOSE

The purpose of this thesis is to develop algorithms that can detect a faulty functioning system level and determine if it is possible to isolate which component that causes the faulty behavior. A faulty functioning system level could e.g. be a stop in line, a broken pump, a suction leakage on the line, a clogged filter or a stuck level sensor.

The algorithms will during driving be able to detect if the system is faulty functioning and will then provide knowledge in which component that is broken or faulty and needs maintenance. The workshop staff will then directly know what part that needs to be replaced or repaired which results in a reduced time inside the workshop.

If specific faults cannot be completely isolated during a system operation, a proposed method for isolating the fault inside the workshop shall be suggested.

### 1.3 DELIMITATIONS

- The diagnostic algorithms will be based on the results from experiments performed on a experimental rig that will be constructed during this thesis work.
- The pumps that will be used in the rig are prototypes and have very limited specifications.
- The rig will be controlled by Labview.
- The pressure sensors that will be used are originally from other systems related to the engine.
- Modeling of the system as well as the controller will be developed in another master thesis, which is performed in parallel with this one.

### 1.4 METHOD

In order to reach the goal of this thesis, the following tasks were identified:

1. Literature study
2. Define system layouts
3. Development of experimental rig
4. Experiments
5. Development of diagnostic algorithms

The first step in this thesis is to perform a literature study in the field of fault detection and diagnosis methods. The aim is to retrieve a deeper knowledge of the FDD field and identify suitable methods that are applicable for this thesis, with respect to time and resources. This will result in a chapter containing the current state of the art and a method evaluation.

The second step is to define different system layouts, considering the system price, the ability to detect faults and the requirements for the control performance. These layouts are to be compared and evaluated with each other.

In order to investigate the system behavior during normal and faulty conditions, a rig needs to be designed and developed. The aim is to replicate the real system as much as possible in order to get relevant measurements during the experimental phase.

The experiments that will be performed on the system, are designed for identifying what faults are detectable or not for the different system layouts. The idea with the measurements is that they should provide a foundation for being able to develop the diagnostic system. This part will also include a sensor and sampling time evaluation.

## 2. FRAME OF REFERENCE

*In this chapter, a summary of the existing knowledge and performed research in the field of fault detection and diagnosis is presented. The chapter starts with a short introduction to the field and continues with existing research and methods. This is then followed by an evaluation and a conclusion with the aim of identifying the applicable theory and methods for this thesis.*

### 2.1 FAULT DETECTION AND DIAGNOSTIC STRATEGIES

#### 2.1.1 BACKGROUND

During the last decades there has been an increasing demand for efficiency and product quality along with more safety reliable systems in industrial applications. One of areas that have played a big role in accomplishing this has been fault detection and diagnosis. An early detection and isolation of a fault can prevent product deterioration, major damage to the system itself and sometimes even prevent damage to the human health. When the first machines were built, the only way to locate malfunctions was by using the human senses such as feeling, seeing, hearing and smelling. When sensors and microprocessors were introduced the fault detection and diagnosis was taken to a whole new level. This made it possible to monitor the system variables during a system operation. Fault detection and fault diagnosis has since then played a big role in the development of industrial applications such as power plants, chemical processes, ships, airplanes, heavy duty trucks and other vehicles (Gertler, 1998), (Chiang, et al., 2002), (Svärd, 2012).

#### 2.1.2 ON-BOARD DIAGNOSTICS

For heavy duty trucks and automotives, diagnostics has become mandatory in order to meet the requirements of the emission regulations that was introduced in 1988 for the United States and later for Europe in 1992 (Euro I), (McDowell, et al., 2007). From that point, requirements for the on-board diagnostics (OBD) have continuously evolved to be able to meet the requirements that today exist in the Euro VI standard.

#### 2.1.3 FAULT DETECTION AND DIAGNOSIS

##### 2.1.3.1. Definitions

According to (Iserman, 2006), a *fault* is an unpermitted deviation of at least one characteristic property or parameter of the system from the acceptable / usual / standard behavior. Depending on the industrial application and its functionality, the presence of different kinds of faults is implied, but regarding of what fault is present, fault detection and diagnosis implements the following tasks (Gertler, 1988),

- **Fault detection**, is the indication that something is wrong or that an abnormal event has occurred in the system.
- **Fault isolation**, the determination of the exact location of the fault, which could be a component, follows fault detection.
- **Fault identification**, is the root cause and magnitude of the fault, follows fault isolation.

The definition of *fault diagnosis* is sometimes defined differently and will in this thesis be considered as the combination of fault detection, fault magnitude and fault isolation as in (Gertler, 1998), since fault identification is often performed offline and it is often very hard to find the root cause in a faulty component without further investigation. Fault detection and isolation is in many papers and literatures abbreviated as FDI or FDD, since the word “diagnosis” is often used as a synonym for “isolation” (Gertler, 1998). In this thesis, the abbreviation FDD will be used. The principle of a FDD system can be seen in Figure 2.1, where observations of physical quantities is obtained in order to execute fault detection tests followed by isolation of the fault, resulting in a diagnostic statement with the aid of supplementary information that is application specific. The difference between a diagnostic statement and an isolated fault is that isolation only tells where the fault is located. A diagnostic statement does on the other hand tell where the fault is located, the magnitude of the fault and what actions that are needed.

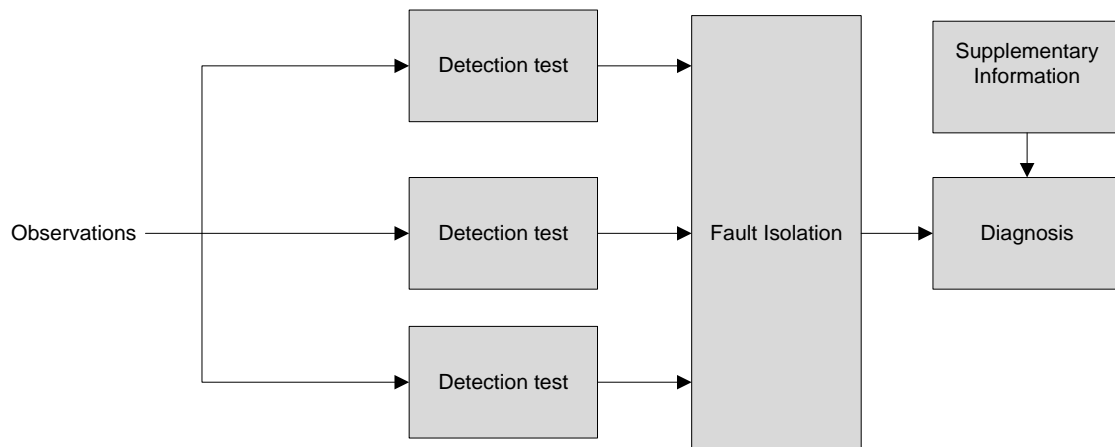


**Figure 2.1.**The principle of a FDD system.



**2.1.3.2. Methods**

During the last years there has been multiple strategies developed in the field of FDD and the major difference in these strategies is the knowledge used for formulating the diagnostics. The system knowledge can either be based on *a priori* knowledge, e.g. model-based, where the complexity is system dependent, or on black-box models, which are purely data-driven. There are also other methods that are model-free but are often combined with the model-based methods. These methods will therefore be categorized as ad-hoc methods in this thesis. The *a priori* knowledge used in model-based methods can broadly be classified as quantitative or qualitative and is based on the fundamental understanding of the system physics (Venkatasubramanian, et al., 2003). Quantitative models are built by mathematical relationships based on the underlying system physics of the system, while qualitative models consists of relationships derived from knowledge of the underlying physics. The diagnostic methodology is in this thesis explained according to the method classification illustrated in Figure 2.2.

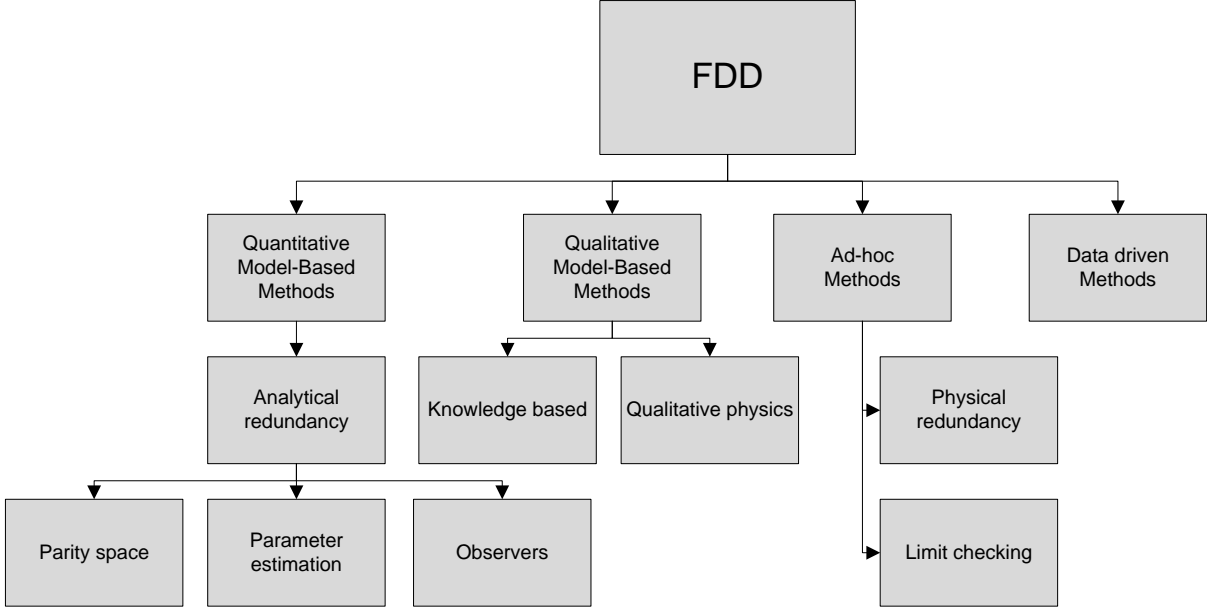


Figure 2.2. Classification scheme for an explaining the FDD methodology.

The choice of method or combinations of methods, when developing a diagnostic system, is depending on the complexity of the system and the required level of fault detection needed. The next sections will briefly go through each method and discuss how they are connected to each other.

*2.1.4 QUANTITATIVE MODEL-BASED FAULT DETECTION AND DIAGNOSIS*

As has been mentioned earlier, the field of diagnostic strategies is growing as the systems become more complex with the years; hence a lot of research is being performed in this area and mostly in quantitative model-based fault detection and diagnosis. This is one of the most widely used strategies in the field of FDD and utilizes an accurate model of the system based on differential equations and state-space models. The mathematical model will act as a reference for the real system behavior and *analytical redundancy* is achieved. Analytical redundancy exists when it is possible to determine a variable in two different ways, by only performing one observation (Hess, et al., 2006). There is however a grey zone here as the quantitative models can be

simplified, moving towards the qualitative models, but still provide analytical redundancy (Katipamula & Brambley, 2005). The section below will go through each method that requires an accurate model in order to be applied successfully for diagnostics.

### 2.1.4.1. Residual generation

Methods that use the analytical redundancy compare, during operation, signals from the real system against parameters in or out from the mathematical model. The comparison is based on the consistency between the signals and is called *residual generation* (Chiang, et al., 2002). A *residual* has the value of zero if there are no faults present and non-zero when a fault is present. In order to avoid a fault free system to be diagnosed as faulty, the residual threshold levels are often greater than zero. The system condition can then be evaluated based on the residuals. As an example, consider a residual generator  $R_i$  that has the input  $y$ , which is data from a sensor located in a system. The residual  $r_i$  is then the output from the residual generator,  $r_i = R_i(y)$ . After this a detection test,  $d_i$  is performed by a residual evaluator,  $T_i$ . The detection test is then performed in a certain quantity,  $\beta_i$  and compared to a threshold  $J_i$  (Svärd, 2012). The detection test can then be written as,

$$d_i = T_i(R_i(y)) = \begin{cases} 1 & \text{if } \beta_i > J_i \\ 0 & \text{if } \beta_i \leq J_i \end{cases} \quad (1)$$

An illustration of the residual generation principle can be found in Figure 2.3.

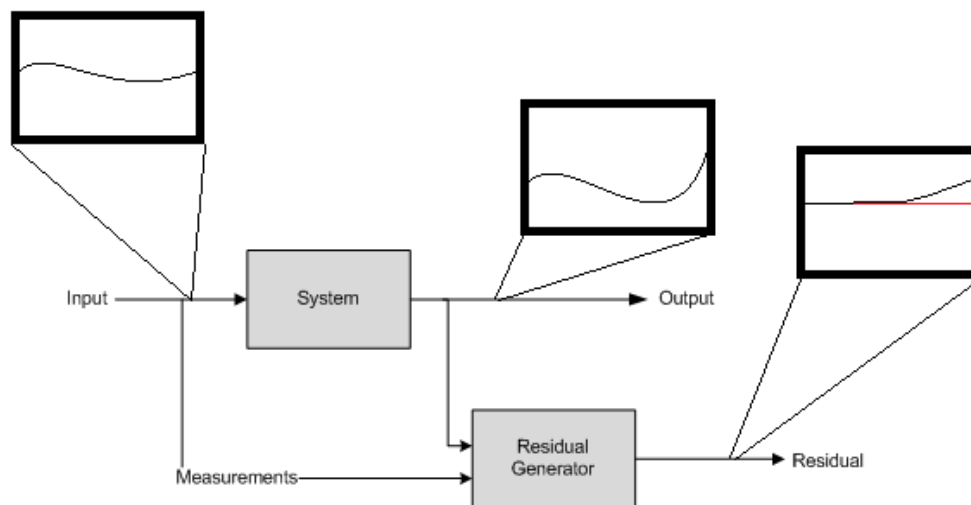


Figure 2.3. Residual generation principle.

There are four commonly used approaches for residual generation and evaluation: Parameter estimation, Observers, Parity relations and also Kalman-filters, which one may consider as a more data-driven method. Since all of these methods require an accurate mathematical model to obtain residuals, it has been chosen to classify them as quantitative model-based methods.

#### 2.1.4.1.1. Parameter estimation

A popular approach for generating residuals is the parameter estimation method in which the residuals are the difference between the nominal model parameters and the estimated model parameters, e.g. storage or resistance quantities, based on input and

output signals of the system. The estimation of the parameters occurs during system operation which enables detection and isolation of a fault. Consider a system with the input signal,  $u$  and the output signal  $y$ , as in Figure 2.4. Then the nominal model parameters will be compared with the estimated parameters, generating a residual which is then compared to a predefined threshold (Witczak, 2007). Due to the difficulty of constructing accurate models for complex non-linear systems, the application of this method is therefore very limited to simpler linear systems. For a deeper mathematical understanding of the parameter estimation method, the reader can find more information in (Witczak, 2007).

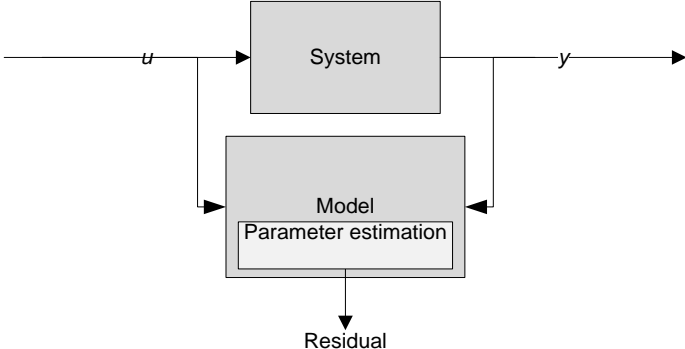


Figure 2.4. Parameter estimation residual generation principle.

**Observers and Kalman-filter**

Residuals generated with an observer is another method that also estimates signals or states in the model. The difference is that these signals are then compared with the measured signals in the real system. In order to estimate signals or states, many different observers or filters can be used, e.g. a Kalman filter (Witczak, 2007) or a Leunberger observer. The method has been used in several applications, e.g. for a electro-hydraulic brake in (Huh, et al., 2008) or a three tank system in (Hossein Sobhani & Pshtan, 2011). During this literature study, there was only applications found where sensor and actuator faults are detected by method. For a deeper understanding, the interested reader can find the mathematical approach in (Witczak, 2007) and in (Zhang, et al., 2010). The principle of the observer-based method is shown in Figure 2.5, where the input signal is  $u$  and the output signal is  $y$ .

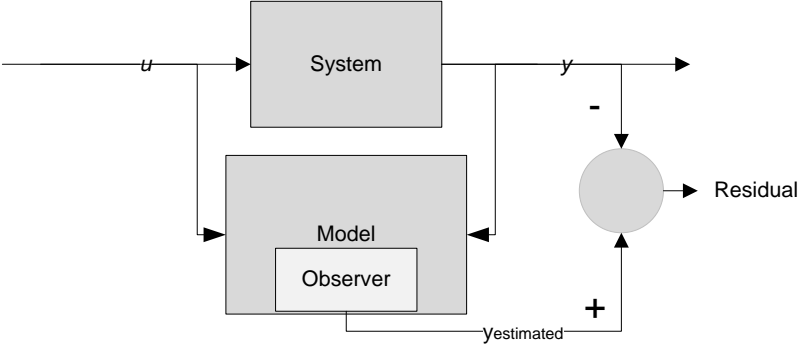


Figure 2.5. Principle of observer-based residual generation.

#### 2.1.4.1.2. *Parity relations*

The parity relations origins from the fault detection and diagnosis used for control and navigation systems for aircrafts, which was introduced by (Potter & Suman, 1977) and further developed by (Chow & Wilsky, 1984). This method aims to re-arrange or transform the system into parity equations and these equations will serve as residuals that are sensitive to a specific fault. This makes it possible to identify and locate the fault that is causing a faulty system behavior without further isolation (Iserman, 2006). The major drawbacks with this method are the required computational effort required as yields for the other residual generation methods as well. There was however a successful implementation of adaptive parity equations for fault detection on a DC-motor in (Höfling & Iserman, 1996), where the computational effort was reduced in comparison to previous work. For the interested reader, the mathematical description of parity relations can be found in (Witczak, 2007), for both linear and non-linear systems.

#### 2.1.5 *QUALITATIVE MODEL-BASED FAULT DETECTION AND DIAGNOSIS*

The pure quantitative model-based approaches described in the section above gains the system knowledge from accurate mathematical models while the qualitative model-based methods are based on a priori knowledge developed from causal relationships. By utilizing the system physics and simpler mathematical relationship between observations and system failures causal relationships can be derived (Milne, 1987).

##### **2.1.5.1. Knowledge-based**

The knowledge-based fault detection and diagnosis are based on the fundamental knowledge of the system physics and the relationships between causes and system level failures. This method is divided into sub methods named expert-systems, pattern recognition and cause-effect relationships. This thesis will, from this method, consider the latter, where the system knowledge is usually obtained by performing causal analysis or by analyzing the system characteristics during normal conditions and faulty conditions. The testing of the faulty conditions should be based on hypotheses that connects possible observations with particular faults, e.g. an abnormal observation of the physical quantity  $z$  indicates that fault  $F$  has occurred (Milne, 1987), (Venkatasubramanian, et al., 2003). The system characteristics during faulty and non-faulty conditions can then be compared in order to apply suitable detection methods. Causal analysis is often performed with the help of graphical tools that explains the relationships between faults and causes. Two of these methods are described below (Chiang, et al., 2002).

**2.1.5.2. Causal modelling methods**

*2.1.5.2.1. Fault tree analysis and Sign directed graphs*

There are multiple methods that serve as graphical tools in which the relationships between faults, events and conditions are constructed. These can be described as causal models. One of them is Fault tree analysis (FTA) (Iserman, 2006), originally developed at Bell telephone laboratories in 1961 (Venkatasubramanian, et al., 2003), and is a top down method that is commonly used in safety critical applications. The fault is the top node in the tree which is built up by underlying nodes, representing the causes. The nodes are connected with logical operations, such as AND- and OR- blocks. An illustrative example of a basic fault tree can be found in Figure 2.6.

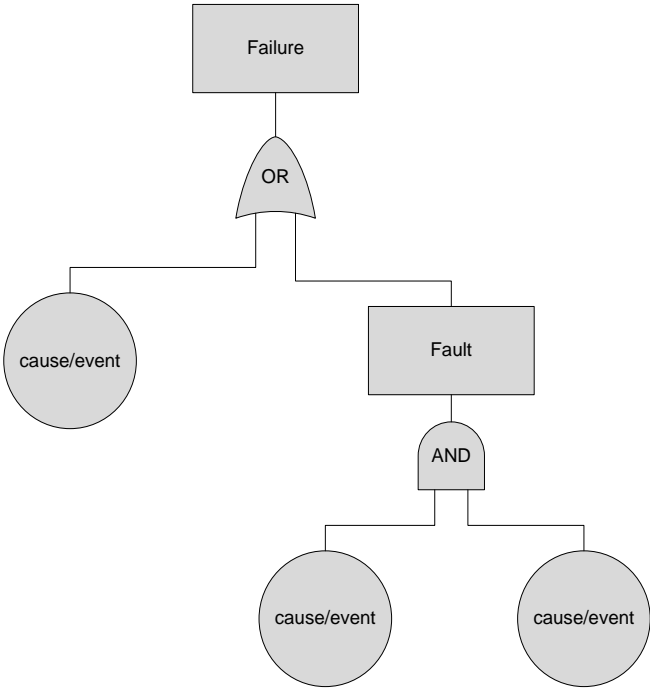


**Figure 2.6. The principle of Fault tree analysis.**

Another method is based on causal analysis and is called sign directed graphs (SDG), and acts as a map showing relationships of system variables including behavior of the equipment involved (Chiang, et al., 2002). The first attempt of applying SDG into diagnostics was performed in (Iri, et al., 1979), on a buffer tank in a chemical process. A basic example of an SDG, describing the level *h* in a tank, can be found in Figure 2.7.

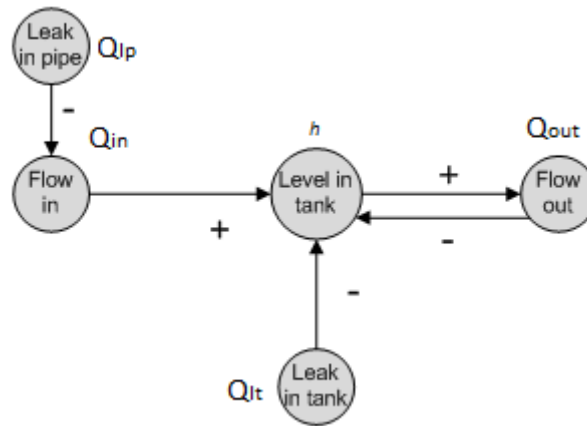


**Figure 2.7.** A simple signed directed graphs, showing the relationship between the system process variables.

Now, imagine that the symptoms are that the level  $h$  is decreasing and  $Q_{in}$  and  $Q_{out}$  remains the same. The SDG then reveals possible faults by inserting signs according to the behavior, zero if the node is unchanged, negative if the node is increasing, positive if the node is a root node and empty if the next node is unchanged, see Figure 2.8.

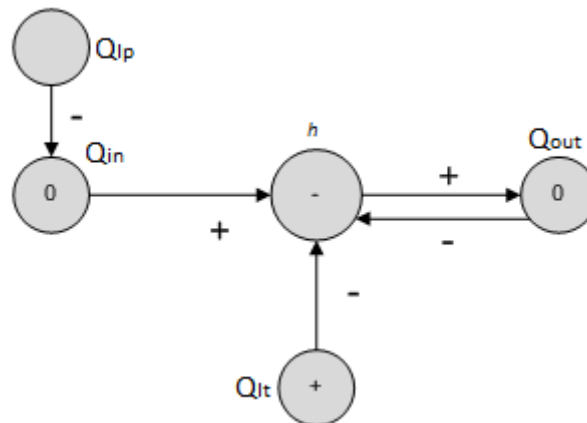


**Figure 2.8.** The signed directed graph with symptoms.

Since this is a simple example, intended for method description, one can directly see that the node that is causing the level to decrease is a leakage in the tank, thus the SDG's is more useful when the system is more complex.

### 2.1.6 AD-HOC METHODS

The methods that are in this thesis, categorized as ad-hoc methods are called limit checking and physical redundancy. These methods does not solely build a diagnostic system as they are dependent on a physical system knowledge before they can be applied, e.g. in order to perform a limit check, the suitable limit has to be derived from the systems physical behavior, either by modeling or testing.

#### 2.1.6.1. Physical redundancy

The original approach in this method is based on multiple sensors that measure the same physical quantity. By placing two sensors at the same location in a system, the difference in the measured values will indicate if a sensor is broken. If a third sensor is

introduced it is possible to determine which sensor is broken with a voting method described in (Willsky, 1976). The method is very efficient for identifying faulty functioning sensors but also adds extra costs and hardware to the system (Gertler, 1998). This method is usually used in safety-critical systems that require functioning sensors at all times, regarding the system costs. Some of the applications that have applied this are aircrafts, space vehicles and nuclear power plants (Venkatasubramanian, et al., 2003). Physical redundancy can however be applied in a different way than described above. Imagine there are five sensors in a system. By taking the measurements from four sensors in a system, one can together with an analytical relationship, calculate or estimate a value of the sensor value and then compare it against its measured value (Venkatasubramanian, et al., 2003).

### **2.1.6.2. Limit checking**

One of the simplest methods and most commonly used in fault detection is the limit checking of measured variables. The physical quantity is measured with an existing sensor in the system and the sensor signal is then compared against a limit threshold, which is either static or dynamic. If the measured signal is within the upper and lower limit boundaries the system is assumed to be normal. If the limits are exceeded an alarm or a fault code would trigger with the underlying assumption that a fault has occurred. Consider a physical quantity  $y$ , a simple limit check of this quantity would then be,

$$y_{low} < y \leq y_{high}. \quad (2)$$

It is also possible to use the derivatives from the measured signals and create combinations of thresholds, or fuzzy thresholds (Iserman, 2006). As the reader may have realized, the methods are strongly connected to each other, since the above can be seen as very simple residuals.

## *2.1.7 DATA DRIVEN METHODS AND SPECTRUM ANALYSIS*

### **2.1.7.1. Principal component analysis**

These methods are based on large amounts of collected data from the system and are usually used in large-scale systems. All of these methods are either based on the theory of probability and statistics or machine learning. A commonly used data-driven fault detection method is the Principal component analysis (PCA), which uses multivariate statistics in order to detect and diagnose faults (Chiang, et al., 2002). In (Antory, 2007), air leakages in the intake manifold on an automotive diesel engine was proven to be detectable and isolated with the PCA method. As has been mentioned before, the data-driven methods require large amounts of data in order to be successfully implemented.

### **2.1.7.2. Spectrum analysis**

A system that contains rotary mechanical parts or other systems with periodical behavior often causes oscillations in different signals. This information can be used in fault detection and isolation, if the deviations from the normal oscillatory behavior are related to faults caused by system components. The method is based on the theory of digital signal analysis in which the frequency spectra often is of interest together with correlation functions and FFT (Iserman, 2006). Fault detection in a Urea injection dosing system was in (Sun, et al., 2012) investigated by using spectral analysis and FFT with promising results.

### 2.1.8 FAULT ISOLATION

The above described methods focus on the fault detection and in order to perform a diagnosis, the faults needs to be isolated in the best possible way. In most of the cases some faults may give the same observations, which is why complete isolation is a very difficult task. If every fault had its own signature in the observed quantities, the fault isolation would not be a problem. The ability to isolate faults depends on (Ding, 2008),

- Number of the possible faults
- Possible distribution of the faults in the system
- Characteristic features of each fault
- Available information about the possible faults

To accomplish isolation with residual generation methods Bayesian fault isolation, (Pernestål, 2007), structured residuals or fixed direction residuals, (Chiang, et al., 2002), has been implemented with good results. The Bayesian method is based on the probabilities given all information at hand and the structured analysis is based on *fault decoupling*. This means that each residual corresponds to a different subset of faults (Svärd, 2012). Data driven- and spectrum analysis- methods include fault isolation schemes in most of the literature studied, (Chiang, et al., 2002), and these will not be discussed further in this thesis. The other methods are in the reviewed literature, described as only being fault detection methods. A popular tool for constructing a isolation structure is by using a fault signature matrix (Svärd, 2012), (Salvador, et al., 2010), (Bartys, 2013) and (Mattone & De Luca, 2006). A rearranged example from (Svärd, 2012), can be found in Table 2.1, where complete isolation is possible due to decoupled faults.

**Table 2.1. Fault signature matrix. An x means that a test is sensitive to certain fault.**

Test	Fault 1	Fault 2	Fault 3
$T_1$	x	x	
$T_2$		x	x
$T_3$	x		x

In the isolation structure, test  $T_1$  is for example sensitive to Fault 1 and Fault 2. If the tests  $T_1$  and  $T_2$  has alarmed, one can conclude (with the assumption that a single fault is present) that Fault 1 or Fault 2 has occurred. Since both tests include Fault 2, it is certain to say that Fault 2 has been isolated. The diagnostic statement can be written as,

$$D = T_1 \cap T_2 \cap T_3 = \{f_1, f_2\} \cap \{f_2, f_3\} \cap \{f_1, f_3\} = f_2 \quad (3)$$



## 2.2 EVALUATION AND CONCLUSION OF THEORY AND RESEARCH

### 2.2.1 EVALUATION OF METHODS

From a theory explaining perspective it is practical that the studied literature divides the fault detection and diagnostic methods into categories. In practice, these methods are often combined since no method is flawless for all possible applications. Below follows an evaluation of the methods based on the constraints in this thesis.

The quantitative model-based methods that utilizes residual generation, such as parameter estimation, parity relations and observers has in the reviewed papers and literature shown satisfying results with respect to the diagnostic demands. These methods are mostly used where the requirements on the diagnostic performance are essential, e.g. the OBD for emissions required on the heavy duty vehicles that was mentioned earlier. Evaluating the amount of papers and literature focusing on the residual generation methods, e.g. (Svård, 2012), (McDowell, et al., 2007), (Ding, 2008) and (Mattone & De Luca, 2006), it becomes very clear that this is where most of the research is performed in FDD. These methods are on the other hand, highly dependent on accurate models that have been validated and tuned which can consume a lot of time and resources. Another reason that speaks against residual generation methods is that they are hard to implement on a ECU's with limited memory and computational power. Further, if a change is performed on the system, the process of updating the diagnostic system becomes very inefficient. With these limitations in mind, a full residual generation method is too complex with respect to the time given for this thesis.

The data-driven approaches are mostly used for large scaled systems such as power plants or chemical process industries where the computational power is not a issue. This also yields for the spectrum analysis methods and might be more suitable when rotating machinery e.g. a gearbox is the system to be diagnosed. With the future use of this thesis in mind, a possible ECU implementation of the algorithms, none of these methods are the first choice for implementing in this thesis.

Physical redundancy methods are very useful when more than two sensors are implemented since a method can be realized in order to determine if sensors are faulty functioning. The method is however very limited for detecting sensor faults. Adding extra sensors to the system, (for on-board fault detection) would of course add a lot of extra costs and would in that sense not be a very satisfying choice in this thesis. Looking at this approach from another perspective, this can however be utilized in the workshops. Consider a system, where a fault has during operation been isolated into a certain area within the system (e.g. one of two components). By adding the extra sensor to the system in the workshop, the fault can then still be fully isolated, resulting in less time in the workshop.

Qualitative model-based methods has in the literature shown to be very simple but useful in both investigating possible system faults and forming logical statements for a knowledge base. Since these models are suitable for providing a non detailed physical knowledge of the system, they often serve as basis for the knowledge based approaches. The final result is often a set of IF- THEN- and ELSE- rules with limit checking, which represents the final diagnostic system. The diagnostic algorithms will be system specific but since the complexity of the diagnostic system is lower, it will also be easy to perform

changes to it. This approach offer the most expedient way to meet analytical needs when more complex methods are more time consuming.

### *2.2.2 CONCLUSION*

Based on the information found in this literature study, one can draw the conclusion that no method is individually applicable to this thesis, but that some are more suitable than others with respect to the application field, time and resources.

Since this thesis includes both system layout decisions and the development of the diagnostic system, quantitative methods, e.g. parameter estimation will not be the first choice. There is however room for simplified models that is necessary to provide required analytical redundancy, e.g. a temperature model or flow model for a specific component. As there will exist several sensors that are measuring the same physical quantity and the final system layout has not yet been determined, it is a good idea to investigate how physical redundancy can be applied in the system.

Causal models can also be used in the form of FTA and SDG, together with experiments performed on the actual system during normal and faulty conditions. From the knowledge obtained from the models and experimental data, suitable limit checks or trend checks can be developed for fault detection, with the aim of accomplishing complete fault isolation.

As regular limit and trend checks might not be enough for the detection of all faults, the simplified quantitative models mentioned earlier should be efficient for accomplishing more sophisticated detection limits.

To summarize and clarify the above, the fault detection- and isolation methods will be developed in steps, starting from the most simple detection limits and redundancy principals for single signals. The complexity of the methods will then be increased, with the aid of the methods presented in this chapter, until complete fault isolation is achieved for at least one system layout.

### 3. IMPLEMENTATION

*In this chapter, suggested system layouts with symbol descriptions are presented and discussed followed by the development of the experimental rig. The approach for developing the diagnostic system is then presented shortly and is in the next chapter presented in detail.*

#### 3.1 SYSTEM LAYOUTS

As the development of diagnostic algorithms is dependent on the available sensor signals in the system, several layouts have been proposed for further investigation and testing. All of these layouts origins from a proposed layout given by the company and have most of the components in common. A symbol description of the components used in the system layouts can be found in Figure 3.1.

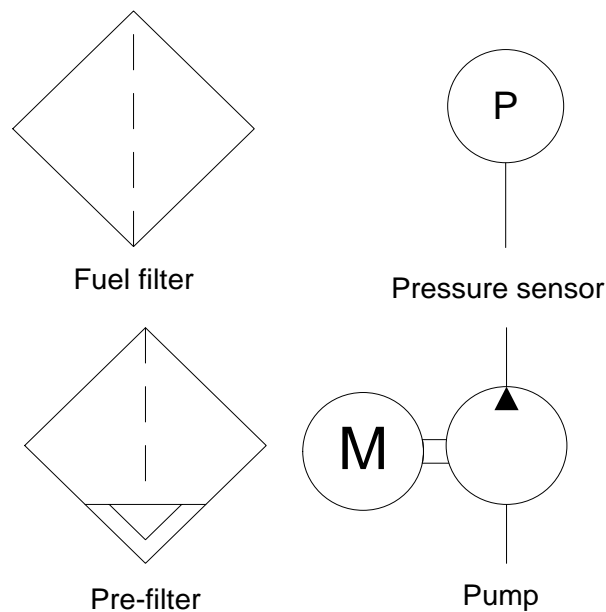


**Figure 3.1.** Symbol description for fuel filter, pre-filter, pressure sensor and pump.

The major difference between the system layouts is the number of used pressure sensors and their locations in the system. The first layout that was given by the company can be found in Figure 3.2. This design only utilizes one pressure sensor, which is required from a control perspective if a feedback control should be applicable. This layout is therefore categorized as the minimum required.

The common signals that are available for all of the system layouts are shown below.

- Low pressure circuit
  - RPM level for each feed pump
  - RPM level for each transfer pump
  - Current consumption for each feed pump
  - Current consumption for each transfer pump
  - Fuel level in main tank
  - Temperature in main tank
  - Fuel level in tech-tank
  - Temperature in tech-tank
  - Pressure before high pressure circuit
  - Possible fuel quality sensor
  - Temperature in feed pumps
  - Temperature in transfer pumps
- High pressure circuit
  - Temperature in high pressure circuit
  - Pressure in high pressure circuit
  - Mass flow through injectors

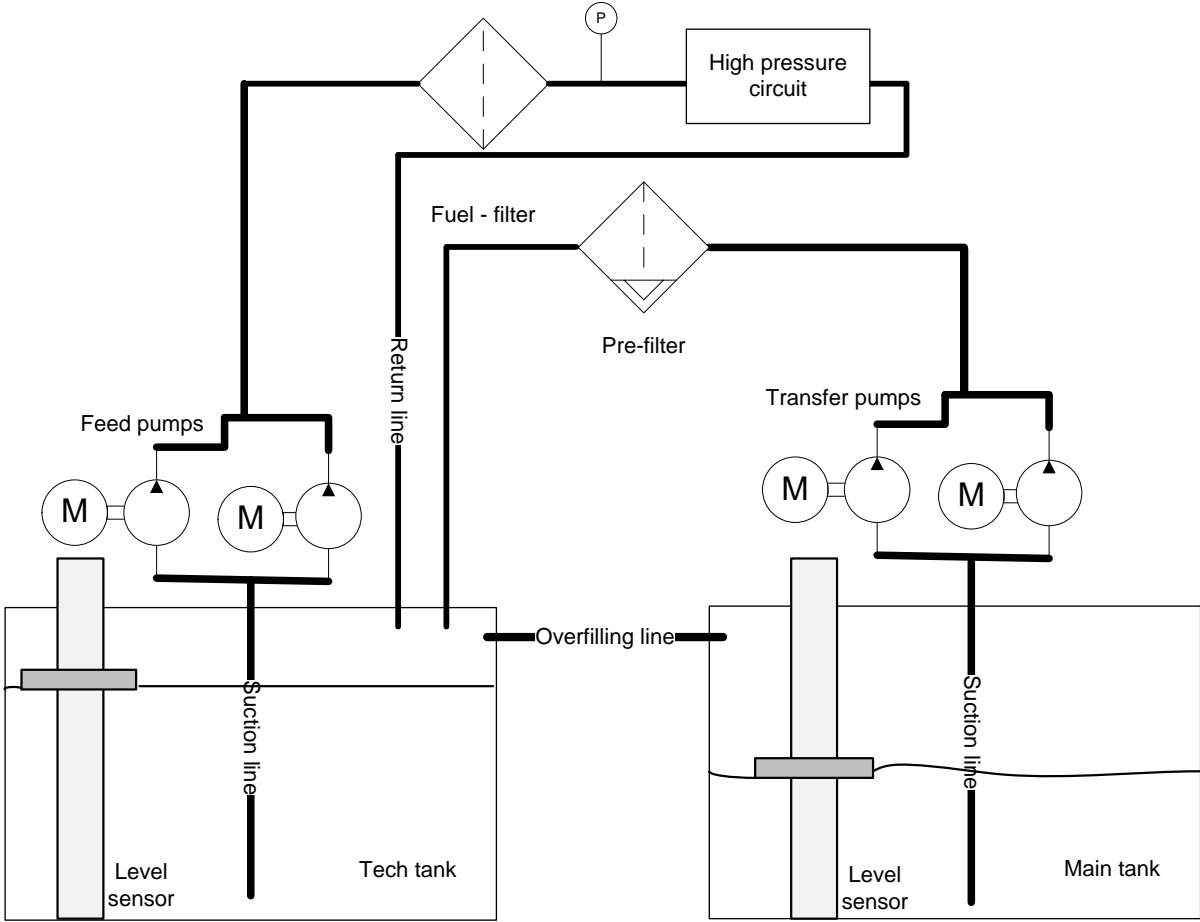


Figure 3.2. A schematic drawing for system layout A.

The second layout utilizes two pressure sensors, one before the fuel-filter and one before the high pressure circuit, which can be seen in Figure 3.3. The advantage of using one sensor on each side of the fuel filter is that it can provide knowledge of what is happening inside the filter with a possible pressure difference.

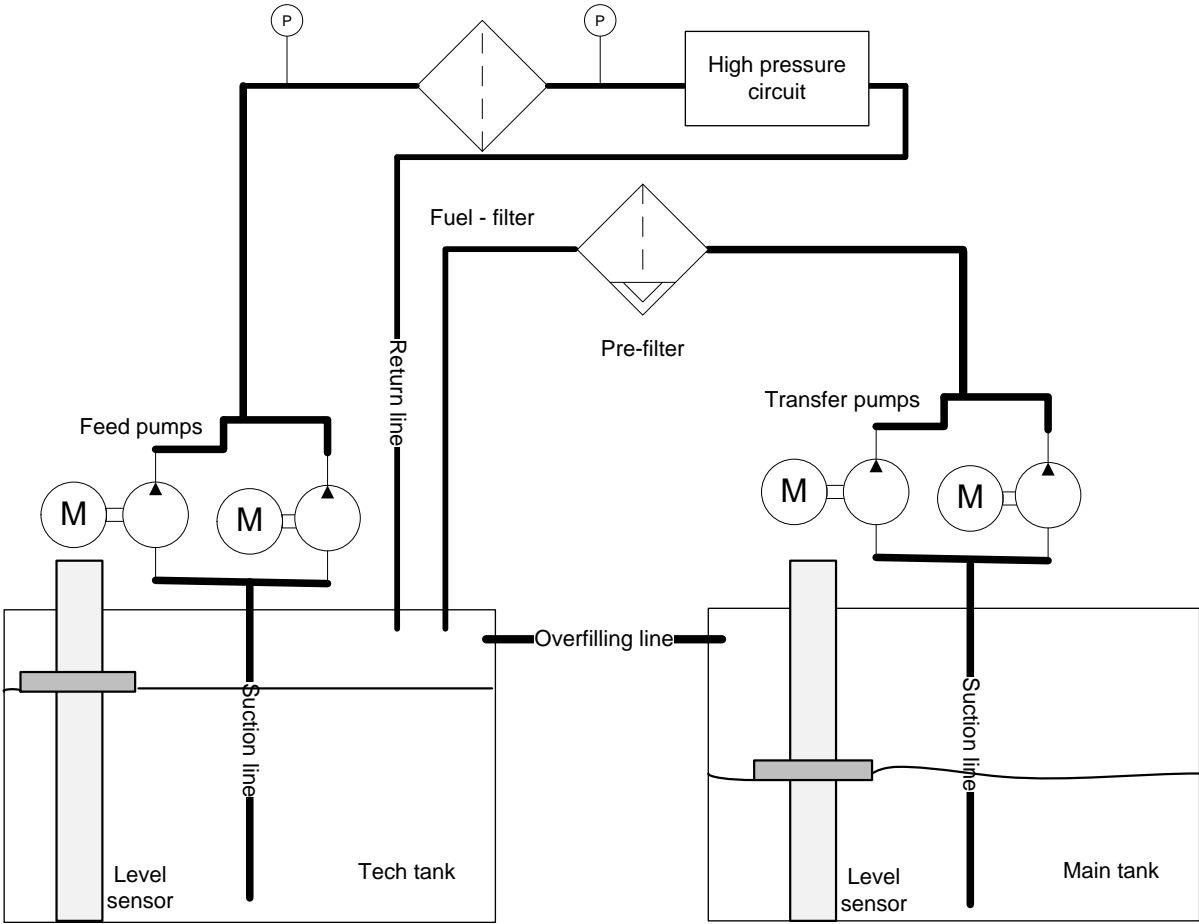
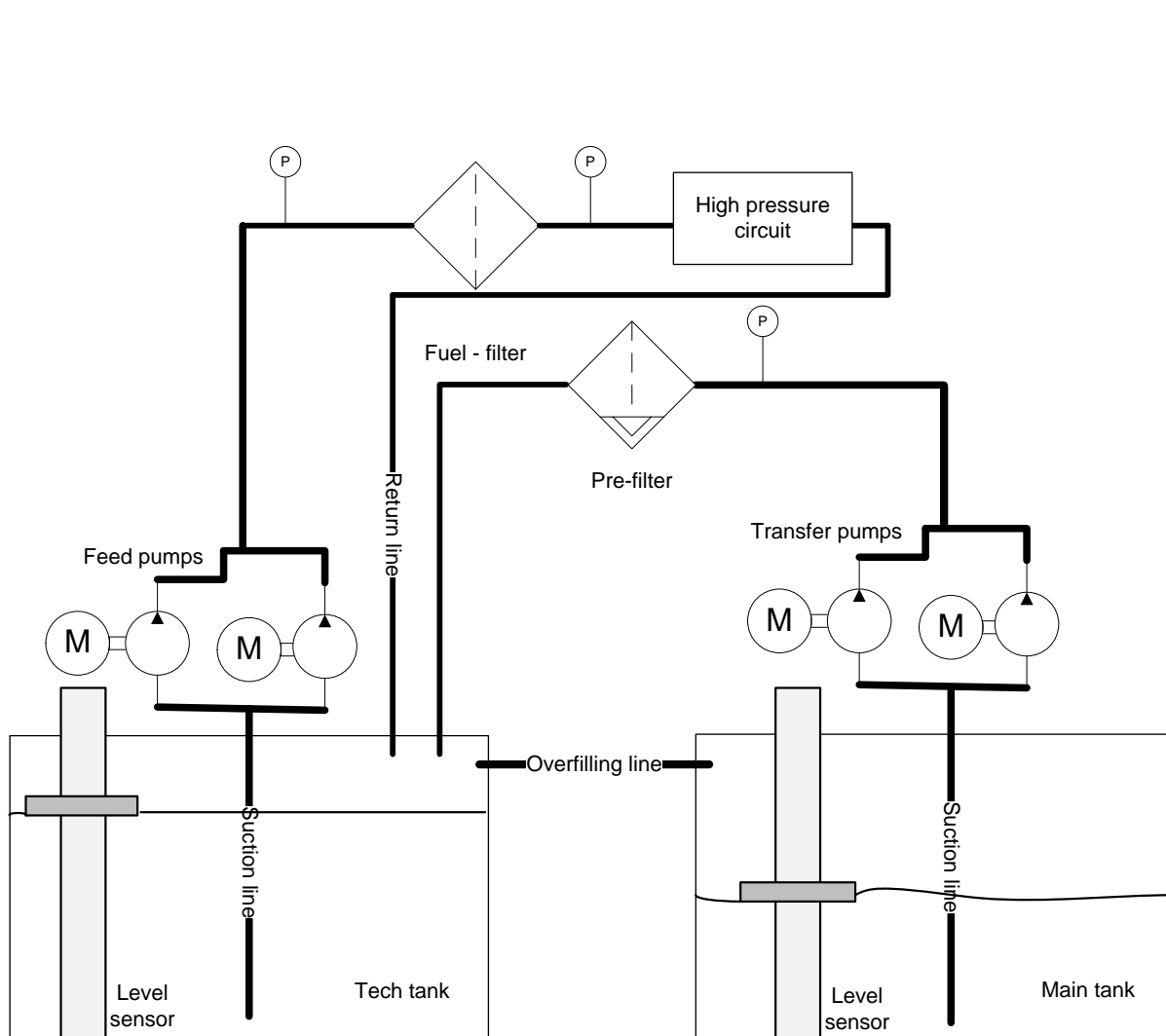


Figure 3.3. A schematic drawing for system layout B.

The first two proposed layouts give extra information for the behavior after the feed pumps but do not add any knowledge for the behavior after the transfer pumps. A third pressure sensor is therefore introduced in the third proposed layout, which can be seen in Figure 3.4. This third pressure sensor placed after the feed pumps and before the pre-filter is intended to provide additional information regarding the status of the pre-filter and the feed pumps.



**Figure 3.4. A schematic drawing for system layout C.**

As there is a possibility that the pressure sensor, located in between the feed pumps and the fuel filter, may be shown to be unnecessary a fourth layout is proposed. This layout has one pressure sensor after the transfer pumps and one before the high pressure circuit, which can be seen in Figure 3.5.

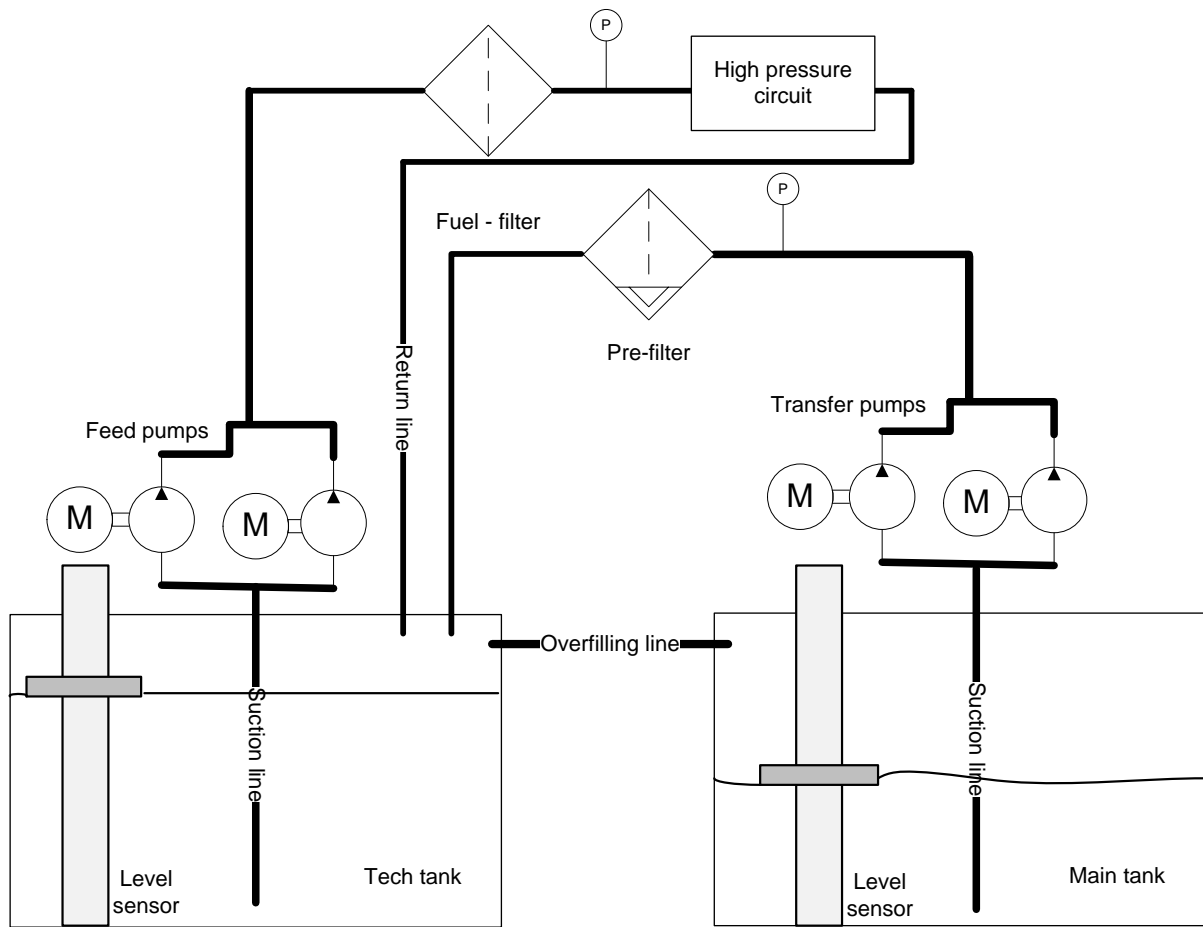


Figure 3.5. A schematic drawing for system layout D.

The number of available signals and the system price for each proposed layout can be found in Table 3.1.

Table 3.1. System layouts overview with respect to number of available signals for fault detection and diagnosis and system price.

System layout	Number of available signals for fault detection and diagnosis	System price
A	21	Low
B	22	Middle
C	23	High
D	22	Middle



## 3.2 EXPERIMENTAL RIG

To be able to develop a diagnostic system for the proposed system layouts, system knowledge is essential. From the beginning of the project, the idea was to utilize an already constructed rig for experiments. This rig was however not only designed for the purpose of this thesis, but also for other tests which contradicted the project planning. In order to still be able to investigate how the system behaves during normal and faulty conditions, the decision of constructing an own independent rig was made.

The purpose of the rig is to provide an easily modifiable test system, where system faults can be generated manually and where the number of pressure sensors can be applied for the different proposed layouts. The aim was, during the development, to replicate the real system as much as possible in order to get the most relevant measurements during the experiments. A picture of the developed rig can be found in Figure 3.6 and a schematic drawing, explaining the system in Figure 3.7.

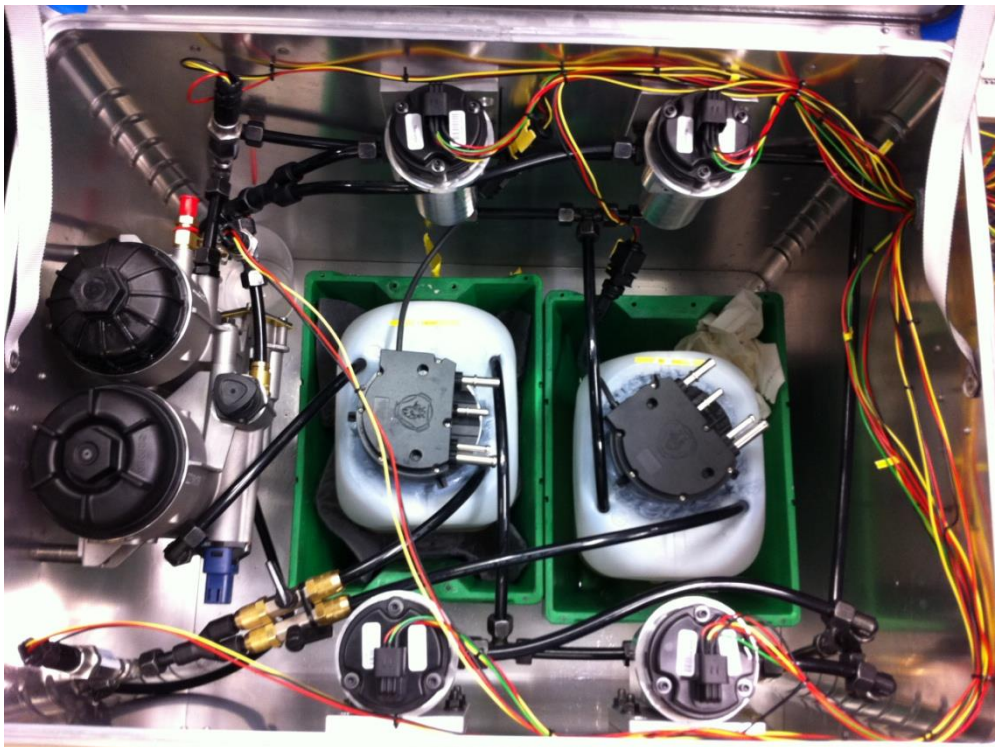
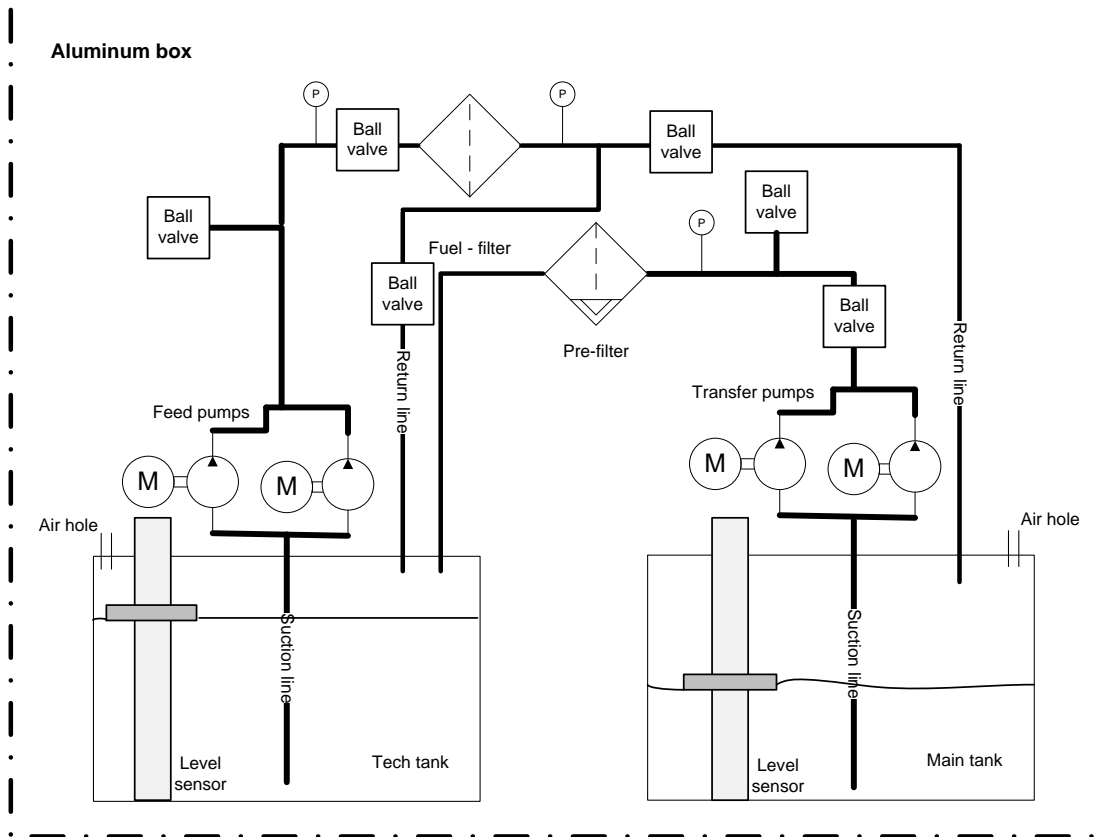


Figure 3.6. A picture of the final rig that was developed.



**Figure 3.7. Schematic drawing of the developed rig.**

The transfer pumps are connected in parallel and have the purpose of transporting the fuel from the first tank (main-tank) through the pre-filter, where water separation is possible, and then into the second tank (Tech-tank). The feed pumps are also connected in parallel and transports the fuel, firstly through a second filter (fuel-filter) and then through one of the ball valves one which shall represent the IMV, where some of the fuel returns back to the Tech-tank or the main tank through the return lines. The signals that are available in the developed rig are shown below.

- RPM level for each feed pump
- RPM level for each transfer pump
- Current consumption for each feed pump
- Current consumption for each transfer pump
- Fuel level in main tank
- Temperature in main tank
- Fuel level in tech-tank
- Temperature in tech-tank
- Pressure before high pressure circuit
- Pressure before fuel filter
- Pressure before pre-filter
- Temperature in transfer pumps
- Temperature in feed pumps

The construction of the rig included both hardware and software which are covered in the sections below.

### 3.2.1 HARDWARE

The rig includes four, pumps, two 10 liter tanks, two level sensors, three pressure sensors, two filters, ball valves, electrical connections and a lot of tubing. Below, the purpose and functionality of each component is described.

#### 3.2.1.1. Pumps

The four pumps that have been used are from the company Parker where two of them acts as transfer pumps and the other two as feed pumps. These are all screw pumps which can be categorized as pumps with a positive displacement. This means that the flow is theoretically proportional to the RPM-level of the pumps. All of the pumps are controlled with the help of CAN communication and uses their internal RPM controllers. The lowest RPM level that is possible to demand is set to 1300 RPM's and due to the CAN communication, the resolution for the current consumption is in steps of 0,13 amperes.

#### 3.2.1.2. Tanks

To replicate the tanks, two 10 liters plastic tanks has been modified and used. These tanks are intended to serve as storage for the fuel.

#### 3.2.1.3. Filters

The pre-filter that was mentioned earlier is used for fuel filtration and separation of water in the fuel. The second filter, which is a pressure filter, is used to filtrate the fuel again, but from smaller debris. Both of these filters are placed inside a filter house which has been modified slightly. Since the water separation functionality on the first filter will not be used in this thesis, the functionality has been removed in order to prevent the filter from building up a pressure when these connections are plugged.

#### 3.2.1.4. Level and temperature sensors

To be able to indicate the level in the tanks, two level/temp sensors has been used and these are originally intended for SCR-tanks. The level sensors has a float with built in magnets that triggers the reed relays generating a potential-free resistance with an ohm value that increases or decreases depending on the float position. The level sensors are connected to a  $\psi$ V power supply and then output the voltage between  $\alpha$  and  $\Omega$  for "empty" and "full" respectively. There is also a thermistor integrated in the level sensor unit. With knowledge of the electrical circuit the thermistor resistance changes according to (4).

$$R_f = \frac{R_a R_b (V_{cc} - V_{sense})}{(R_a V_{sense} - R_b (V_{cc} - V_{sense}))} \quad (4)$$

The temperature in Celsius can then be calculated as (5),

$$T = \frac{\beta}{\ln\left(\frac{R_f}{A}\right)} \quad (5)$$

where  $\beta$  and  $A$  are constants depending on the thermistor.

### 3.2.1.5. Pressure sensors

The rig includes three pressure sensors, which can be placed on different locations in the rig for experimental purposes. The sensors that are being used has two different resolutions whereas the first can measure  $\zeta - \theta$  bar and the second can measure  $v-\xi$  bar and both of them outputs a voltage between  $\alpha V - \Omega V$ . Since the normal pressure levels will be below  $\theta$  bar, the latter is also used in order to detect possible pressure peaks occurring in the system. The error for the pressure sensors, depending on the temperature, is described by figure and a table in (Ellnefjård, 2014). This can however not be shown in this report version due to secrecy. The reader shall from this have in mind that the pressure error is depending on the temperature and that the error is lowest around  $50^\circ C$ .

### 3.2.1.6. Ball valves

In order to manually be able to generate faults representing leaks, ball valves have been connected with T-couplings on several places inside the system, where leaks on lines can occur during system operation.

### 3.2.1.7. Labview

All of the sensors and pumps are controlled by Labview running on a NI cDAQ-9174 with two CAN modules (NI 9862 and NI 8473) and two analog input modules (NI 9239 and NI 9219).

### 3.2.1.8. Electrical connections

#### 3.2.1.8.1. Overview

An overview of the communication between the PC, Labview unit, sensors and actuators can be seen in Figure 3.8.

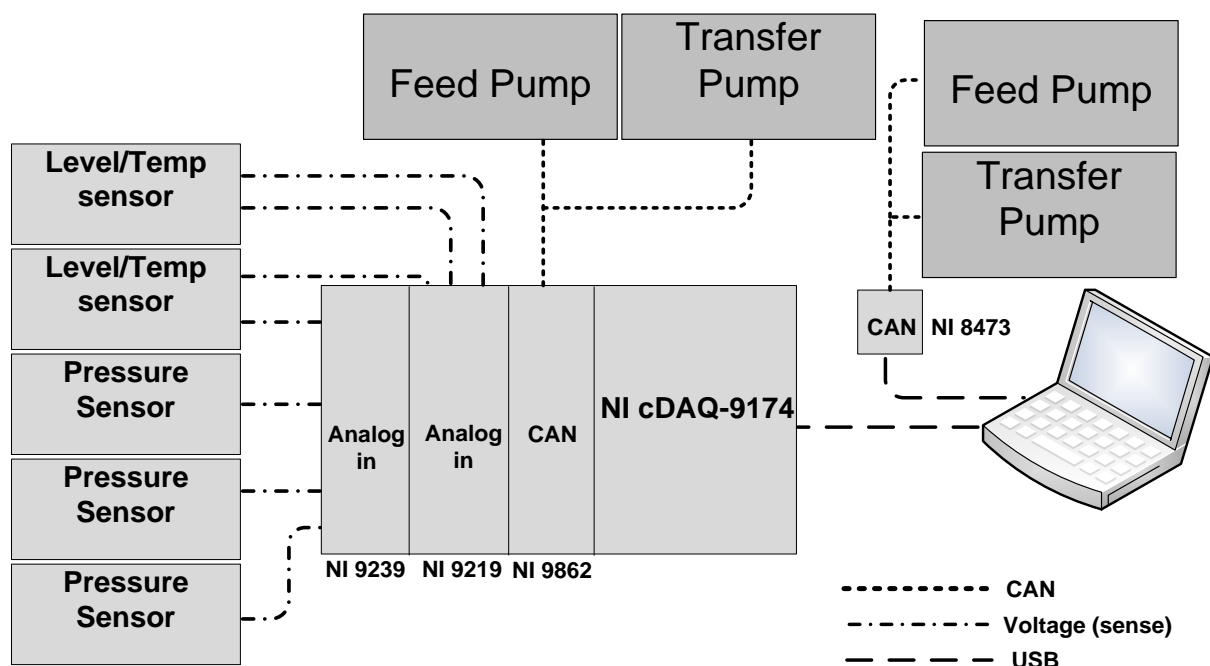


Figure 3.8. Overview of the communication between the PC, Labview unit, sensors and actuators.

#### 3.2.1.8.2. CAN interface

As mentioned earlier, the communication with the pumps is performed through CAN. Since the two feed pumps share the same identifier, which also yields for the two transfer pumps, two CAN busses is needed. One feed pump and one transfer pump is connected to the NI9862 CAN module as the other pair is connected to the NI USB 8473 CAN module. This is needed in order to be able to command and receive information from each pump separately. The information regarding the used identifiers and message frames can be found in APPENDIX A.

### *3.2.2 SOFTWARE*

As was mentioned earlier, the system is controlled and monitored through a Labview interface. The developed Labview program communicates with the pumps through the CAN interface and reads voltage levels from all of the sensors, converting them into the measured physical quantities.

#### **3.2.2.1. System control**

The system can either be directly controlled manually, by sending the demanded RPM level to the pumps, or with simpler controllers based on PID regulators and hysteresis's that has been developed for the test cases that can be executed both manually and automatically.

#### **3.2.2.2. Data logging**

The developed Labview interface has several graphs and indicators, representing the real-time system behavior. These are enough for controlling the system but in order to better analyze the data from the sensors and the pumps, e.g. when a fault occurs, the data needs to be saved for a post analysis. A logging system has therefore been developed, which automatically saves all of the sensor and actuator data into a file when logging is demanded.

#### **3.2.2.3. Data analysis**

In order to analyze the data that has been collected with the logging system described above, a MATLAB script has been developed. This script creates vectors of the measured quantities and removes the unnecessary information within the files. The vectors can then be used for suitable graphs or for other scripts related to the analysis.

### 3.2.3 CALIBRATION OF SENSORS AND LABVIEW INTERFACE

To be sure that the sensors functions properly and that the conversion of the output voltage to a physical quantity is correct, the sensors and the Labview program has been calibrated.

#### 3.2.3.1. Level sensors

The level sensor was calibrated by manually pouring a known amount of water into the tank and then reading the output voltage. This was then repeated for the range of 1-10 liters. According to the datasheet, the output voltage is linear and thus the factor needed for proper conversion is the gradient,  $k$ , in the linear equation. The conversion from voltage to liters is described as equation (6).

$$level = \left( \frac{U_{out} - U_{min}}{U_{max} - U_{min}} \right) k \quad (6)$$

#### 3.2.3.2. Pressure sensors

The pressure sensors output was calibrated by using a portable pressure calibrator. By applying a known pressure to the sensors, the sensor output conversion can easily be calibrated and tuned with the software. The conversion from the output voltage to bar for the pressure sensors is described by equation (7).

$$p = \left( \frac{U_{out} - U_{min}}{U_{max} - U_{min}} \right) (p_{max} - p_{min}) + p_{min} \quad (7)$$

### 3.3 DEVELOPMENT OF THE DIAGNOSTIC SYSTEM

In order to develop the diagnostic algorithms, one must be able to separate a faulty behavior from a normal behavior of the system. To be able to accomplish this, sensor and actuator data needs to be retrieved from the system during normal and faulty conditions. With a post analysis of the data it is then possible to determine which faults are detectable or not for a specific system layout.

#### 3.3.1 EXPERIMENTS

Since the developed rig is designed to be able to run during both faulty and normal conditions, the different behaviors can be established with designed test cases.

In order to test and record the normal and faulty behavior of the system, one must consider how the system will behave with and without an active optimal system controller since some faults might not be detectable with both. The system will during the tests therefore be controlled both actively and manually.

#### 3.3.2 DATA ANALYSIS

The results and the post analysis of the collected data will be separated into two chapters. In the first chapter, the analysis is focused on determining the normal behavior of the system as the other is focusing on the faulty behavior and how these faults can be detected. Multiple detection methods will be proposed for each fault as all of them might not be applicable to all of the different system layouts. The methods will be presented in pseudo code and flow charts as this thesis will serve as the basis for implementing the diagnostic system on an ECU.

#### 3.3.3 DIAGNOSTIC SYSTEM

The final diagnostic system, for each layout, will be presented in larger flow charts, where the order of the detection tests are presented along with the controller conditions and modes that are needed for proper fault detection and isolation.





# 4. RESULTS AND ANALYSIS FOR NORMAL SYSTEM BEHAVIOR

In this chapter, the normal system behavior is discussed and defined by analyzing the data retrieved from the normal behavioral tests along with other data retrieved from the company, representing the average fuel consumption for different trucks.

To test the normal behavior, one must first define what is normal for the system. In Figure 4.1, the top graph represents the fuel consumption and mechanical feed pump flow for a  $v$  liters  $\phi$  cylinder engine with  $\chi$  hp or  $\psi$  hp. The bottom graph represents the fuel consumption and the mechanical feed pump flow for a  $\epsilon$  liters engine with  $\omega$  hp.

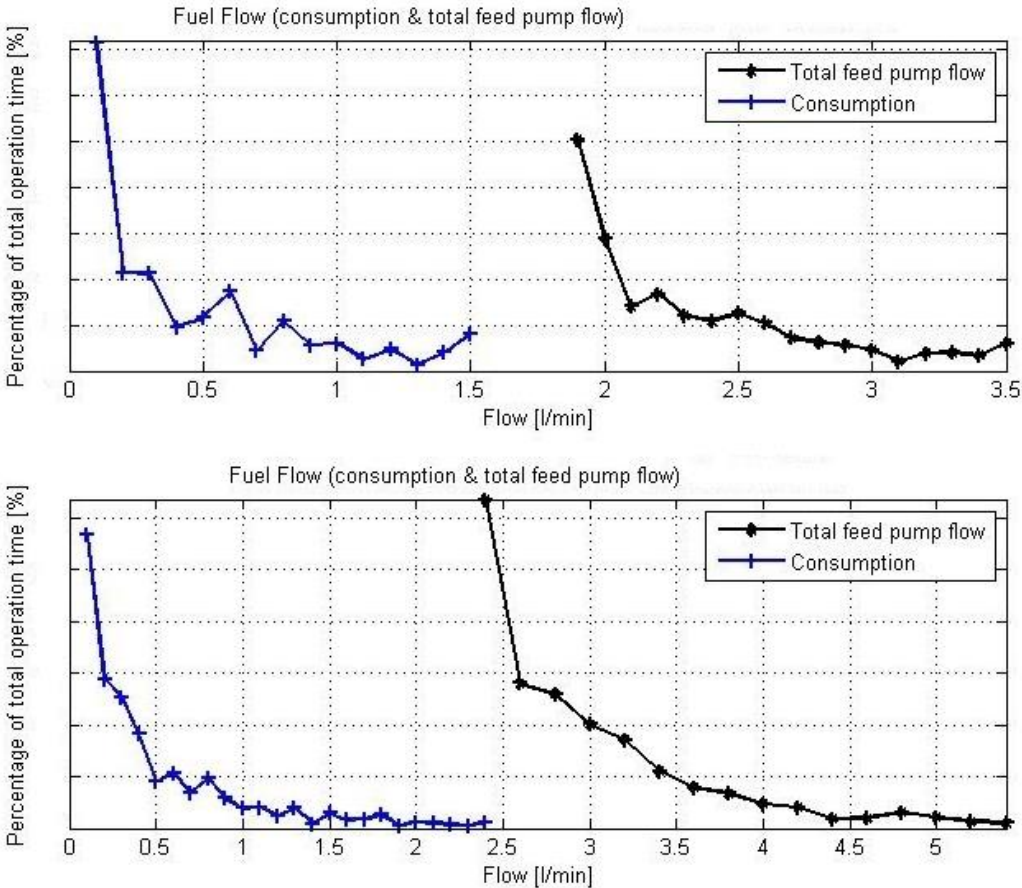


Figure 4.1. Percentage of total operation time for fuel consumption and total flow from feed pumps for a  $v$  liters engine with  $\chi - \psi$  hp (top graph) and a  $\epsilon$  liters engine with  $\omega$  hp (bottom graph).

From these graphs one can see that the new electrical feed pumps must be able to provide a flow of at least 2,5 l/min to satisfy the engine with the highest consumption. A normal fuel consumption is therefore in between 0,01 – 2,5 liters/min.

To be able to deliver the correct amount of fuel during the normal behavior the flow as a function of the RPM needs to be investigated. This was done by executing a test case that is described below.

## 4.1 DETERMINING THE FLOW FOR DIFFERENT RPM LEVELS

To determine the relationship between the RPM level and the flow for each pump the following test case was developed.

- Automatic filling and emptying of the tanks with increasing RPM levels.
  - The transfer pumps starts on 1300 RPM and fills up the tech-tank meanwhile the feed pumps are off.
  - When the tech-tank level reaches 90%, the transfer pumps stops and the feed pumps starts on 1300 RPM and fills up the main tank.
  - When the level reaches 90% in the main tank, the sequence starts again but with an increased RPM level.

The RPM level, the tank level and the derivative of the tank level data that was collected during the test can be found in Figure 4.2 and Figure 4.3. The rest of the test data that was collected can be found in APPENDIX B.

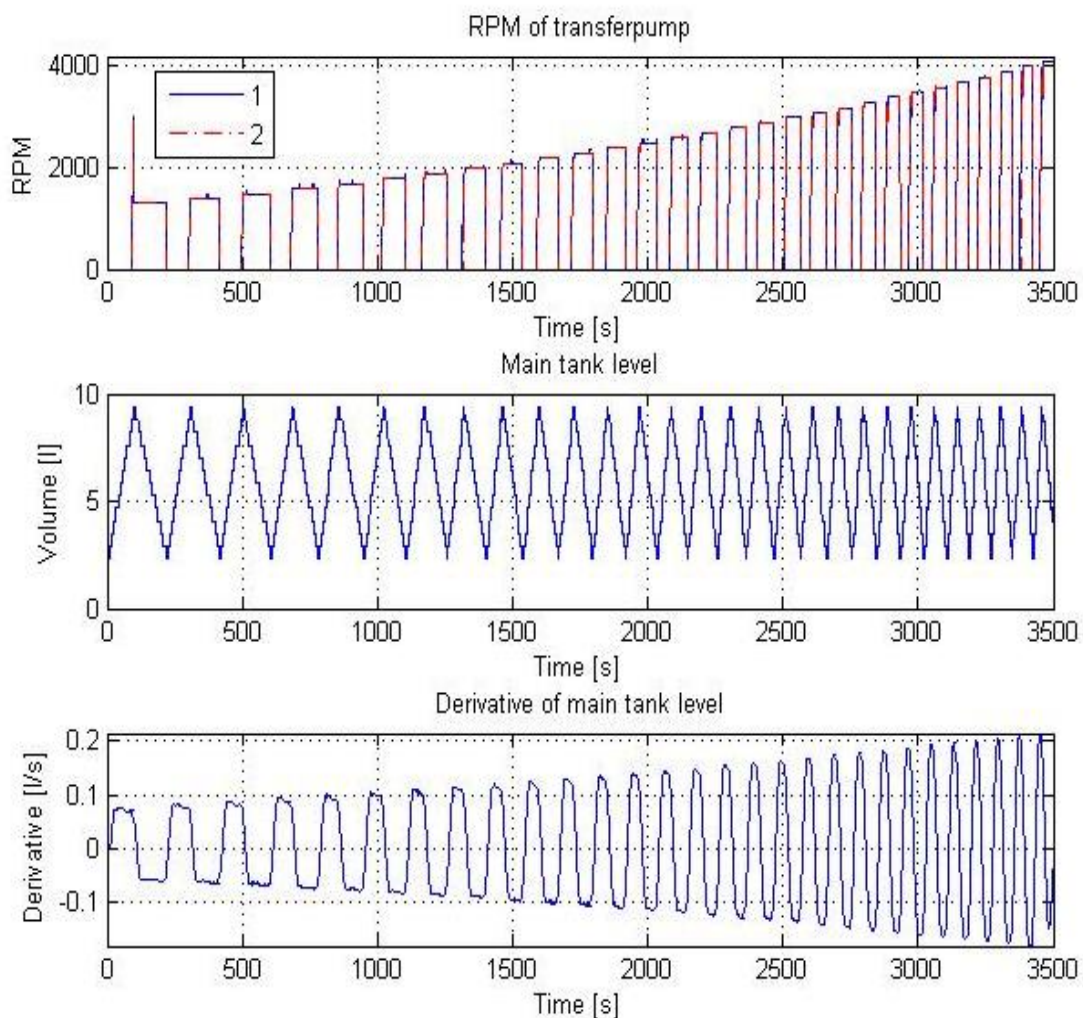


**Figure 4.2.** Data from the test, representing the RPM level for the transfer pumps, the level in tech tank and the derivative of the tech tank level (flow). In the top graph, the blue signal is from feed pump 1 and the red signal is from feed pump 2. Note that the filling time for each tank decreases as the RPM level is increased and generates an illusion of a non-linear relationship between the RPM and the flow. This is not the case as the same amount of fuel is transported in each sequence.

As the test was executed automatically with an increasing RPM level the tank gets emptied faster for each increase, which can be seen in the middle graph. By looking at the derivative of the tech tank level signal, one can see that the flow is nearly proportional to the RPM-level for the transfer pumps.

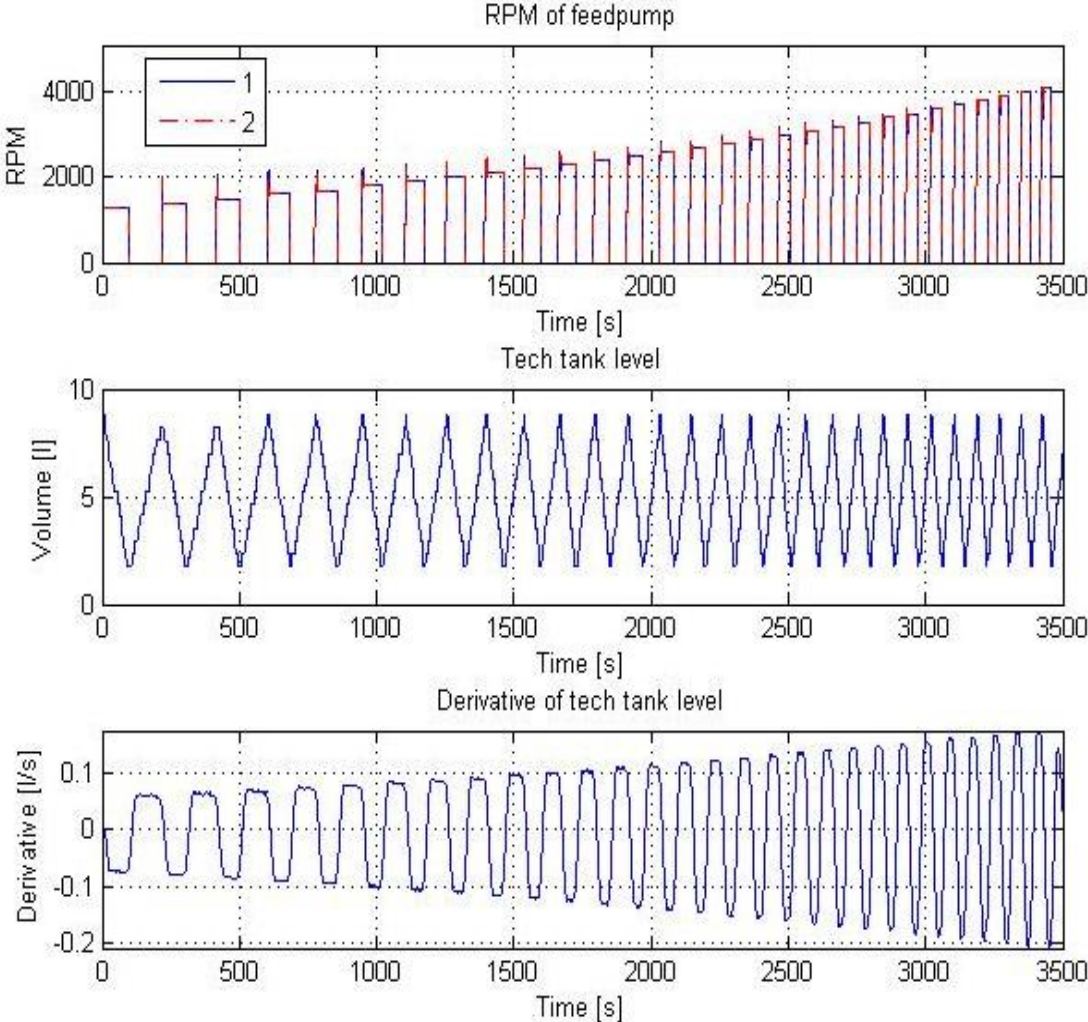


**Figure 4.3. Data from the test, representing the RPM level for the feed pumps, the level in main tank and the derivative of the tech tank level (flow). In the top graph, the blue signal is from feed pump 1 and the red signal is from feed pump 2.**

By only considering the data where either the transfer pumps or the feed pumps are running, the volume that is being moved from one tank to the other can be calculated for each RPM level. Thus, the flow for the feed pumps and transfer pumps as function of the RPM level can be found in Figure 4.4.

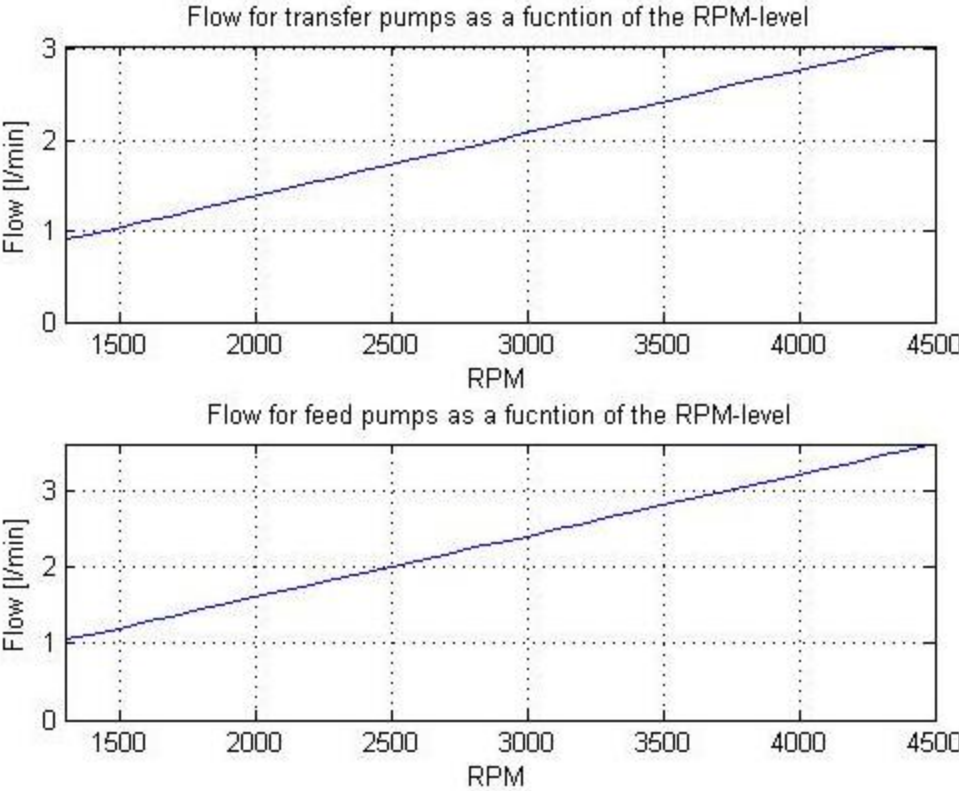


**Figure 4.4.** Upper graph describes the flow for the transfer pumps as a function of the RPM level while the lower is the flow from the feed pumps as a function of the feed pump RPM-level.

## 4.2 DEFINITION OF NORMAL BEHAVIOR

As was shown in Figure 4.4, the flow of the feed pumps on the lowest RPM level (1300) is in the normal consumption range that was presented earlier. Therefore, a normal behavior will in this thesis be considered as a system where either one or two feed pumps are running on the lowest RPM-level where they separately deliver the fuel amount around 1,1 l/min with a pressure of 5-10 bar. The RPM level for the transfer pumps will only depend on the level in the tech-tank and thus, a normal RPM level for the transfer pumps will be in between 1300 – 3000 RPMs where the pressure is determined by the hydraulic circuit.

### 4.3 DATA FROM NORMAL SYSTEM BEHAVIOR

After determining the flow for the different RPM levels, the normal system behavior described above can be tested. The test that has been designed for this is described below.

- PI-controlled / manually controlled pressure for feed pumps and level hysteresis for transfer pumps.
  - The transfer pumps runs on 3000 RPM's when the level in the main tank goes below 25% and stops when the level reaches 90%.
  - The feed pumps RPM level is either controlled with a PI-regulator, where the reference is the pressure after the fuel-filter, or where the RPM is set to 1300 RPM's and the valve is adjusted so that a pressure around 5-10 bar is reached.

The purpose this test case is to replicate a real system behavior and can be used during both normal and faulty conditions.

This test was therefore executed in two different ways as some faults may only be detectable with a certain type of system control. In the first test the PI-regulator controlled the RPM level where the reference input was a feed pressure of 5-10 bar. The valve representing the IMV was slightly closed so that the RPM level would saturate nearby 1300 RPM. Data from this test of the normal behavior can be found in Figure 4.5, where RPM levels and the current consumption are presented as a function of time.

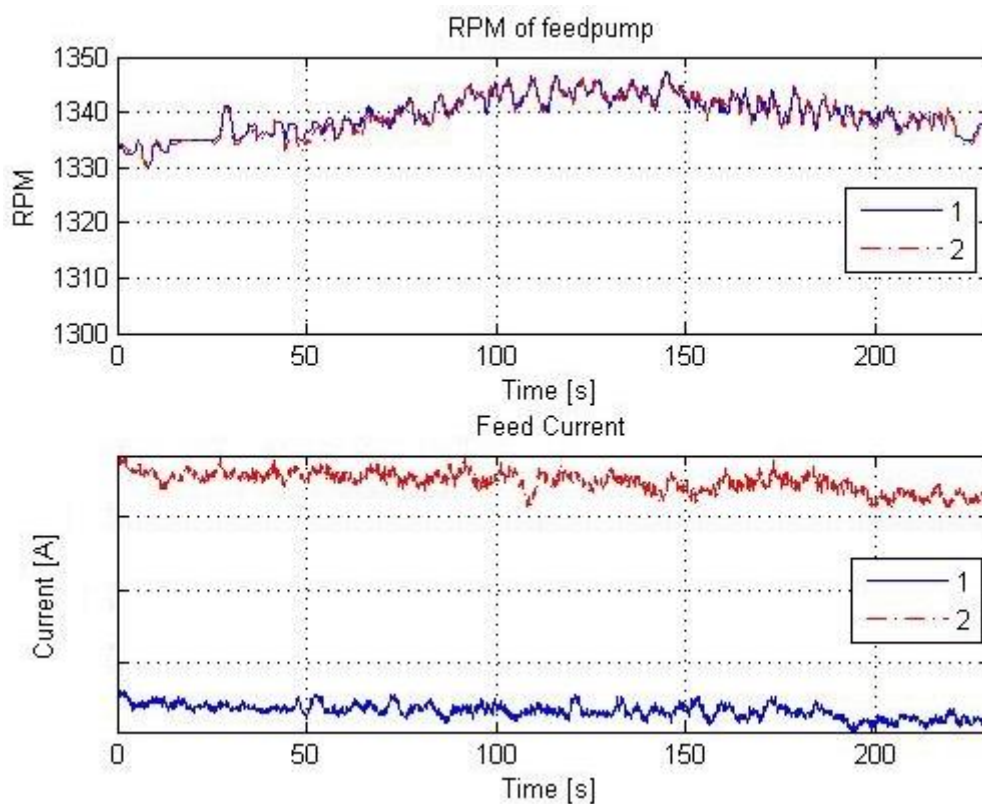


**Figure 4.5. Behavior for RPM levels and current consumption during PI-regulated feed pumps with a pressure around 5-10 bar. The blue signal is from feed pump 1 and the red signal is from feed pump 2.**

Even though the two feed pumps operates at the same RPM level, transfer pump 2 consumes more current than feed pump 1, which can be seen in the lower graph presented in Figure 4.5. The reason this was further investigated as it could either depend on the pump location inside the rig or the internal current measurement inside the pumps. To test if the pump location inside the rig was causing this phenomenon, the two feed pumps were simply switched. The result from this did not have any effect. After further investigation, it turned out to depend on the internal measurement rounding together with the CAN-communication. The internal pump controller uses a current sensing resistor to sense the current draw and internally rounds up to the closest hex byte. This hex byte is then transmitted on the CAN status message as the current feedback byte. From this current feedback byte it is then possible to read the current by converting it to a decimal value and multiplying by 0.13. The current feedback byte is described in a table on the corresponding page in (Ellnefjård, 2014).

The current draw that is transmitted in the CAN status message may therefore vary depending on the current sensing component accuracy and internal rounding. E.g. when the speed is set to 0 RPM the current feedback byte will read 01 (0,13 A) or 02 (0,26 A).

For the same time sequence as in Figure 4.5, the feed pressure before and after the fuel filter can be seen in Figure 4.6, together with the upper and lower error boundaries that depends on the temperature. As can be seen, the pressure sensor after the fuel filter has a higher accuracy and thus, the error boundaries are smaller.

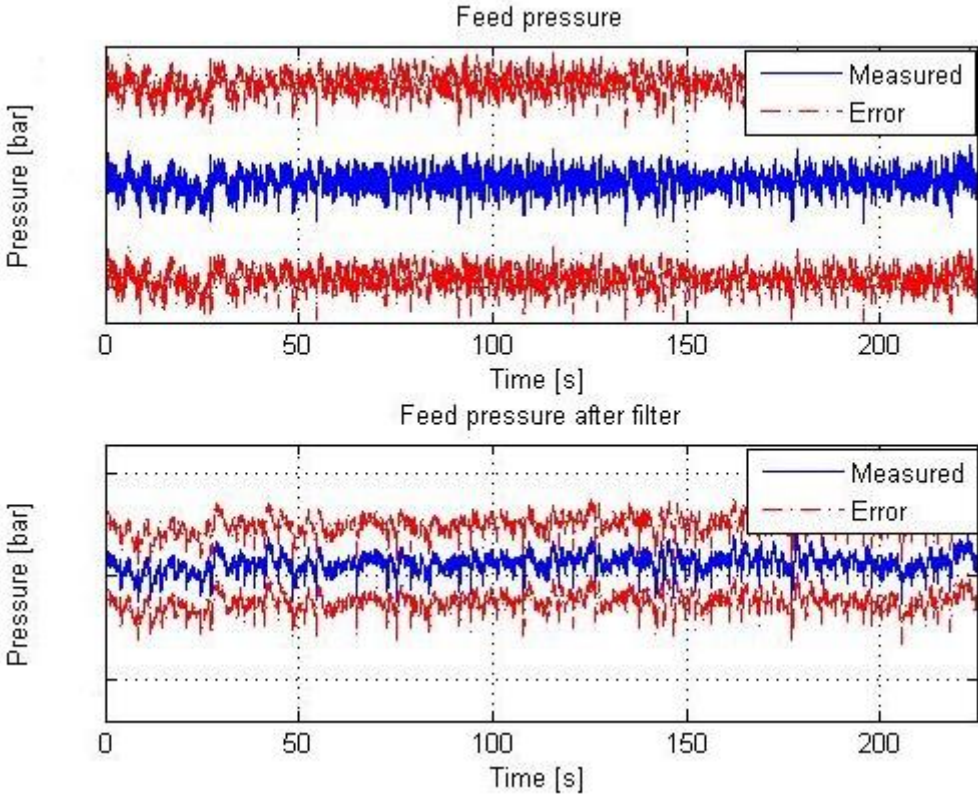


**Figure 4.6. Pressure before and after the fuel filter during PI-regulated feed pumps with a pressure around 6 bar. The red dot-dashed line is the upper and lower error boundaries that depends on the temperature.**

Both of the signals contains a lot of noise and is therefore in the need of filters which will be suggested later in the report.

The transfer pumps was during this test controlled with a simple level hysteresis for the tech-tank and the RPM levels, current consumption and transfer pressure can be found in Figure 4.7.

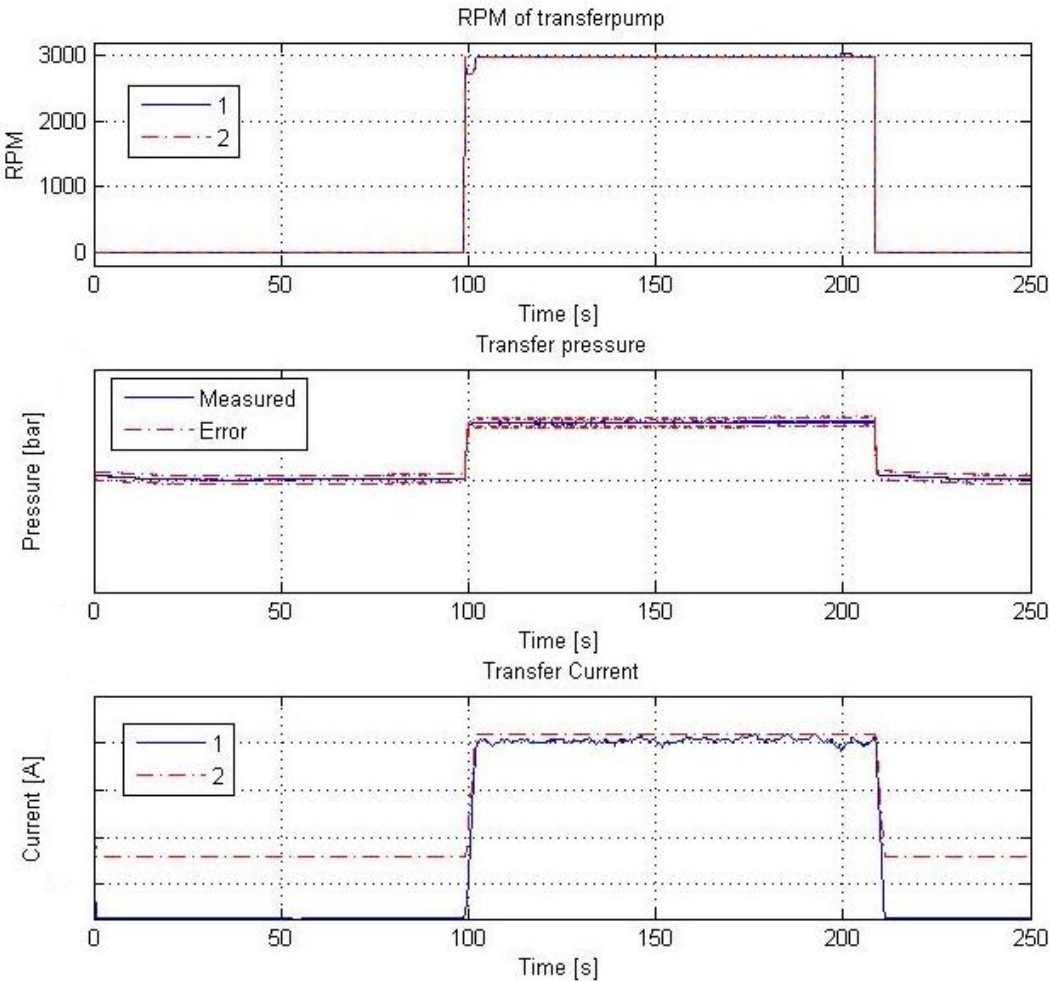


**Figure 4.7. RPM levels, transfer pressure and current consumption when controlled with a tech-tank level hysteresis during PI-regulated feed pumps. For the RPM- and the current plot the blue signal is from transfer pump 1 and the red signal is from transfer pump 2.**

As was mentioned before, the current consumption phenomena exists for the transfer pumps as well, which can clearly be seen in the figure above. All of the data that was recorded during this test can be found in APPENDIX B.



As was described earlier, the test was both executed with a PI-controller for the feed pumps and with a constant feed pump RPM level. In the latter one, the ball valve, representing the IMV, was manually put in a position that saturates a feed pressure of 6,5 bar. The RPM levels and the current consumption recorded in this test can be seen in Figure 4.8.

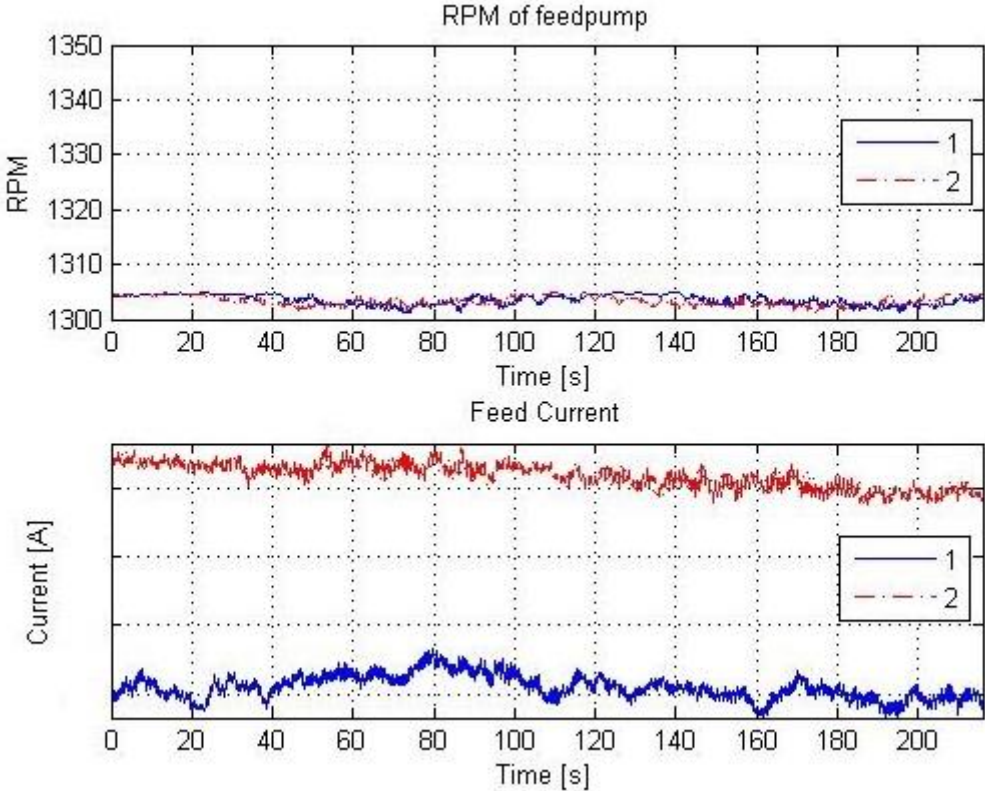


**Figure 4.8. Behavior for RPM levels and current consumption during constant a constant RPM level of 1305 for the feed pumps with a feed pressure around 5-10 bar. The blue signal is from feed pump 1 and the red signal is from feed pump 2.**

In Figure 4.8, one can see that the internal RPM controller integrated in the pumps maintains the demanded RPM level around 1305 with a small random error. This error is more visible with a smaller RPM axis, as in Figure 4.9.

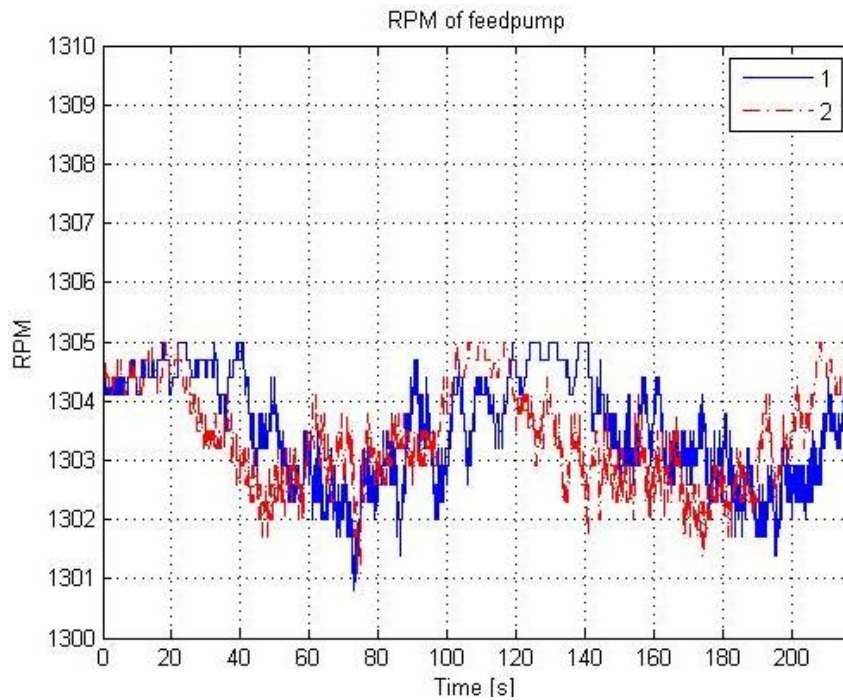


**Figure 4.9.** The feed pump RPM levels with a smaller RPM axis. The blue signal is from feed pump 1 and the red signal is from feed pump 2.

In Figure 4.9, one can see that the random error goes up to the size of 4 RPM's maximum. Another interesting fact that can be concluded is that the random error oscillates over time. This is also a result from the chosen internal controller in the pumps, which is not possible to change in this thesis. The feed pressure before and after the fuel filter, with upper and lower error boundaries, can be found in Figure 4.10.

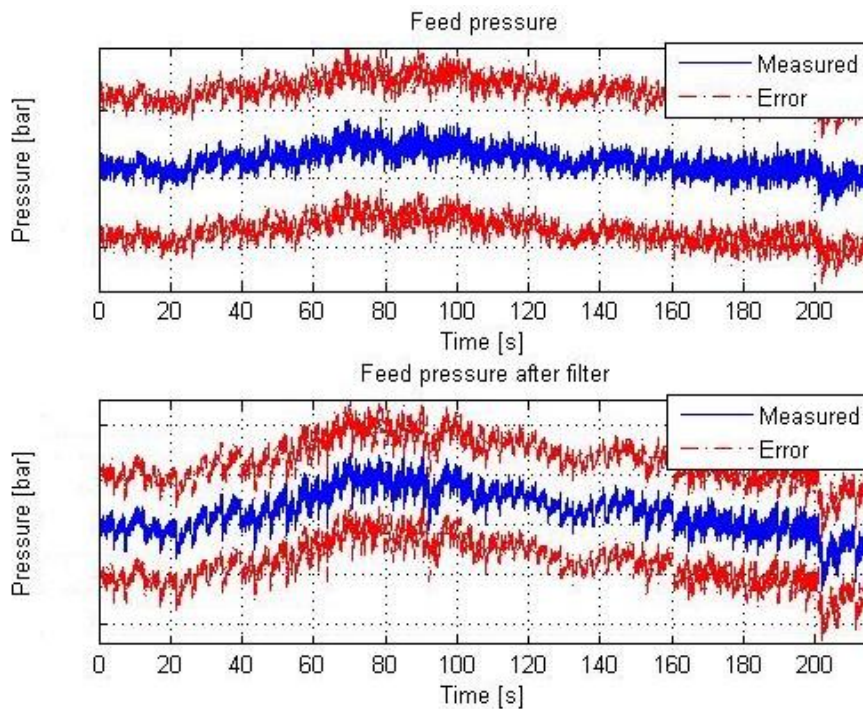


**Figure 4.10.** Pressure before and after the fuel filter during constant a constant RPM level of 1305 for the feed pumps with a feed pressure around 5-10 bar. The red dot-dashed line is the upper and lower error boundaries that depend on the temperature.

The RPM levels, transfer pressure and the current consumption for the transfer pumps that was recorded in this test can be found in Figure 4.11. As the hysteresis control is used in this test as well, the signals characteristics are very similar to the ones retrieved in the previous test. The rest of the data that was recorded during this test can be found in APPENDIX B.

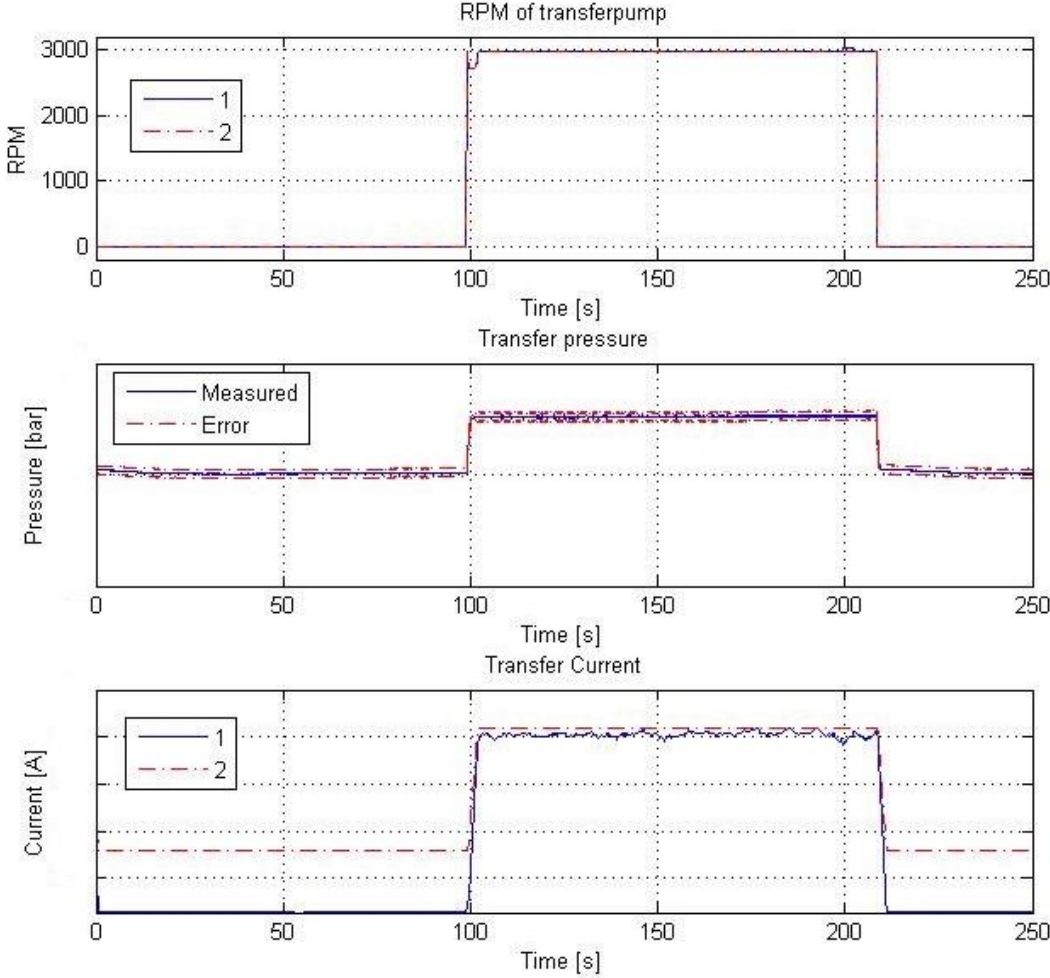


**Figure 4.11. RPM levels, transfer pressure and current consumption when the transfer pumps are controlled with a tech-tank level hysteresis and the RPM level demand is constant for the feed pumps. For the RPM- and the current plot the blue signal is from transfer pump 1 and the red signal is from transfer pump 2.**

4.3.1 RELATIONSHIPS BETWEEN PARAMETERS DURING NORMAL BEHAVIOR

To later be able to develop diagnostic algorithms, it is very useful to investigate how the currents and the pressures are related to the RPM levels. From the data retrieved during normal system behavior, the relationships between different system parameters can be evaluated. The current consumption for the transfer pumps can during a normal system behavior be seen in Figure 4.12.

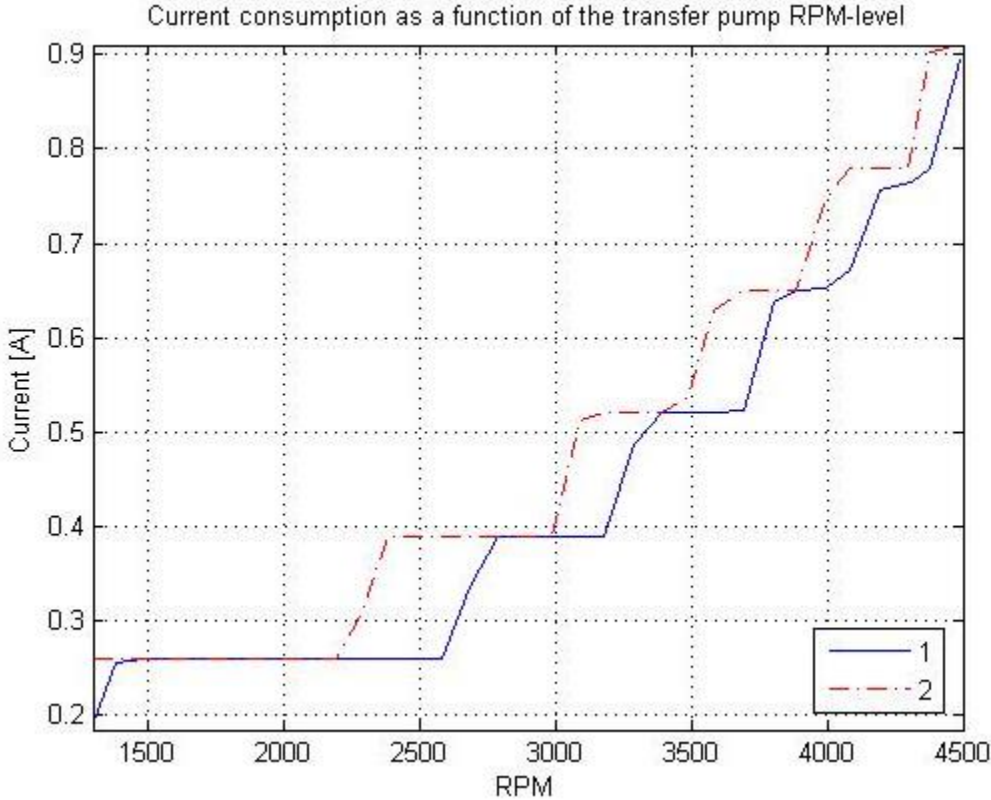
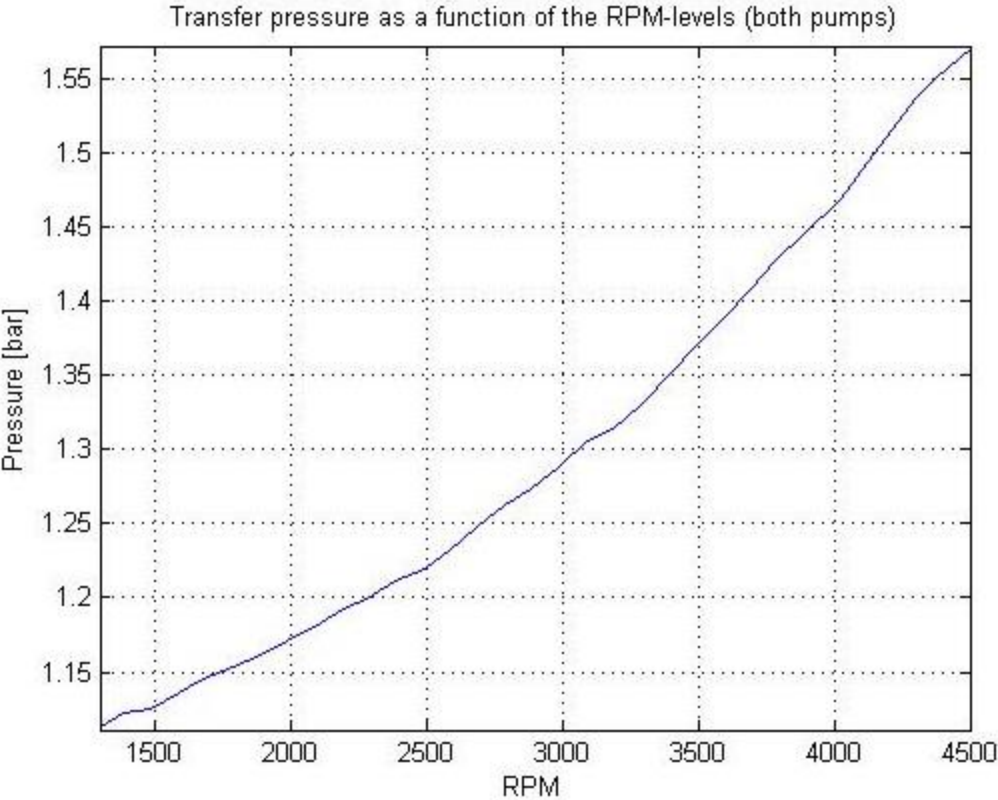


Figure 4.12. The current consumption for transfer pumps 1 and 2 as a function of the RPM level during normal system behavior. The blue signal is transfer pump 1 and the red signal is transfer pump 2.

The above presented figure, one can clearly see the current consumption difference phenomena that depend on the internal current measurement and the CAN communication that was mentioned earlier in the report.

The transfer pressure as a function of the RPM level can be seen in Figure 4.13.



**Figure 4.13. Transfer pressure as a function of the RPM-level during normal system behavior, running both transfer pumps at the same time.**

As can be seen in the graph, the absolute transfer pressure is around 1,5 bar during normal conditions, depending on the RPM level.

The two latest graphs shown above describes how the transfer pressure and current consumption are related to the RPM-levels for the transfer pumps, which is fairly straight forward in comparison with the rest of the system. The reason for this is that both the current consumption for the feed pumps and the feed pressure is depending on the combination of the chosen RPM-level and the ball valve position (IMV demand in the real system). Since the experimental rig does not provide any information of the ball valve position a behavior relationship between these variables becomes more difficult. An example of the pressure and the current consumption behaviors, where the ball valve is slightly closed, can be found in Figure 4.14.

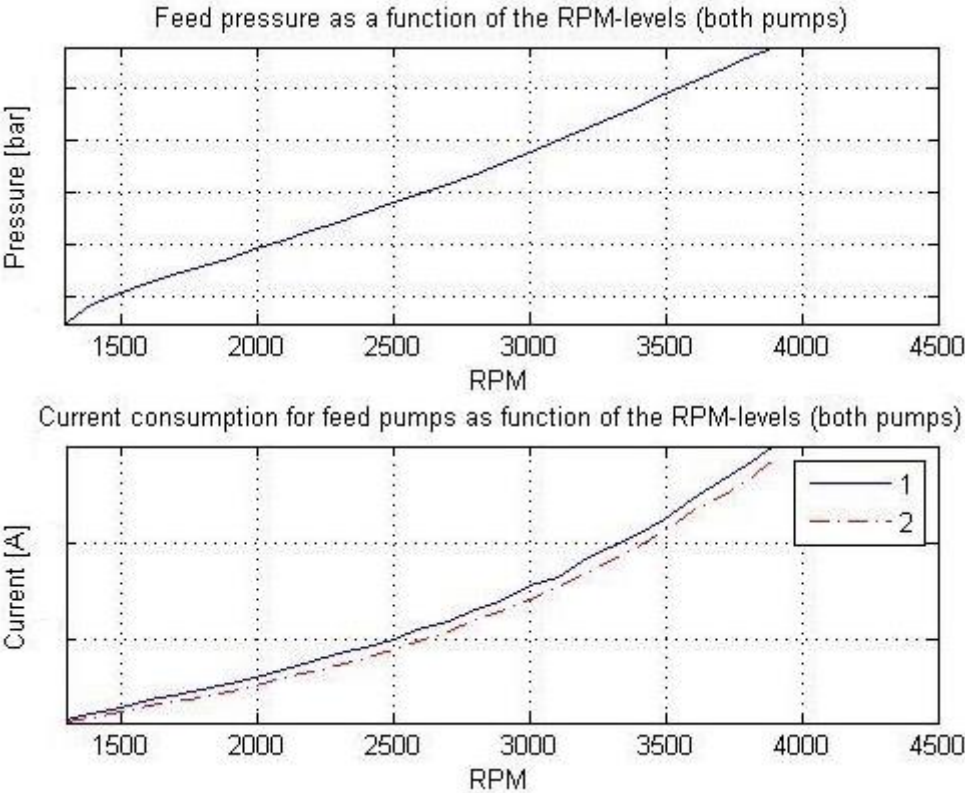


**Figure 4.14. Feed pressure and current consumption for the feed pumps when the ball valve, representing the IMV is slightly closed. In the lower graph, the blue and the red signal is from feed pump 1 and 2 respectively.**

## 5. RESULTS AND ANALYSIS FOR FAULTY SYSTEM BEHAVIOR

*In this chapter, the faulty system behavior results are presented and analyzed. Fault detection and isolation tests are then presented for each fault.*

As the normal behavior was tested and established in the previous section, it is now possible to investigate how the system behaves during faulty conditions, i.e. when a specific fault occurs. Different faults that have been identified and can occur during system operation are stated below.

- 5.1 Leak in pipe/hose between main feed-pumps and fuel filter
- 5.2 Leak in pipe/hose between transfer-pumps and pre-filter
- 5.3 Leakage on suction line to feed-pump
- 5.4 Leakage on suction line to transfer-pump
- 5.5 Open pre-filter
- 5.6 Open fuel filter
- 5.7 Clogged pre-filter
- 5.8 Clogged fuel filter
- 5.9 Stop in line between transfer pumps and pre-filter
- 5.10 Stop in line between fuel filter and high pressure circuit
- 5.11 Stop in line between feed pumps and fuel filter
- 5.12 Non-operating transfer-pump
- 5.12 Non-operating main feed-pump
- 5.13 Broken/stuck level sensor in main fuel tank
- 5.14 Broken/stuck level sensor in tech-tank
- 5.15 Transfer pumps are not shutting off
- 5.15 Feed pumps are not shutting off
- 5.16 Temp sensor in main-tank broken
- 5.17 Temp sensor in tech-tank broken
- 5.18 Pressure sensor(s) indicating wrong pressure (high, low)

To be able to compare the results of a normal system behavior and a faulty, the system will be controlled in the same way as for the normal behavior. When the system is operating, faults will be manually generated by manipulating the system components related to a specific fault. For some faults, test cases are not possible to apply in the developed rig and are therefore analyzed from a system experience perspective where the system behavior is also affected by the final chosen controller. After each performed analysis related to the results for a specific fault, suggested fault detection methods will be presented and discussed.

## 5.1 LEAK IN PIPE BETWEEN FEED PUMPS AND FUEL FILTER

The system was from start operating during normal condition. A leakage was then generated by manipulating the ball valve attached on a T-coupling in between the feed pumps and the fuel filter. The leakage occurs during 60 seconds and the leaked amount of fuel was then measured afterwards. Relevant signals worth investigating are those where a noticeable change occurs, which in this test are the feed pump current consumption, RPM levels and the feed pressures. This test was executed with the two different system controls that were described earlier. The useful data that was recorded during each test can be found in Figure 5.1 and Figure 5.2, respectively.

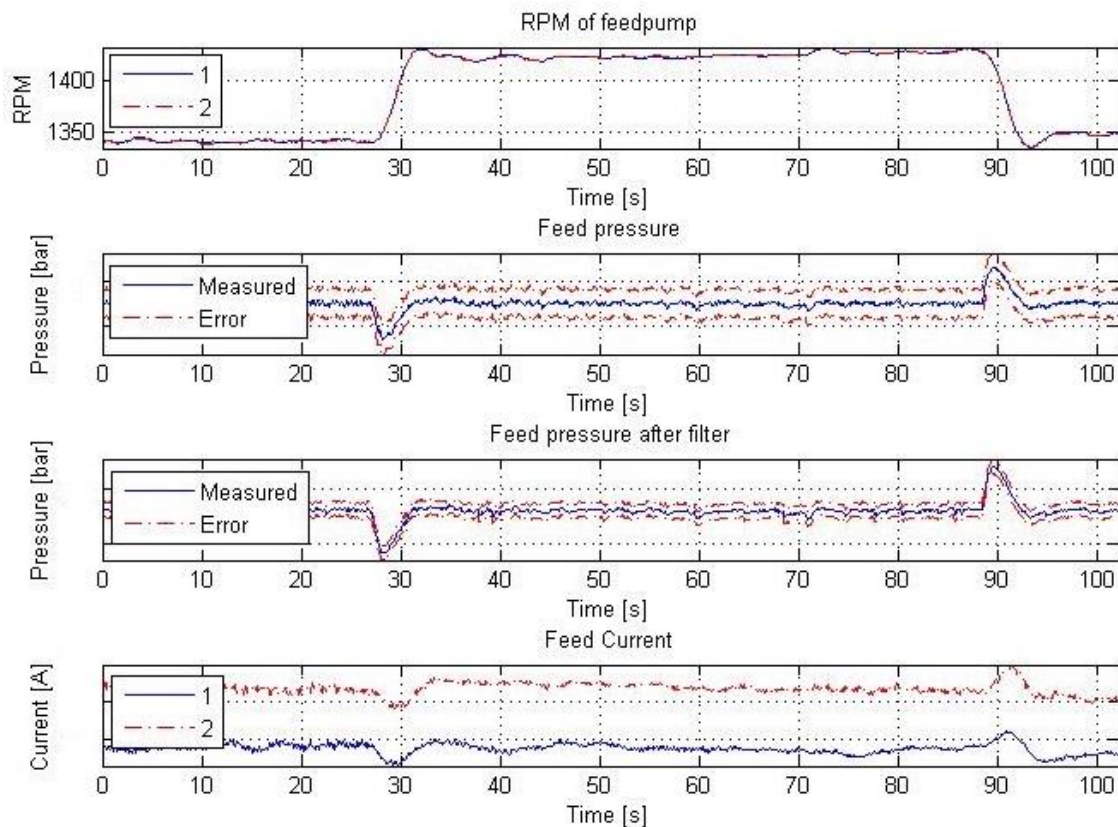


**Figure 5.1.** RPM levels, feed pressures and current consumptions during a leakage of  $\text{¥ l/min}$ , starting at  $t=28$  and ending at  $t=88$ . The feed pressure was controlled with a PI-regulator, replicating the normal behavior. For the RPM- and the current plot the blue signal is from feed pump 1 and the red signal is from feed pump 2.

As can be seen in Figure 5.1, the leakage is in this case visible in all of the presented signals since the usage of a relatively slow controller. As the feed pressure is controlled with a simple PI-regulator, the system pressure drop occurring is recovered from the leakage by increasing the control signal, i.e. the RPM level. The current consumption goes down because of the pressure drop but increases as the pressure level is recovered. Since the RPM level deviation is also depending on the fuel demand from the engine one cannot only use this for fault detection with an active controller. Further tests and analysis is therefore continued below.



The same leakage test was executed with a constant RPM level for the feed pumps and data can be found in Figure 5.2. Since there is no pressure regulator used in this second test, the pressure drops when the leakage occurs and does not recover from that level until the ball valve is closed. The same yields for the current consumption as the feed pumps will work with less resistance.

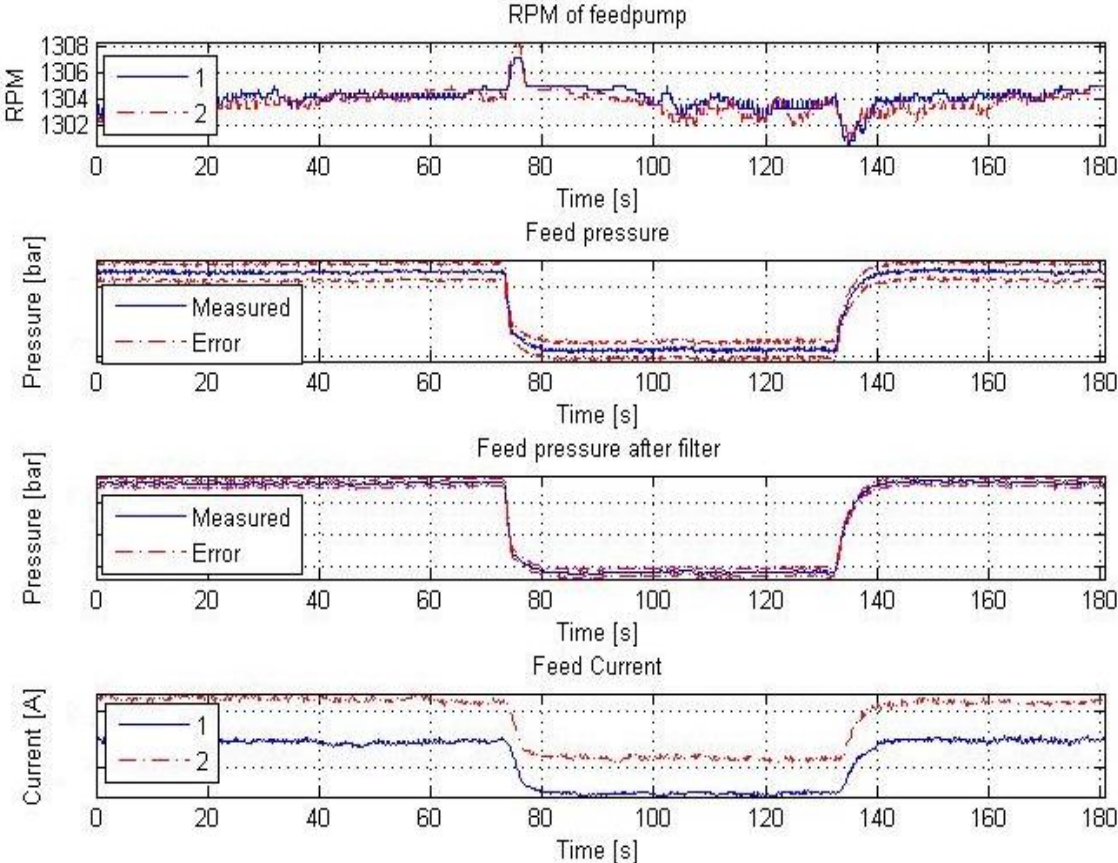


**Figure 5.2. RPM levels, feed pressures and current consumptions during a leakage of  $\xi$  l/min, starting at  $t=72$  and ending at  $t=132$ . The feed pumps RPM level is set to constant, 1305 RPM's, replicating the normal behavior. For the RPM- and the current plot the blue signal is from feed pump 1 and the red signal is from feed pump 2.**

To see how the fault affects the dynamic behavior a step from 1300- to 2300 RPM's was performed. The behavior for a normal case and the faulty case can be seen in Figure 5.3.

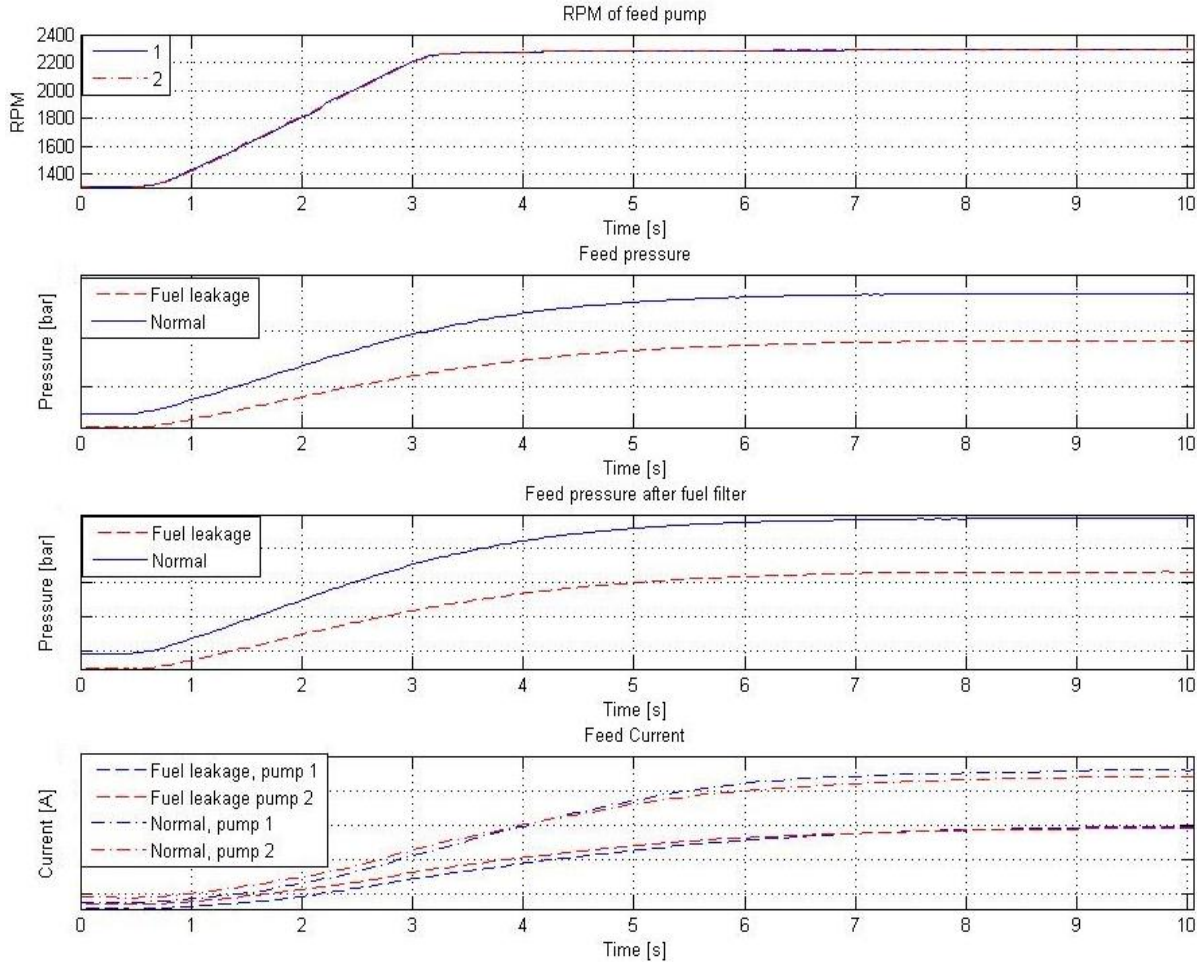


**Figure 5.3. RPM levels, feed pressures and current consumptions during a step from 1300- to 2300-RPM's. Behaviors during both normal and faulty conditions are presented.**

From the above figure, it can be seen that the static pressure difference between the normal and the faulty behavior is increasing with the RPM level. Several step response tests were therefore performed to determine the relationship of pressure as a function of the RPM level for both normal behavior and faulty behavior during a leakage. This can be seen in Figure 5.4 on the next page.

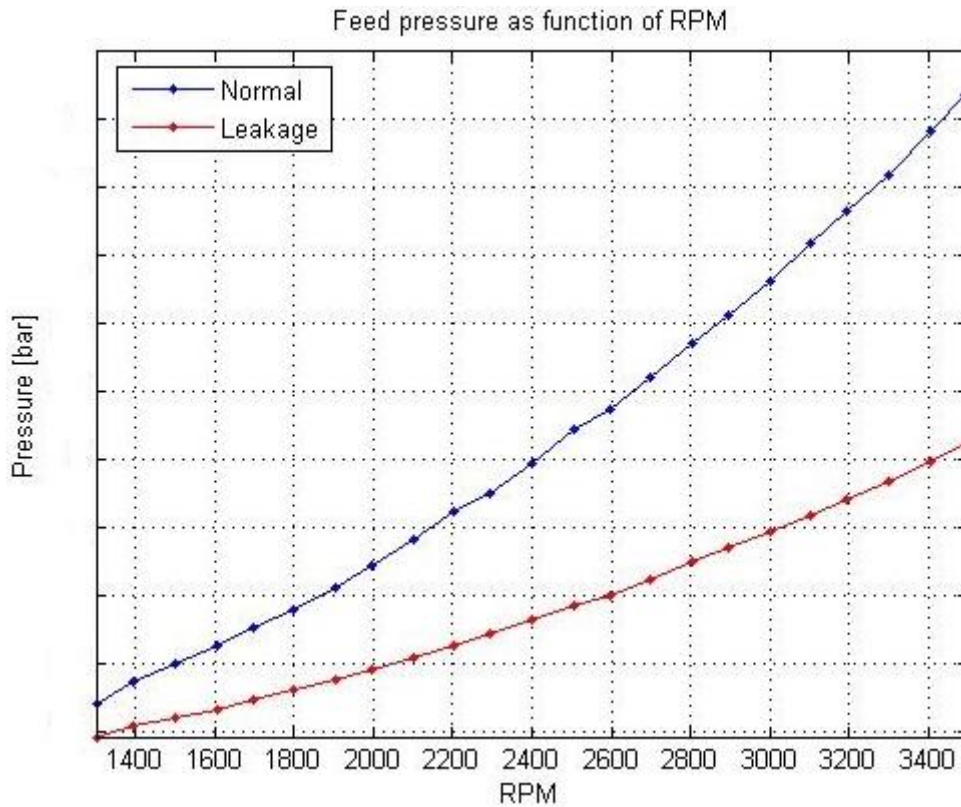


**Figure 5.4. The pressure as a function of the feed pump RPM-level during normal behavior (blue line) and the behavior during a larger leakage (red line).**

The above figure verifies that the error between the normal behavior and the behavior during a leakage is increasing with the RPM level. The leakage was however relatively large during this test which makes the error large for the lower RPM levels as well. If the leakage was smaller, the red line would move towards the blue line in the graph. Since the pressure sensor has a constant ratiometricity error, i.e. the error for the ratio between the output voltage and the applied supply voltage, smaller leakages is more easily revealed on higher RPM levels.

The step response test was also performed for different positions of the ball valve, representing the IMV, in order to investigate changes in the dynamics with respect to the size of the leakage and the ball valve position. A comparison between two tests with different ball valve position and leakage sizes can be seen in Figure 5.5.

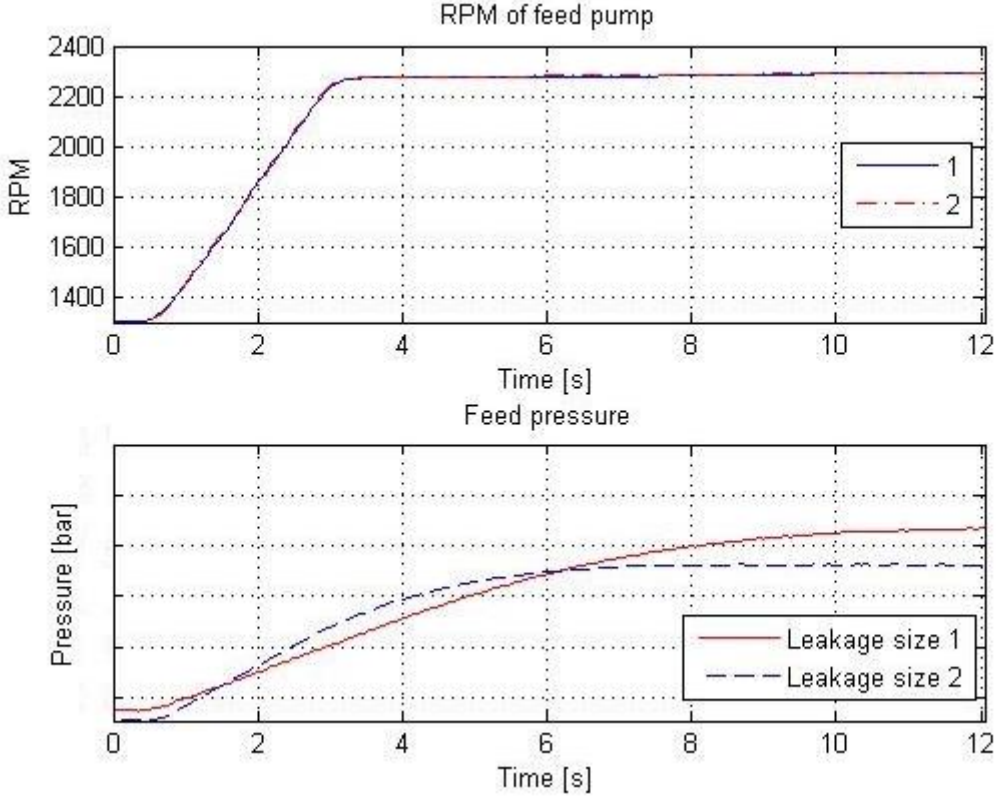


**Figure 5.5. RPM levels and feed pressure for two different leakage sizes, during a step from 1300 to 2300 RPM's. In the RPM graph, feed pump 1 and 2 is presented as blue and red, respectively.**

It is clear that the IMV demand and the leakage size affect the dynamics for the feed pressure increase as the rise time and the derivative changes. It is therefore not possible to detect a leakage by only using this information.

**Fault detection**

A leakage that occurs between the feed pumps and the fuel filter during a system operation where the normal system controller is active would cause the RPM level to be increased to maintain the demanded pressure level. If this type of fault shall be detectable with an active controller, one must know the relationship between the RPM level needed for maintaining the demanded pressure and the IMV fuel demand range.

There is another way to detect this fault when the original system controller is deactivated, which is by performing a separate test when the IMV is demanding the same amount of fuel, e.g. when the engine is running in a known mode. The fuel that is not consumed by the engine will then return to the tech-tank. The test should then increase the RPM level in steps and compare the saturated pressure level for each step with values that has been obtained during normal behavior, i.e. during the known mode with normal conditions. If the error between the pressures increases with the RPM level

a leakage is present. As the normal reference pressure with respect to each RPM level is depending on whether the filter is clogged or not, different reference pressures need to be established for this. As the leakage is more easily detectable on higher RPM-levels it is suggested that the test ends on the maximum RPM level. A simple flowchart of a suggested detection test algorithm can be found on the corresponding page in (Ellnefjård, 2014).

As can be seen in the algorithm shown above, the error between the measured pressure and the normal pressure has to increase with the RPM level in order to indicate a leakage. The error is compared to a variable that equals the last pressure error gained in previous RPM level and shall be initialized as two times the total pressure sensor error.

One must also consider that this can be caused by a pump with lowered pump performance, which is why the error detection limit must take this into account. The effect of a pump with lowered pump performance needs to be investigated in order to know that smaller leakages can be detected with confidence. This investigation is however not performed in this thesis. This can be detected with another test. If it turns out that the detection test is true, i.e. that there is a leakage present, the same test can be performed for each feed pump separately. If the relationship between the RPM level and the pressure level are the same for the two pumps, it is safe to say that there is no internal leakage in either of the pumps. If the result is different, the pump that gives the lowest pressure level has a lowered performance.

## 5.2 LEAK IN PIPE BETWEEN TRANSFER PUMPS AND PRE-FILTER

The behavioral test of this fault is very similar to the previous test; a leak was generated by opening a ball valve placed on a T-coupling attached in between the transfer pumps and the pre-filter. As in the previous leakage test, the ball valve was opened during 60 seconds and the leaked amount of fuel was measured afterwards. The test was first executed for three different RPM levels, 2000-, 1300- and 3000 RPM's. In Figure 5.6 the transfer pump RPM level, transfer pressure and the transfer pump current consumption is shown for the test with 2000 RPM's.

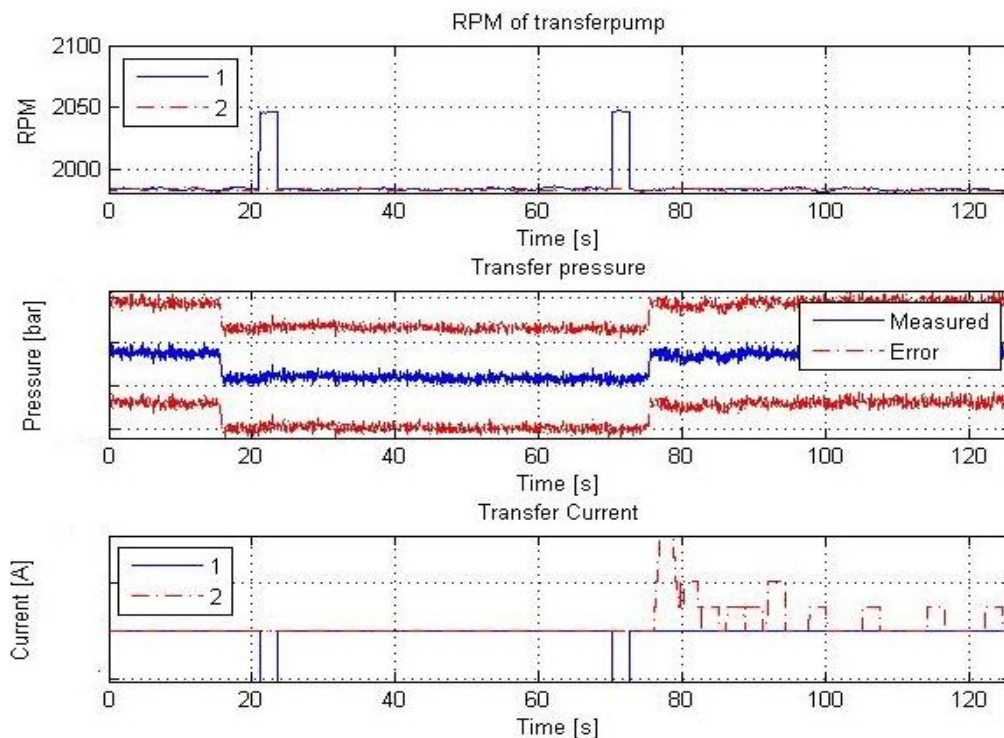


**Figure 5.6. RPM level of transfer pumps, transfer pressure, and current consumption for the transfer pumps. A leakage of  $\lambda$  l/min occurs at  $t = 12$  and ends at  $t = 72$ . For the RPM- and the current graph the blue signal is from transfer pump 1 and the red signal is from transfer pump 2.**

When the leakage occurs, the transfer pressure slightly drops and the internal controller in one of the transfer pumps increases the RPM level since the same amount of current is fed to the pump at a lower resistance, in that instant moment. Even though the leakage can be seen as a larger one, the pressure drop is too low and the current consumption only differs when opening and closing the ball valve. As can be seen, the change in RPM level and current consumption is only occurring for transfer pump 1.

It was realized that it was hard to interpret the data when different RPM levels for different positions of the ball valve was tested, resulting in different size of leakages and pressure drops. Another test was therefore designed, where the position for the ball valve was constant and the RPM levels were increased from 1300 to 3000 RPM's. This test did however show that smaller leakages did not affect the sensor and actuator signals at all.

Since it might not be possible to isolate this fault with only the static behavior, a test where the dynamics are in focus is needed. Therefore, a step response test was

performed during the presence of a leakage. The normal behavior and the faulty behavior, during the step from 2000 to 3000 RPM's, can be seen in Figure 5.7.

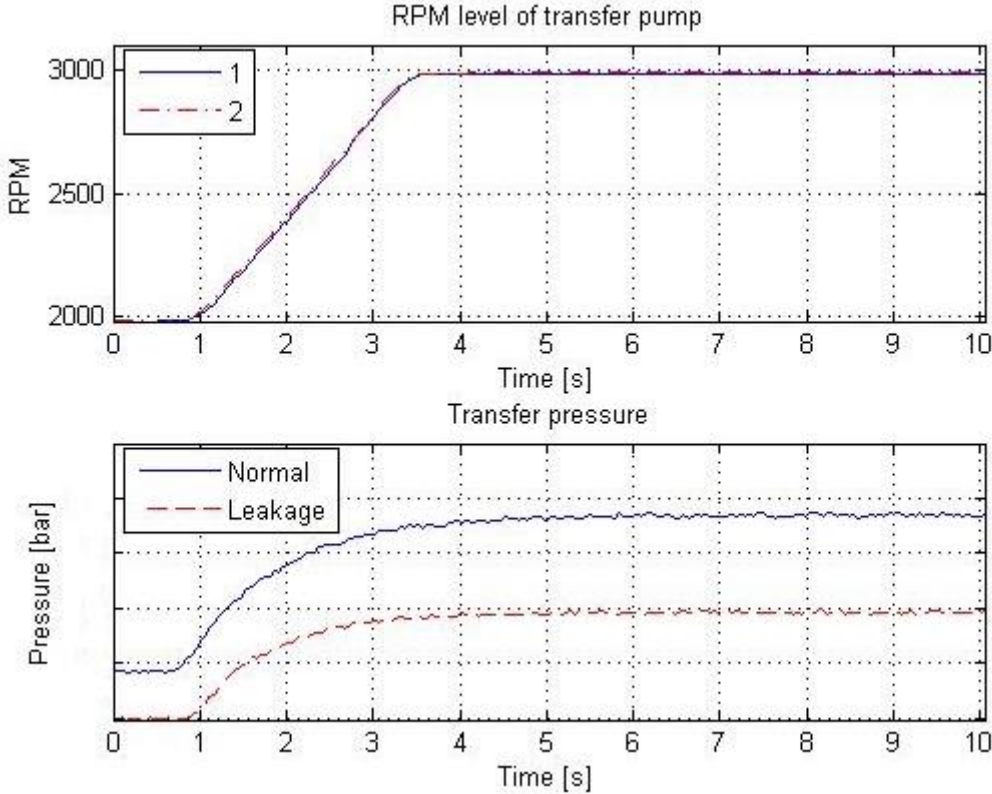


**Figure 5.7. RPM level of transfer pumps and transfer pressure, during normal conditions and when a leakage is occurs. For the RPM-level graph the blue signal is from transfer pump 1 and the red signal is from transfer pump 2. In the transfer pressure graph, the blue line is for the normal behavior and the red line is for the faulty behavior.**

As can be seen from the above step response comparison, the same phenomenon that was noticed for a leak occurring on the feed pump side with the pressure difference is present for this fault as well. Multiple step response tests were therefore performed in order to establish the pressure error as a function of the RPM level. The relationship for faulty and normal behavior can be seen in Figure 5.8 on the next page.

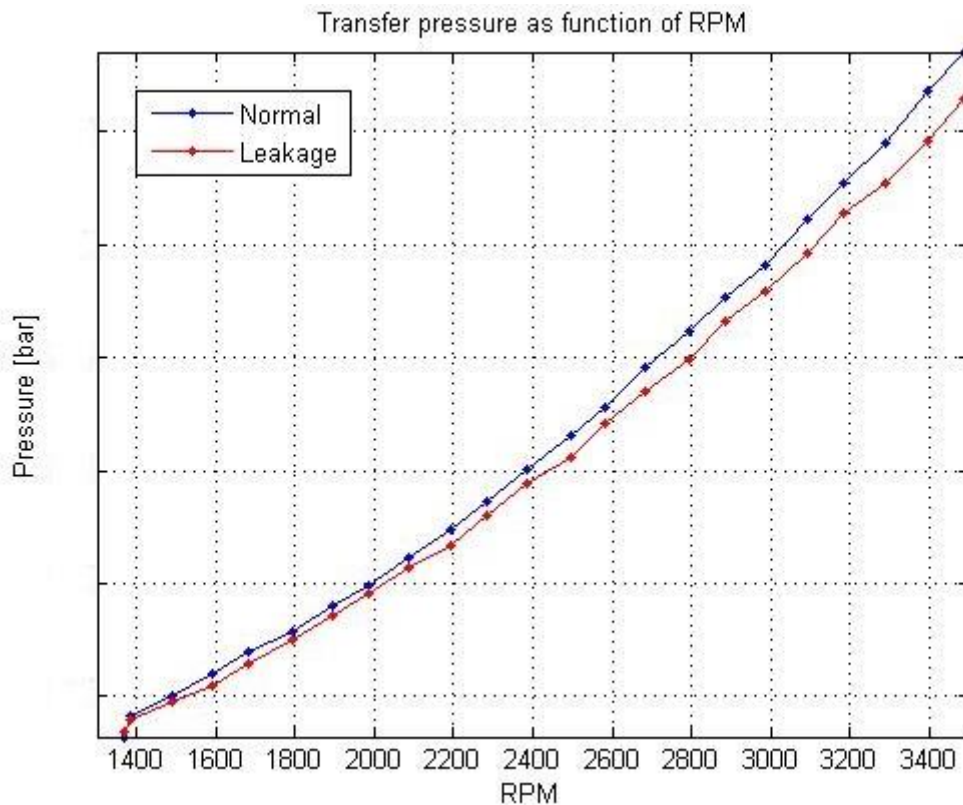


**Figure 5.8.** The pressure as a function of the transfer pump RPM-level during normal behavior (blue line) and the behavior during a smaller leakage (red line).

One can from this result draw a similar conclusion as was done for a leakage occurring on the feed pump side. The error between the normal and the faulty behavior is increasing with the RPM level. The amount of fuel that leaked during this test was  $\mu$  liters at 1300 RPM's which is a relatively small leakage.

### Fault detection

Detecting a leakage that occurs in between the transfer pumps and the pre-filter with the aid of the transfer pressure sensor and a simple detection limit is only possible for larger leakages. Another method for detecting this fault is by using the same principle that was suggested for detecting a leakage on the feed pump side, see test algorithm on the corresponding page in (Ellnefjård, 2014). The difference is that this test can be performed during system operation, as long as there is enough fuel in the tech-tank.

In the detection test, the RPM level would then be increased in steps and the saturated pressure level for each step would then be compared with an already obtained pressure collected during normal conditions. An increasing error would then indicate that a leakage has occurred. The algorithm is very similar to the one presented for detecting a leakage on the feed pump side and is therefore not presented once more. The reader is referred to the flowchart shown for detecting a leakage in between the feed pumps and the fuel filter.



As was discussed for a leakage that occurs on the feed pump side, one must in this case also consider the error that can arise from a pump with decreased performance and that the normal pressure level depends on how clogged the pre-filter is.

The above described detection methods are however only possible if a pressure sensor is used before the pre-filter. A third alternative method that does not include the pressure sensor would then be using the average RPM level that is needed for maintaining the demanded fuel level in the tech-tank. An average RPM level that is, with a larger margin, higher than the normal average would then indicate that a leakage is present. A pseudo code for this detection method is presented as (8) in (Ellnefjård, 2014).

This test is however not very efficient with respect to smaller leakages and requires excessive testing with an active controller before determining what a normal average is. One must also consider that this can be completely caused by a pump with decreased performance. This must in that sense be taken into account when determining the fault detection limit.

### 5.3 LEAKAGE ON SUCTION LINE TO FEED-PUMP

This test was performed by manipulating the suction line, so that air is mixed with the fuel during a normal behavior state, where the feed pumps operates at 1300 RPM's at a pressure at 6 bar. The data containing information of system behavioral changes is presented in Figure 5.9.

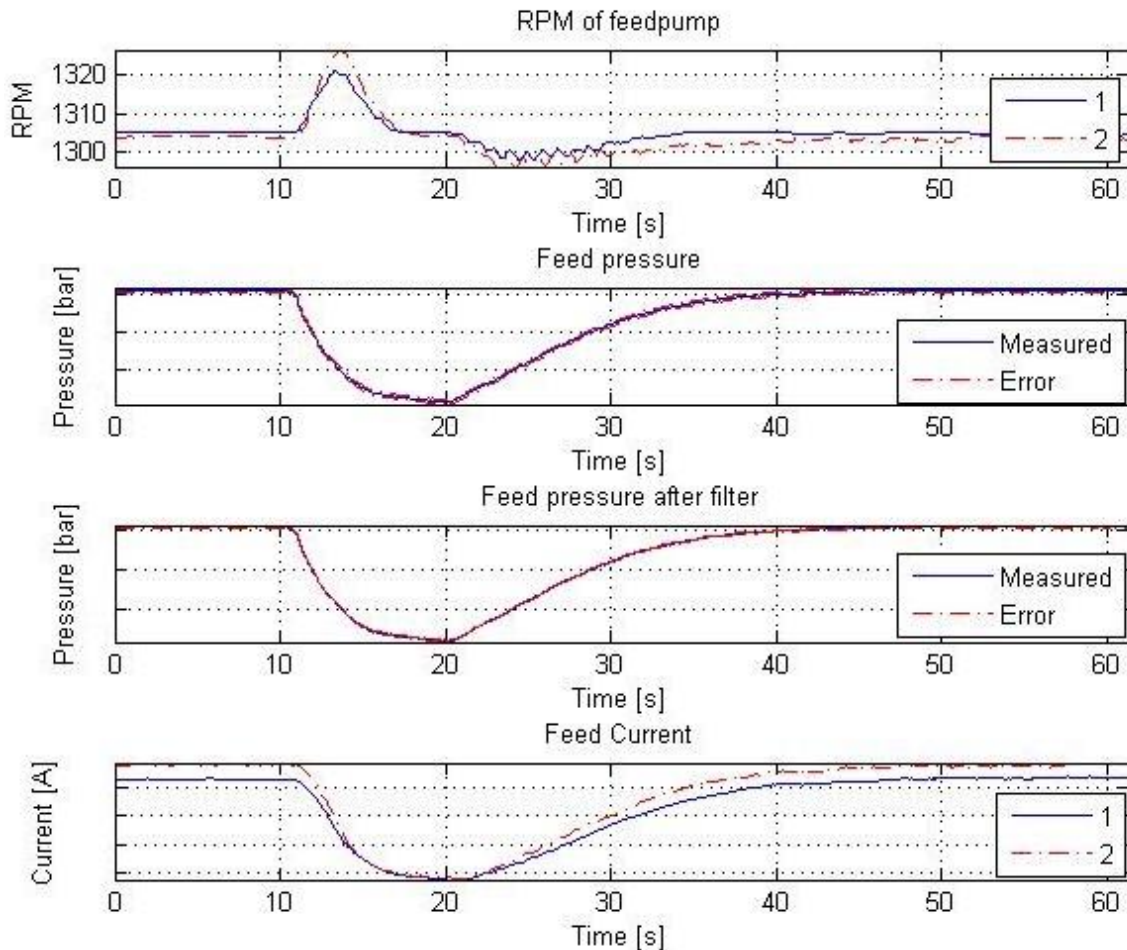


**Figure 5.9. RPM level of feed pumps, feed pressure before fuel filter, feed pressure after filter and current consumption for the feed pumps during a suction leakage at  $t = 11$ . For the RPM- and the current graph the blue signal is from feed pump 1 and the red signal is from feed pump 2.**

As can be seen in the graphs a major pressure drop occur in the system, both before and after the filter, when the air is mixed with the fuel inside the suction line. The resistance for pump work decreases and therefore lower energy consumption is required to maintain the same RPM level. The result is of course different if a controller is used for the pumps as RPM level will increase to maintain the demanded pressure level. This is shown in the next page.

In Figure 5.10, the feed pumps are controlled with a PI-regulator to maintain a pressure of 6,5 bar. In this case, the RPM level is increased by the controller to recover the correct pressure level when the fault occurs, which results in an increased current consumption. After 40 seconds, one can see that the amount of air in the suction line is increased as the RPM level increases once again. This is a result from the difficulties of keeping the suction leakage constant in the experimental rig.

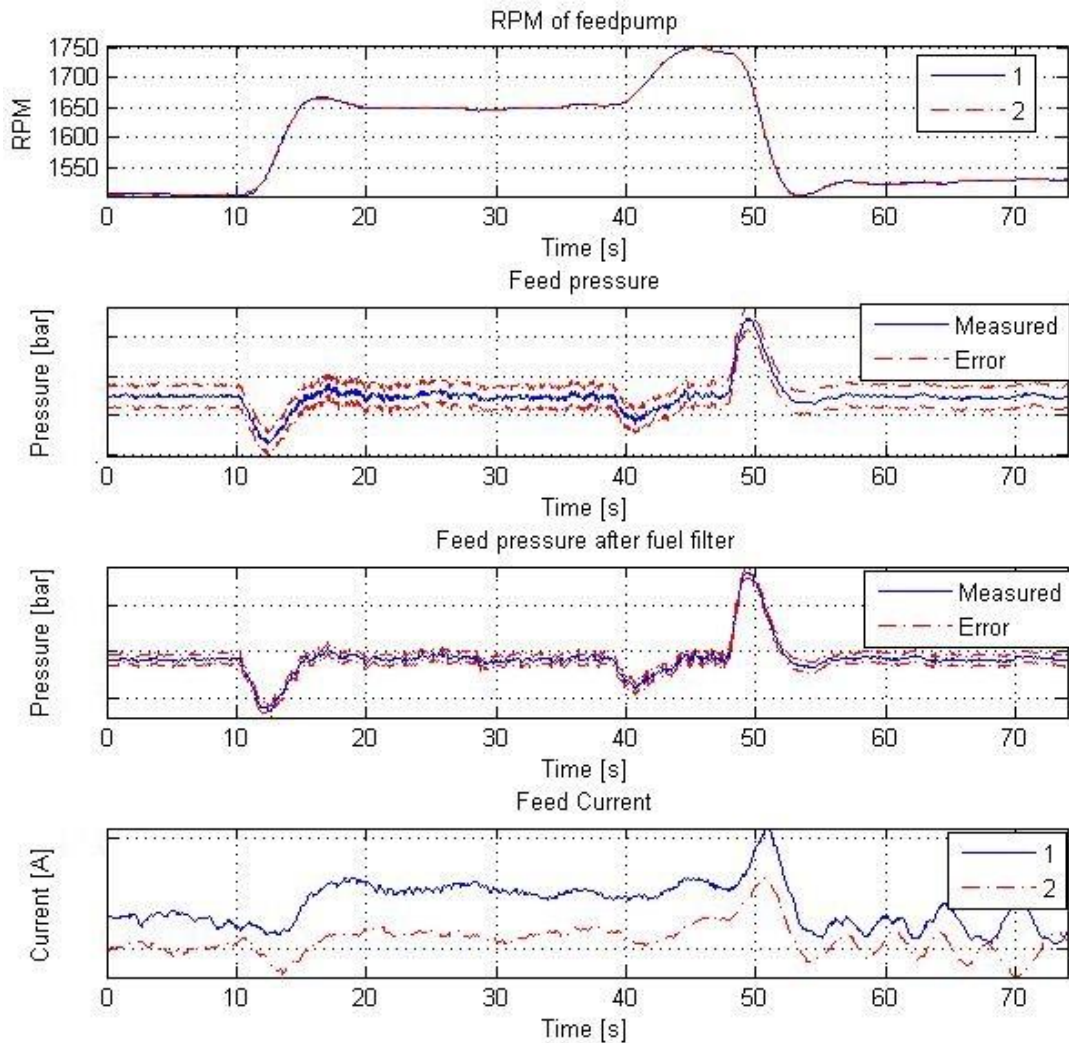


**Figure 5.10.** RPM level of feed pumps, feed pressure before fuel filter, feed pressure after filter and current consumption for the feed pumps during a suction leakage at  $t = 10$ . The feed pumps are controlled with a PI-regulator. For the RPM- and the current graph the blue signal is from feed pump 1 and the red signal is from feed pump 2.

In the feed pressure graph in the figure above, one can also see that the noise is larger than during the normal behavior due to the air bubbles present in the fuel lines which makes it possible to detect this fault by utilizing a high pass filter. The filtered feed pressure signal from the above test can be seen in Figure 5.11 on the next page.

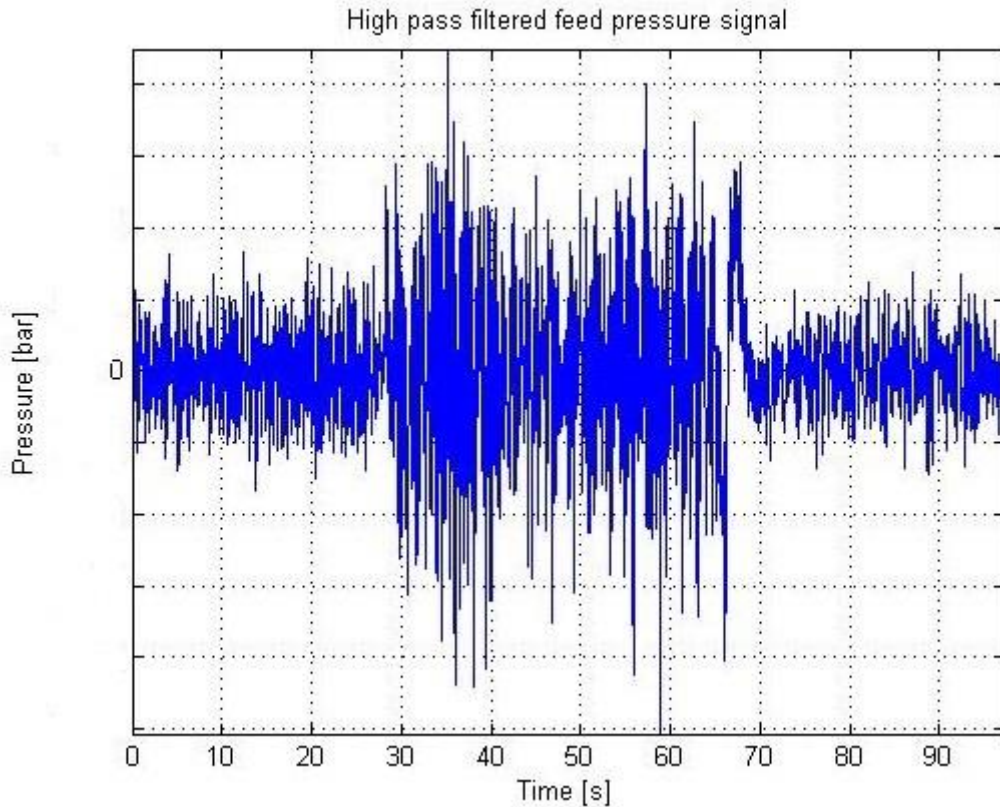


**Figure 5.11. The feed pressure signal after being filtered with a first order high pass filter.**

In the above figure, one can see that the amplitude of the noise is increased when there is a suction leakage present. This is of course one way of detecting this type of fault, which is further discussed under Fault detection. The filter that was used is a Butterworth high pass filter with a normalized cutoff frequency at  $\mu$  where the Nyquist frequency is  $\alpha$  Hz.

The behavior during a step was as for the other faults also investigated during a leakage on the suction line, which can together with the normal behavior be seen in Figure 5.12.

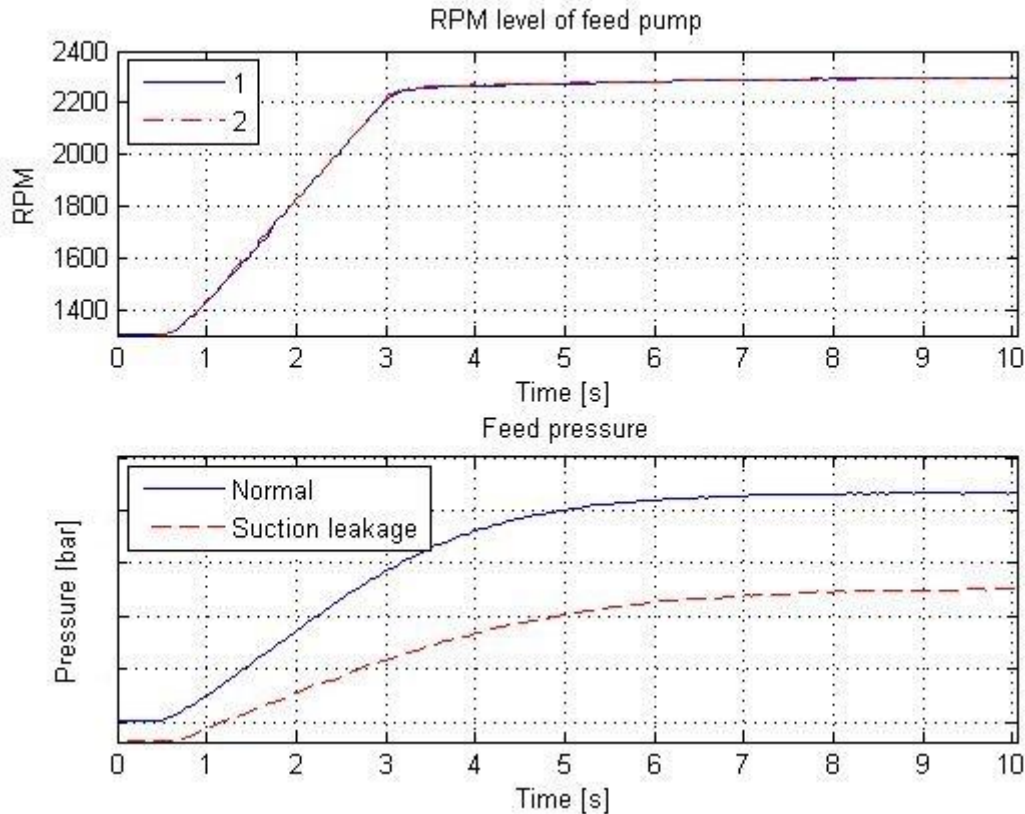


**Figure 5.12. RPM level of feed pumps and feed pressure during a step from 1300 to 2300 RPM's, for both normal and faulty conditions. For the RPM-level graph the blue signal is from feed pump 1 and the red signal is from feed pump 2. In the feed pressure graph, the blue line is for the normal behavior and the red line is for the behavior during a suction leakage.**

The slope of the pressure increase during the suction leakage is clearly different from the normal behavior but as it depends on other factors such as the IMV and the size of the leakage it will be hard to distinguish the fault from the dynamics with an active controller. For the fuel leakage faults that were discussed earlier it was proven that the error increases with the RPM level which is noticeable for this fault as well. The difference is that for this fault, the current consumption is lower than during the normal behavior which is not the case during a fuel leakage.

### **Fault detection**

In the above analysis there were three different detection methods that were mentioned.

The first suggestion was to utilize a similar detection test as suggested for the fuel leakages due to the quasi static behavior, i.e. the increasing pressure error with respect to the RPM level. To distinguish a fuel leakage from a suction leakage would then be possible by using the current consumption since it will be lower than normal during a suction leakage.

The second suggested detection test would be based on the noise in the signal as the amplitude increase is detectable during a suction leakage. To increase the robustness of

the detection test, the amplitude must be larger than the amplitude limit multiple times during a specific time period.

The third approach is more of an ad-hoc test that shall start if there is an amplitude change in the noise. Since the current consumption is lower when a suction leakage occurs, it can be compared with the normal consumption on the highest RPM level where it will affect the most.

The detection method will therefore use both of the two latter tests as the noise amplitude test can run during an active system controller and as the ad-hoc test only can be started in a separate mode. If the noise test is indicating abnormal amplitude levels the fault can be verified by running current consumption error test. The suggested noise detection test written in pseudo code can be found in (9), in (Ellnefjård, 2014). The current error test can as a flowchart be found on the corresponding page in (Ellnefjård, 2014).

## 5.4 LEAKAGE ON SUCTION LINE TO TRANSFER-PUMP

A test to investigate the system behavior during a suction leakage for the transfer pumps was executed with a RPM level of 3000 RPM's. As the operating pressure is lower for the transfer pumps than for the feed pumps, i.e. the pumps work with a lower fluid resistance, the only signal that showed an indication of a faulty behavior was the transfer pressure, which can be seen in Figure 5.13.

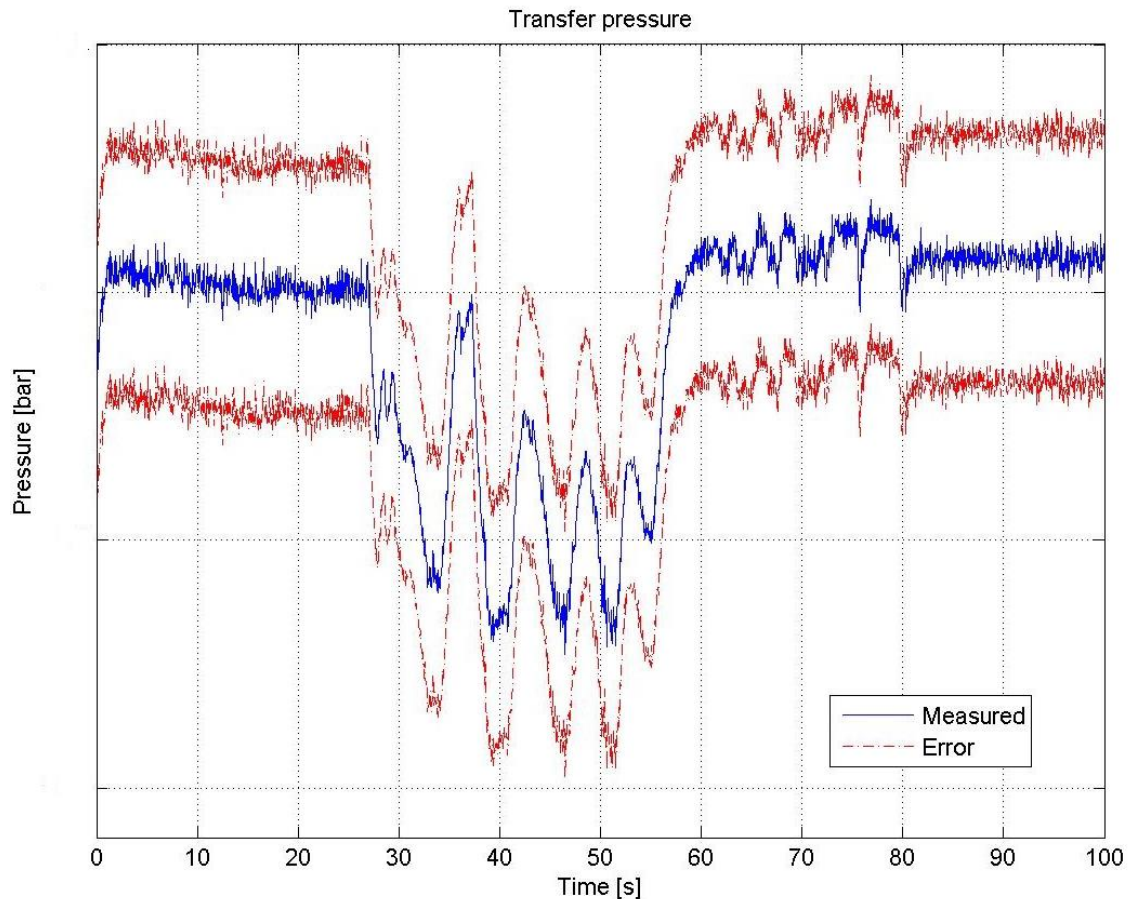


**Figure 5.13. Transfer pressure before pre-filter during a suction leakage, starting at  $t = 27$ . The blue signal is the measured one and the red describes the upper and lower error boundaries that depend on the temperature.**

As the fuel mixes with the air the pressure level drops and oscillates due to the fluctuating fluid resistance for the pumps. The size of the pressure drop is of course depending on how big the suction leakage is which was in this experimental setup not possible to measure. In the above test, it is also worth mentioning that the suction leakage was not constant which explains the pressure going up and down. As the suction leakage will most likely be constant in the real system another test was executed, from which the results can be found below.

A comparison of the pressure during a normal behavior and a faulty behavior, i.e. when there is a constant suction leakage on the line to the transfer pumps, can be seen in Figure 5.14

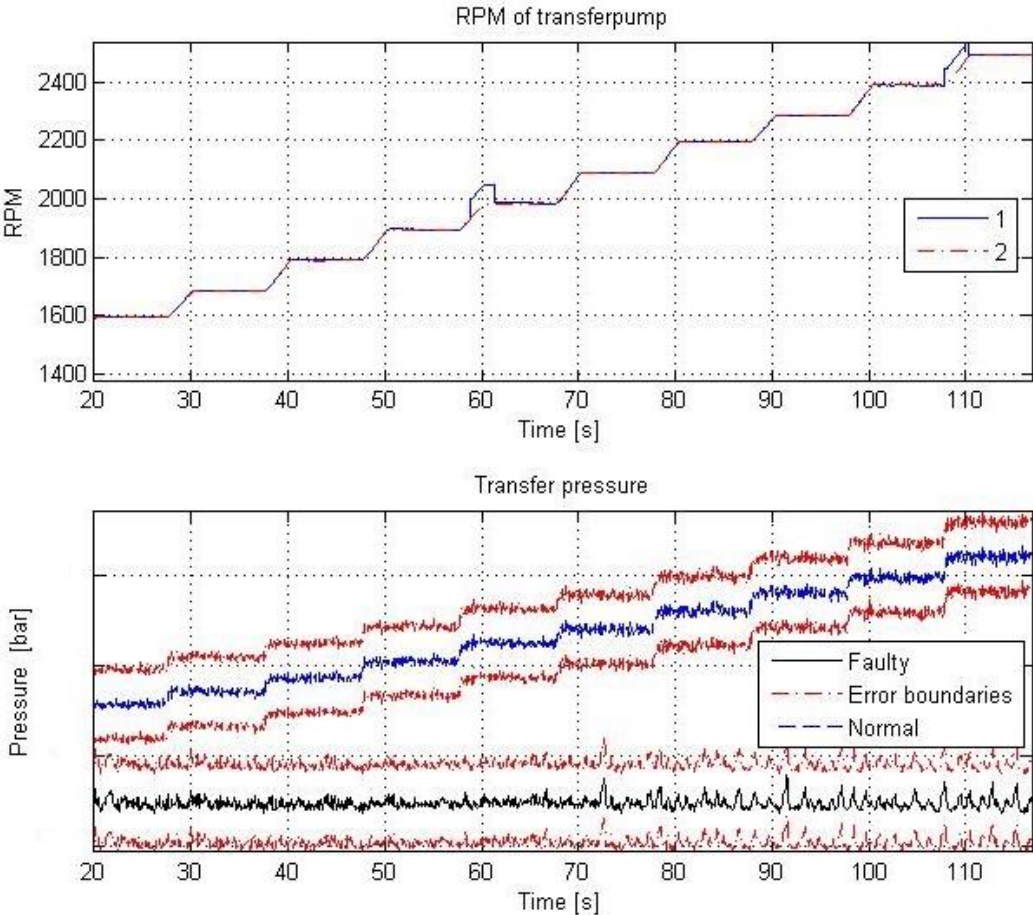


**Figure 5.14. The transfer pumps RPM-level and the transfer pressure, during normal (blue line) and faulty behavior (black line). The pressure is presented with error boundaries (red lines).**

From the above figure, one can see that the pressure does not increase since the suction leakage is very large. As was noticed for the fault leakage on suction line to the feed pumps, there is also different amplitude in the noise of the pressure sensor signal. A high pass filter can therefore be utilized for fault detection in this case as well.



In Figure 5.15 the transfer pressure and the filtered transfer pressure can be seen when a suction leakage occurs at  $t = 16$ . When the suction leakage is present it becomes detectable by the change in the noise which can be seen in the lower graph. The filter that has been used is Butterworth high pass filter with normalized cutoff frequency at  $\mu$ . The Nyquist frequency is in this case  $\alpha$  Hz.

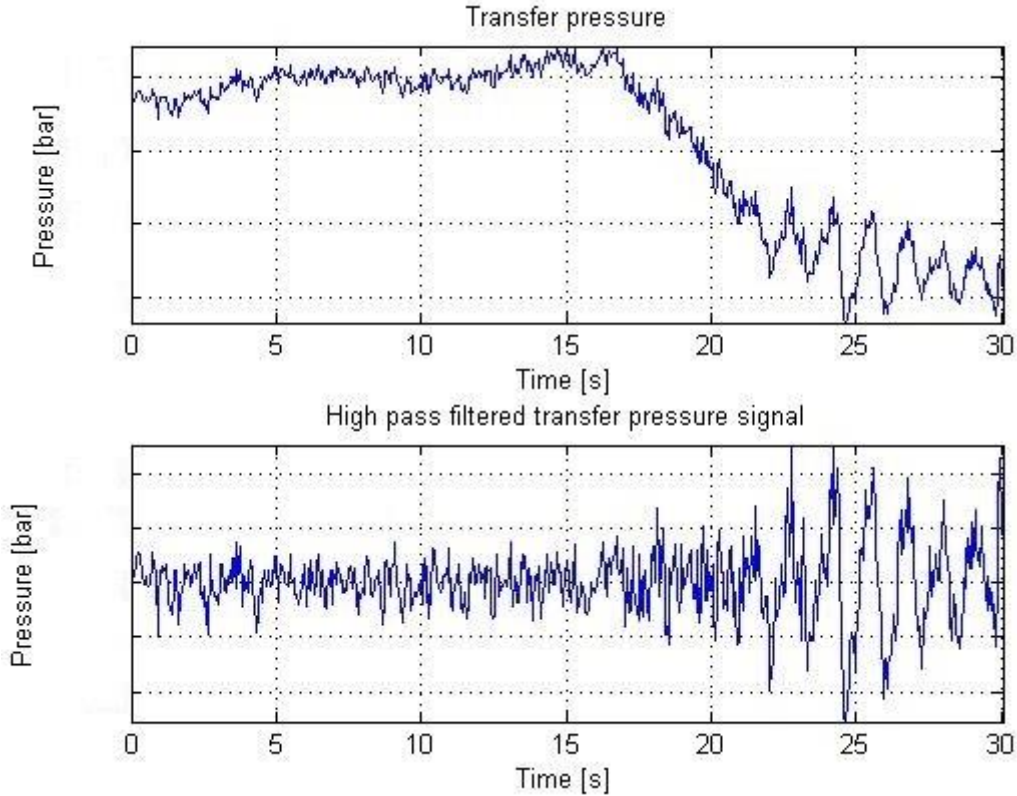


**Figure 5.15. The transfer pressure and the high pass filtered transfer pressure during normal behavior until  $t = 16$ , when a suction leakage occurs.**

From the above figure it is clear that a suction leakage can to the transfer pumps can be detected by looking at the noise amplitude. It is in this case doubled when the suction leakage is present. One can also see that there is another frequency in the noise signal after  $t = 22$ . Filtering the signal once more with a band pass filter and performing a FFT gives the result shown in Figure 5.16. The band pass filter has a lower cutoff frequency at  $\beta$  Hz and an upper cutoff frequency at  $\epsilon$  Hz.

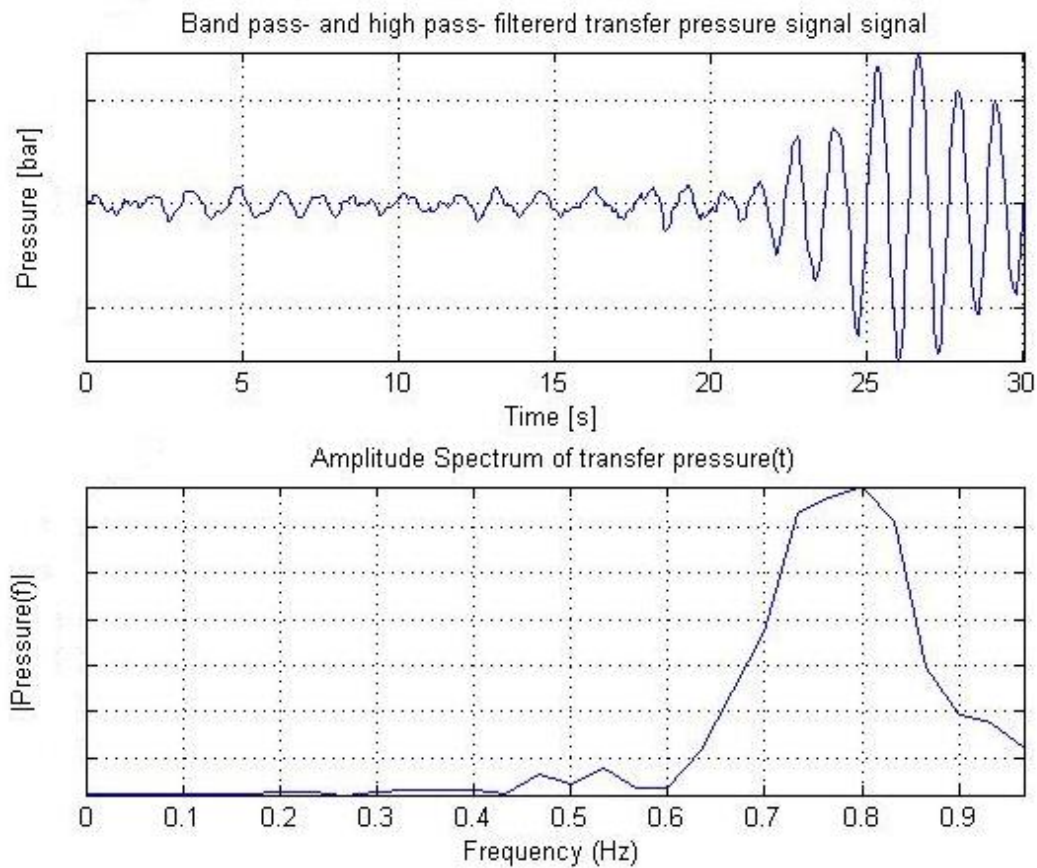


**Figure 5.16. Band pass- and high pass- filtered transfer pressure signal is presented in the top graph. The FFT result is presented in the lower graph.**

In the above figure, one can clearly see that the frequency that is occurring during a suction leakage is fully possible to distinguish and is therefore useful for detecting a suction leakage. This is further discussed under Fault detection.

As for the other faults, it is also important to investigate what information that can be retrieved from the dynamic behavior, in this case a step response.

The transfer pressure behavior for a step from 2000 to 3000 RPM's can for the normal behavior and the behavior during a leakage on the suction line be seen in Figure 5.17.

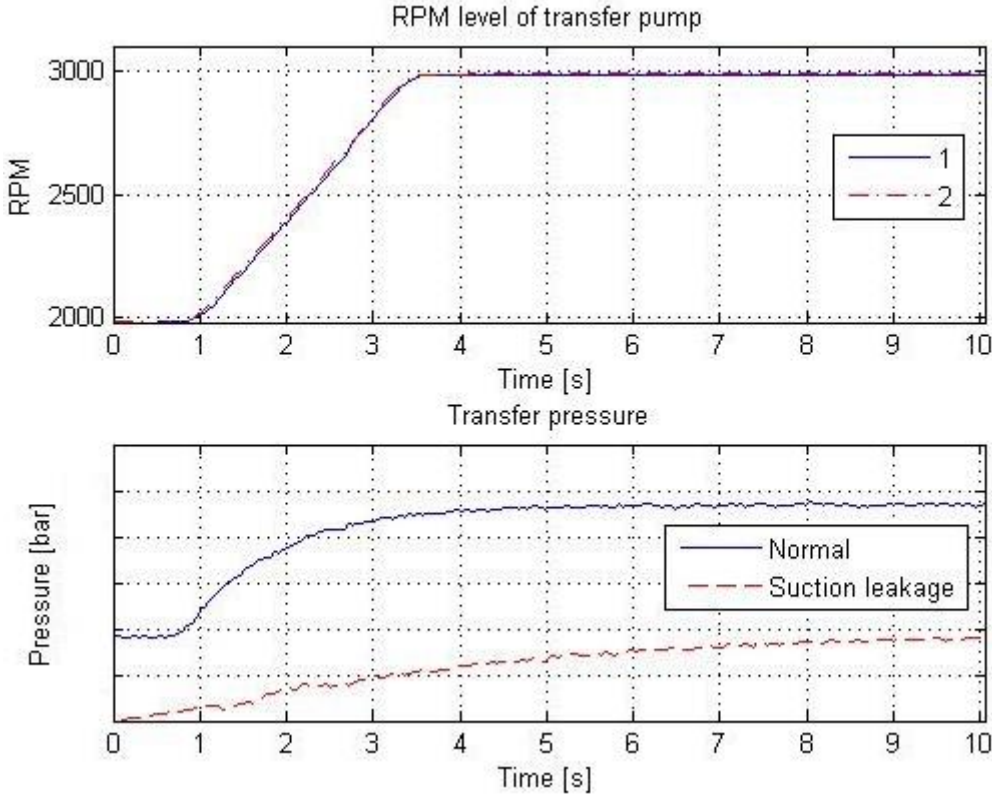


**Figure 5.17. RPM level for transfer pumps and transfer pressure before pre-filter during a step, for both normal and faulty behavior. For the RPM-level graph the blue signal is from transfer pump 1 and the red signal is from transfer pump 2. In the transfer pressure graph, the blue line is for the normal behavior and the red line is for the faulty behavior**

From the step response comparison it is clear that the dynamics are different from the normal behavior during a suction leakage. The suction leakage was in this case relatively large and thus the big difference from the normal behavior. In this case, the derivative is much smaller during the pressure increase and therefore a longer rise time. This information can be utilized for fault detection but is difficult during an active system controller.

**Fault detection**

To detect a leakage on the suction line for the transfer pumps it was in the above analysis suggested to use the noise in the signal or the rise time difference during step responses. On the feed pump side it was suggested to run the pressure and current error test to detect this type of fault which might make the reader wondering why this test cannot be utilized in the same way for this case as well. The reason for this is that the current consumption is much smaller for the transfer pumps as the operating pressure is lower. As was mentioned earlier in the report, the current consumption signal also has a lower resolution, due to the CAN communication, during lower current consumptions levels. Even though the changes in the current consumption level is smaller for this fault

it should still be possible to see a static difference on the highest RPM level for the transfer pumps.

The best way to detect this fault is by using the noise amplitude increase that occurs during a suction leakage. This type of fault detection could also be running constantly as it does not depend on the active controller. This fault detection test would be identical with the one that was suggested for detecting suction leakage for the feed pumps. The noise detection test is written and presented as the pseudo code in (10), in (Ellnefjård, 2014).

If the above test is triggered as true, i.e. that there is abnormal noise in the signal, a second test can be executed to verify that this fault is present. There are two different ways for establishing this.

In the first suggested test, the rise time of the pressure increase is compared with the normal rise time, when the transfer pumps are making a step from the lowest RPM level to the highest. Since the RPM level will be set to maximum, a static comparison between the current consumptions will be performed as well. It might not be necessary to test both the rise time and the current consumption to verify the presence of this fault. This can however be easily modified after testing both of the detection methods. A flowchart for this detection test that includes testing of both the current consumption and the rise time can be found in a figure on the corresponding page in (Ellnefjård, 2014).

The noise and the rise time is however only possible to utilize if there is a pressure sensor located before the pre-filter. For some of the suggested system layouts, this is not the case. There are two other ways for detecting this fault. Either by using the current consumption for the transfer pumps but without the rise time test or with the aid of a tech-tank level model. This model is based on integrating the flow entering and leaving the tech-tank and is described in the other master thesis project that focusing on the control algorithms for the system.

The second suggested test is only functional with a present transfer pressure sensor as it includes further investigation of the pressure signal. It was shown that the pressure oscillates with a frequency around 1 Hz during a suction leakage which can be detected by using a band pass filter, performing a FFT or both. If only the band pass filter is used, the detection test will be identical to the earlier presented noise amplitude detection test. This can however be a bit dangerous since it might be possible that other frequencies can appear during a suction leakage. It is therefore more certain to perform a FFT which can detect abnormalities in the whole frequency spectrum.

## 5.5 OPEN PRE-FILTER

To test how the system behaves when the pre-filter is open a test was executed where the filter was opened during a system operation. The test was performed with a transfer pump RPM level of 1300- and 3000- RPM's. The only signal indicating that a faulty system behavior was during these tests the transfer pressure. The transfer pressure from the test performed with 1300 RPM's can be found in Figure 5.18.

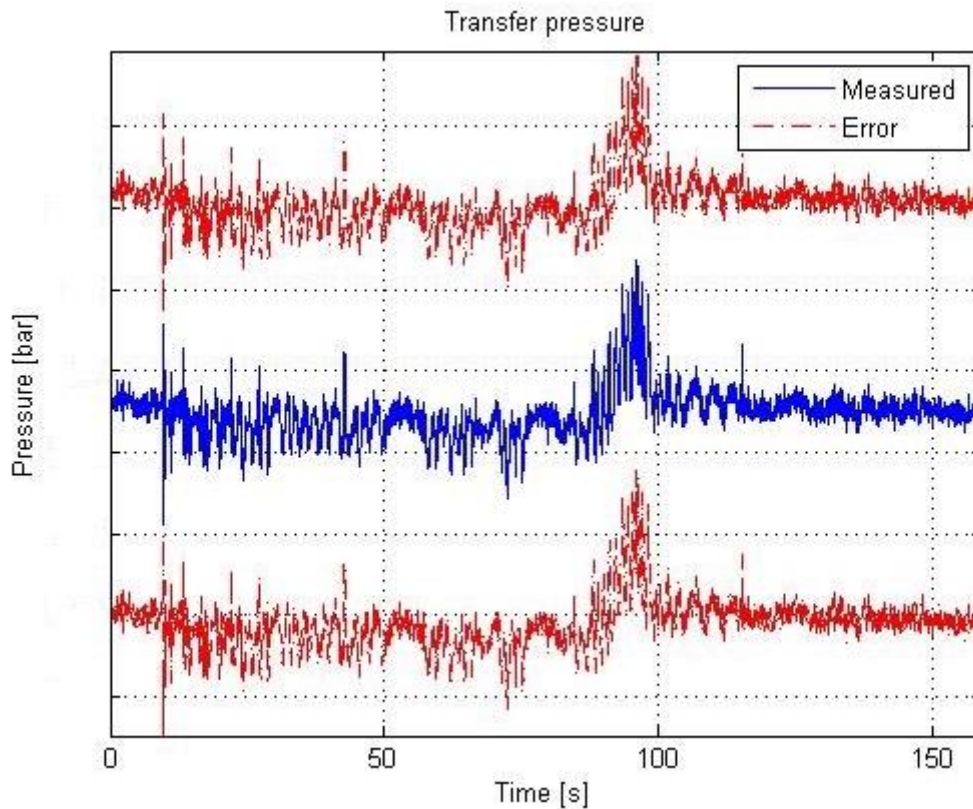


**Figure 5.18. Transfer pressure before pre-filter during open pre-filter, opened at  $t = 10$  and closed around  $t = 90$ . The blue signal is the measured one and the red describes the upper and lower error boundaries that depend on the temperature.**

The transfer pressure is only slightly lowered but there is noticeable change in the signal noise since having the filter opened allows the hydraulic circuit to be more affected by the fluctuations from the pumps. These are more damped when having the filter completely closed. This can, as for some of the other faults, be detected by high pass filtering the signal and compare the amplitude of the noise. The first thirty seconds of the above figure can after being filtered with a first order high pass filter be seen in the lower graph in Figure 5.19 on the next page. The used high pass filter is the same as has been used for detecting the other faults with the noise, i.e. with a normalized cutoff frequency at  $\mu$  with the Nyquist frequency at  $\varepsilon$  Hz.

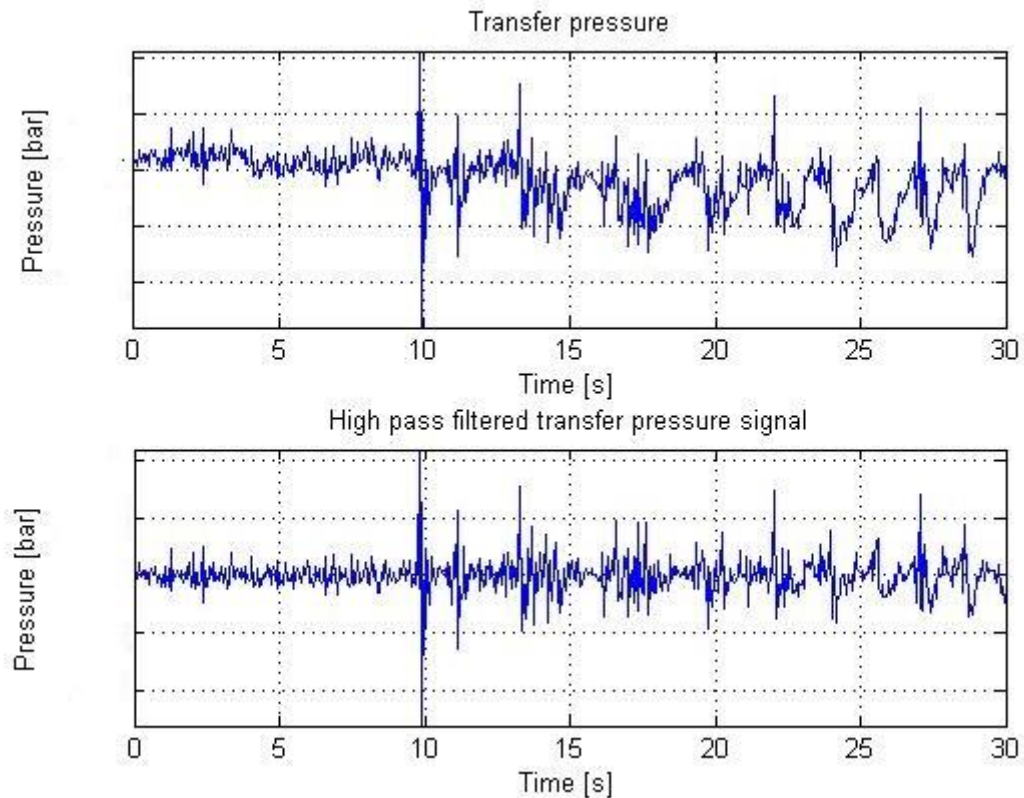


**Figure 5.19. The transfer pressure signal in the top graph and the high pass filtered signal in the lower graph. An open pre-filter occurs at  $t=10$ .**

From the above figure it is very clear that after  $t = 10$  when the pre-filter is open, the amplitude of the noise is larger than normal. The difference between the noise during an open pre-filter and a suction leakage is that there is no frequency change during an open fuel filter as the case is for a suction leakage. A suggested method for detecting this fault will therefore also be by using the noise in the transfer pressure signal. The same signal characteristics were interpreted from the test with 3000 RPM's.

The transfer pressure behavior for an open pre-filter compared with the normal during a step from 2000 to 3000 RPM's can be found in Figure 5.20.

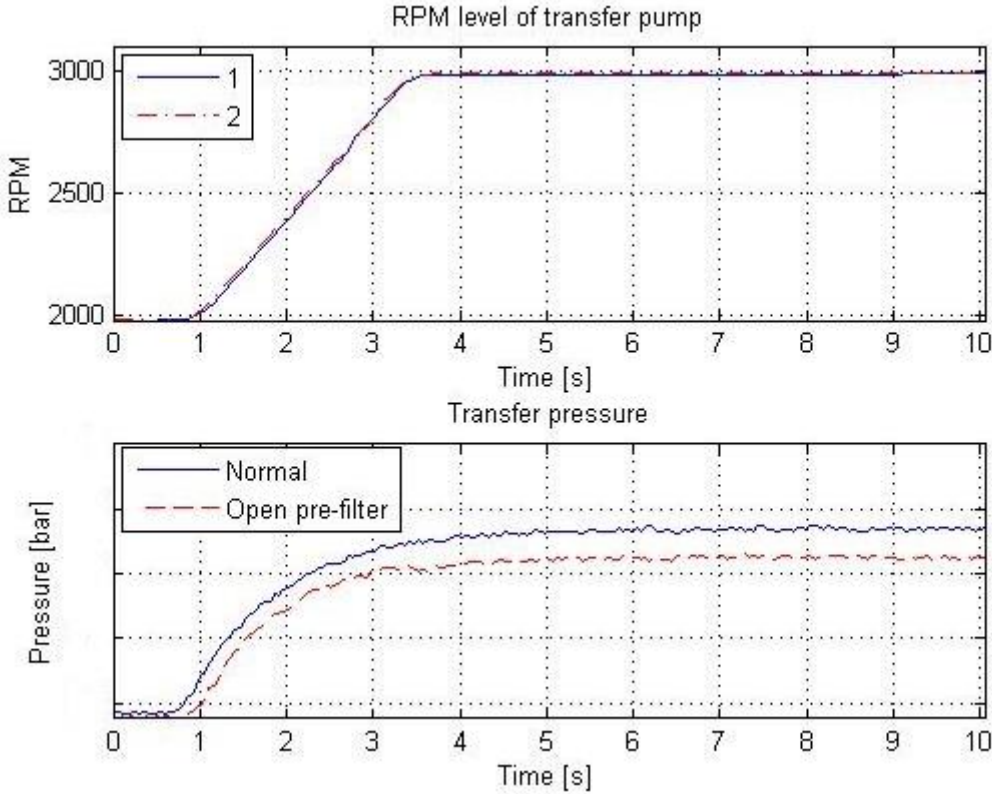


**Figure 5.20. RPM level for transfer pumps and transfer pressure before pre-filter during a step, for behavior during normal conditions and behavior during an open pre-filter. For the RPM-level graph the blue signal is from transfer pump 1 and the red signal is from transfer pump 2. In the transfer pressure graph, the blue line is for the normal behavior and the red line is for the faulty behavior.**

The characteristics of the step response with an open pre-filter is very similar to the normal case and does not provide any useful information more than the static pressure differences which is in this case smaller than the error boundaries for the pressure sensor. The open pre-filter fault is very similar to the fuel leakage except for the noticeable noise change in the pressure signal.

**Fault detection**

As was discussed above, an open pre-filter is very similar to a fuel leakage as it will cause the pressure to slightly drop, depending on how open the filter is. The quasi static behavior that has been analyzed for other faults will in this case be noticeable as well, i.e. the error between the normal pressure and the measured will during an open pre-filter increase with the RPM level. One can say that an open pre-filter is a combination of a fuel leakage and a suction leakage since a suction leakage on transfer pump line also caused an amplitude increase in the transfer pressure noise.

With the above in mind, the best way to detect this fault and still be able to keep full fault isolation, the fault shall first be detected by the change in the pressure noise. This will also be triggered if a suction leakage is present but one can still distinguish the faults by utilizing one of the isolation methods described in the fault detection section for a suction leakage. To clarify this, the faults can be isolated by either using one of the below stated methods.

- The rise time and the current consumption on the maximum RPM level.
- By filtering the signal once more but with a band pass filter or performing FFT.

The difference between these faults is stated below.

- A suction leakage will cause the rise time to be longer and the current consumption will be less than normal on the maximum RPM level. The noise will also oscillate with a frequency around 1 Hz.
- For an open pre-filter the rise time and the current consumption on the maximum RPM level will be close to normal. The signal will contain the frequency around 1 Hz but not near the same amplitude level.

The first detection test will therefore be the same noise amplitude test that is being performed for detecting a suction line leakage, which is written in pseudo code in (10), in (Ellnefjård, 2014). This will then cause one of the above isolation tests to start.

The isolation test that is including the rise time and the current consumption is presented on the corresponding page in (Ellnefjård, 2014) and needs a separate mode for starting. If this test turns out to be true there is a suction leakage present and if not there is an open pre-filter.

If using a band pass filter or a FFT for isolating the faults the test can be started whenever needed, i.e. during an active normal controller.

The above detection test for this fault is however only possible if using a pressure sensor before the pre-filter, which is not the case for all of the system layouts.



## 5.6 OPEN FUEL FILTER

Tests and analysis was also performed when the fuel filter is open. The test was performed on 1300- and 2000- RPM's with a pressure of six bar. The RPM levels, the pressure before the fuel filter, the pressure after the filter and the current consumption can for the test with 1300 RPM's be seen in Figure 5.21.

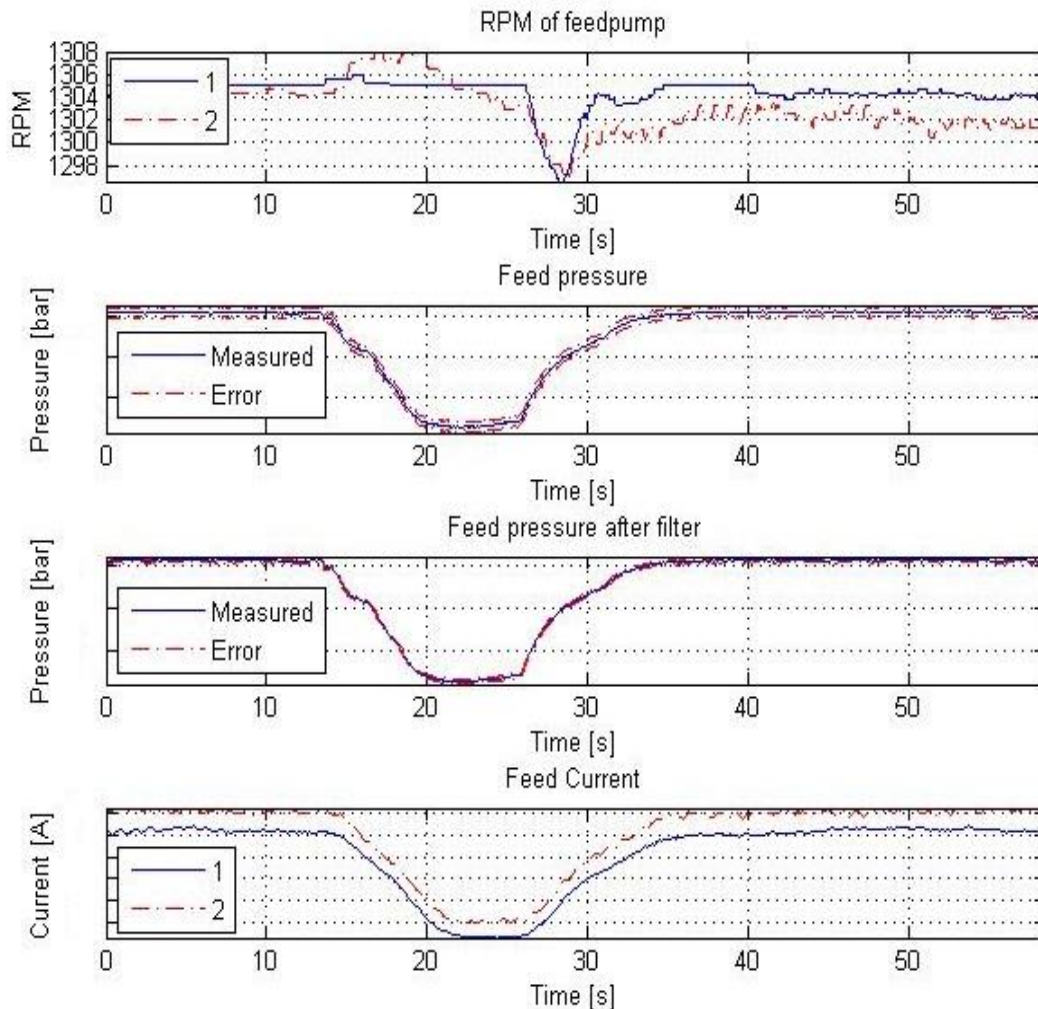


**Figure 5.21.** RPM level of feed pumps, feed pressure before fuel filter, feed pressure after filter and current consumption for the feed pumps with an open fuel filter, opened at  $t = 14$ . The filter is then closed at  $t = 26$ . For the RPM- and the current graph the blue signal is from feed pump 1 and the red signal is from feed pump 2.

The feed pressure drops both before and after the fuel filter when the filter is opened, which also yields for the current consumption as the pump workload is lowered. The data from the test with 2000 RPM's showed similar results.

To see how the system behaves when the feed pumps are pressure controlled another test was performed with the PI controller. The result can be seen in Figure 5.22.

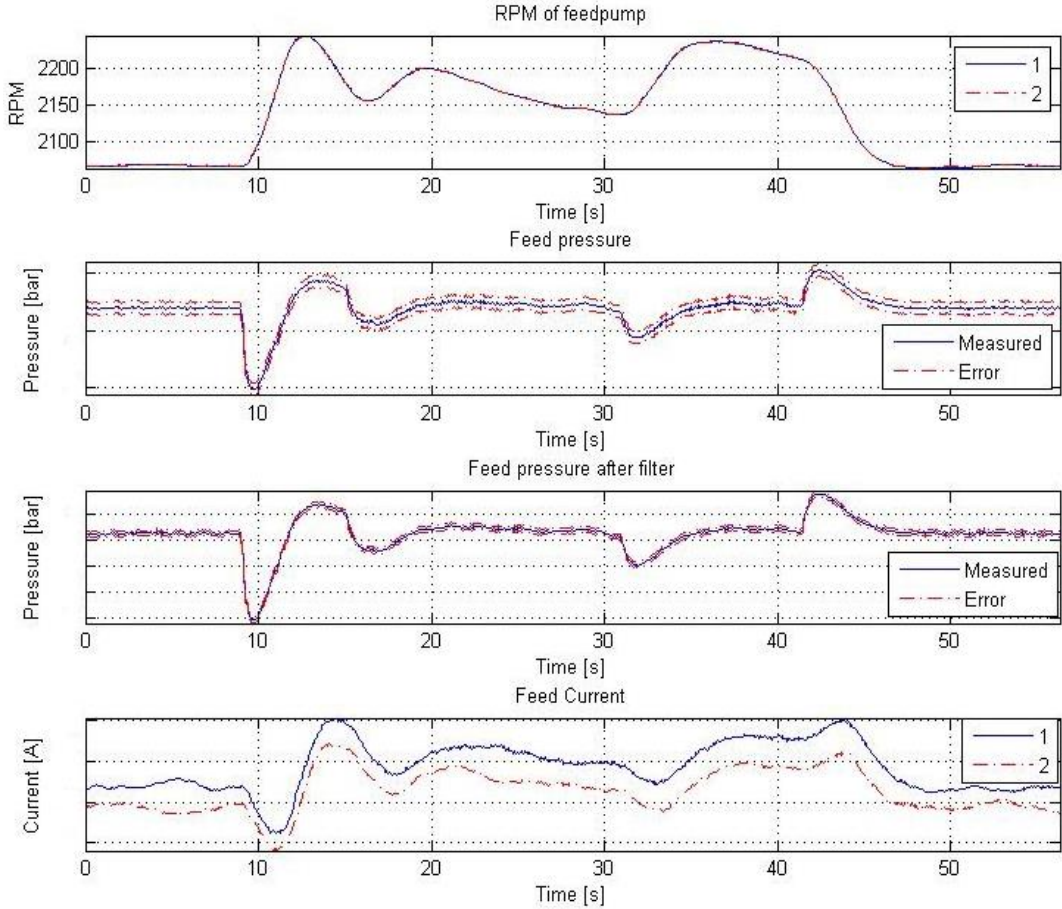


**Figure 5.22. RPM level of feed pumps, feed pressure before fuel filter, feed pressure after filter and current consumption for the feed pumps with an open fuel filter, opened at t = 9. The filter is then closed at t = 41. For the RPM- and the current graph the blue signal is from feed pump 1 and the red signal is from feed pump 2.**

As can be seen, the RPM levels for the two feed pumps are increased in order to maintain the demanded pressure level of 5-10 bar. The behavior is very similar to the ones during a leakage on the suction line and during a fuel leakage in between the feed pumps and the filter in Figure 5.10 and Figure 5.1 respectively. An investigation of the noise change was also performed for this fault and it was shown that there is a change in the noise amplitude for this fault as well. There is however no possibility to separate the noise between a suction leakage and an open fuel filter, which is why further isolation test are needed. This will be suggested and discussed in the fault detection section for an open fuel filter.

As for the other faults presenter earlier, the behavior during a RPM step from 1300 to 2300 RPM's is compared with the normal behavior in Figure 5.23 in order to find more useful information for the fault detection method.

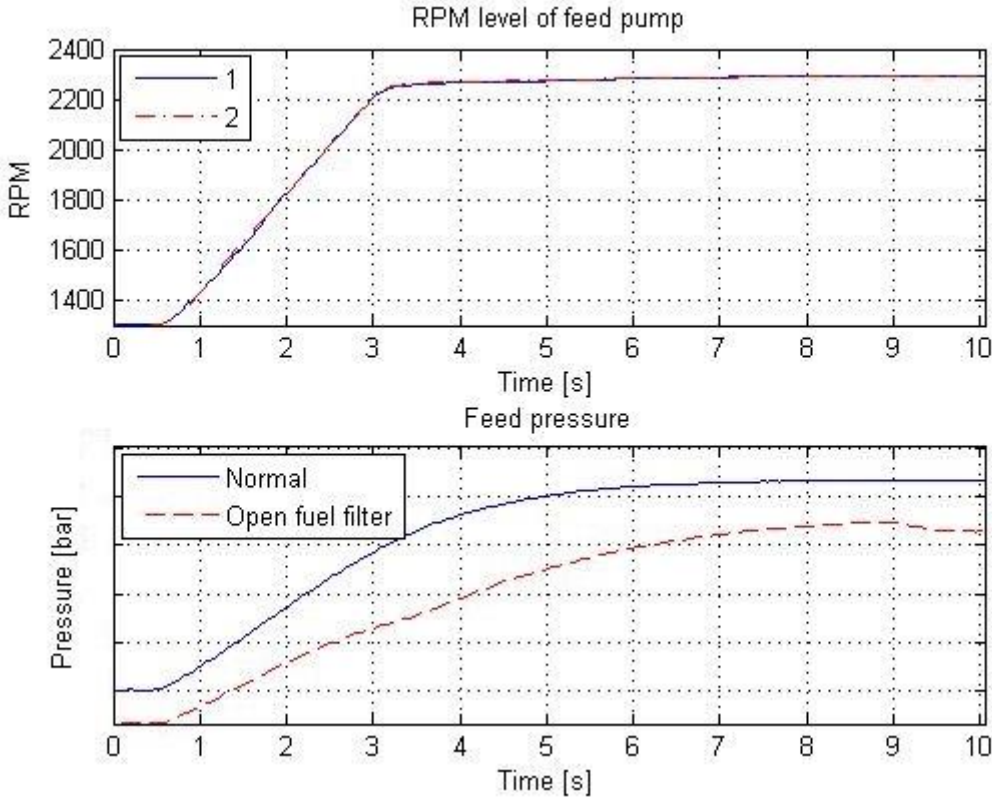


**Figure 5.23.** RPM level for the feed pumps and the feed pressure during a step from 1300 to 2300 RPM's for normal behavior and the behavior during an open fuel filter. For the RPM-level graph the blue signal is from feed pump 1 and the red signal is from feed pump 2. In the feed pressure graph, the blue line is for the normal behavior and the red line is for the behavior during an open fuel filter.

From the above figure, one can see that the pressure has a longer rise time during a suction leakage which could be utilized for fault detection or isolation if necessary.

**Fault detection**

From the above analysis it is clear that this fault is very similar to an open pre-filter. The best way to detect this fault and still being able to achieve fault isolation is therefore very similar to detecting a open pre-filter.

The first detection test that will run during an active controller is the noise amplitude test in (9) that the reader was referred to earlier, see (Ellnefjård, 2014) for more details. If this test is outputting true it means that either a suction leakage is present or that the fuel filter is open. To know which fault is present, the current consumption test for the maximum RPM level needs to be started when possible. This algorithm was shown earlier for a suction leakage and if this test is true there is a suction leakage, otherwise the fuel filter is open.

If the above detection tests are not enough, there is a possibility to consider the rise time as well but this does however require a lot more testing than has been performed.

## 5.7 CLOGGED PRE-FILTER

Generating a system fault representing a clogged pre- filter was done by slightly closing the ball valve attached on the line in between the transfer pumps and the pre-filter. In this test, the ball valve position was fixed while the RPM level for the transfer pumps was increased. The transfer pressure for normal behavior and the behavior during a clogged pre-filter are compared in Figure 5.18.

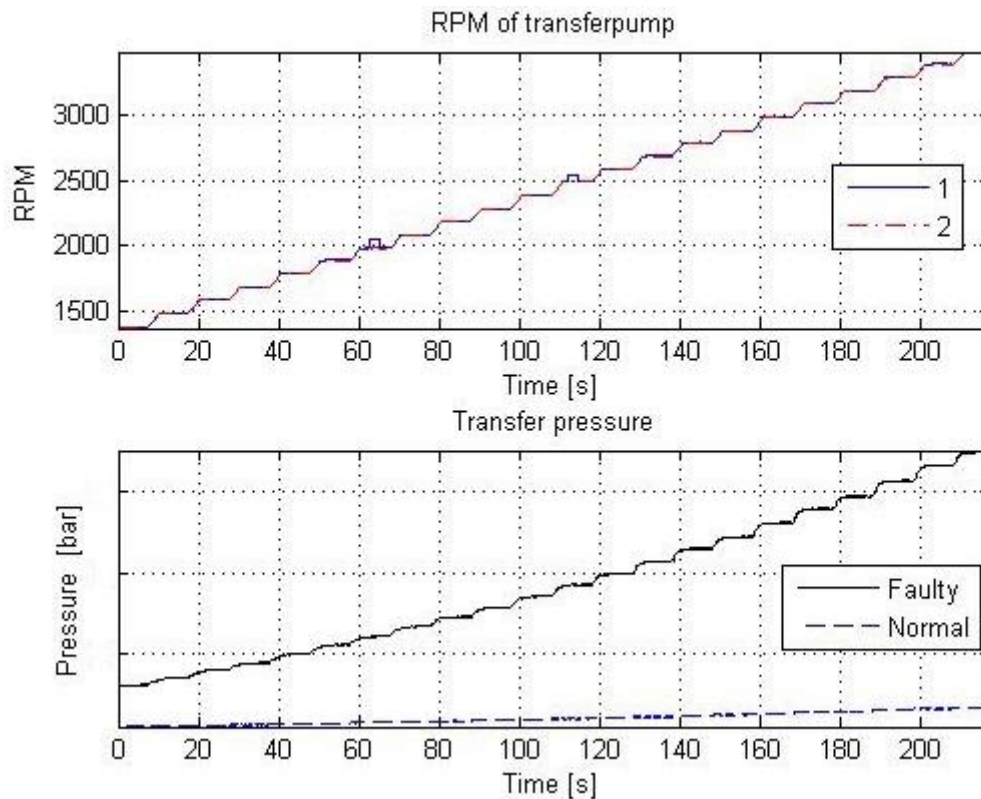


**Figure 5.24. RPM level for transfer pumps and transfer pressure with and without a clogged pre-filter during different RPM levels. For the RPM graph the blue signal is from transfer pump 1 and the red signal is from transfer pump 2. In the transfer pressure graph, the pressure for the faulty and the normal behaviors are presented as black and blue line, respectively.**

From the above figure, one can clearly see that the pressure is a lot larger during a clogged filter in comparison to the behavior during normal conditions. The error between pressure during normal conditions and a clogged pre-filter increases with the RPM level and should easily be detectable. Besides the increased pressure level, the current consumption also increases a lot as well. How to utilize the current consumption and pressure level for fault detection is discussed below.

### Fault detection

A clogged pre-filter causes the transfer pressure and the current consumption for the transfer pumps to increase depending on how clogged the filter is. This fault can be detected by only using the pressure sensor level but as there is a possibility that the pressure sensor can indicate the wrong pressure, the current consumption will be considered as well.

A completely clogged filter would give the same indication as if there was a stop in the fuel line, i.e. no fuel passes by, which is why it should be detected before reaching this

level. The detection test will therefore be designed such that the limits can be divided into steps depending on the pressure as normal, medium clogged and clogged. The simple detection test algorithm can in pseudo code be written as (11) presented in (Ellnefjård, 2014).

To verify that the filter is actually clogged and that the pressure sensor is indicating correctly, the current consumption will be tested for the maximum RPM level. A large deviation will then indicate a clogged pre-filter. If the deviation is not large enough, the sensor is assumed to indicate the wrong pressure. The detection test algorithm can be found on the corresponding page in (Ellnefjård, 2014).

As the pressure sensor is not used in all of the system layouts, the detection test will then only depend on the current consumption with respect to the RPM level. This can easily be done with the use of a look-up table or a polynomial function.

## 5.8 CLOGGED FUEL FILTER

A clogged fuel filter was generated by changing the ball valve position in between the feed pumps and the fuel filter while the feed pumps operates at 1300 RPM's at a pressure around 5-10 bar. Fault relevant data is presented in Figure 5.25.

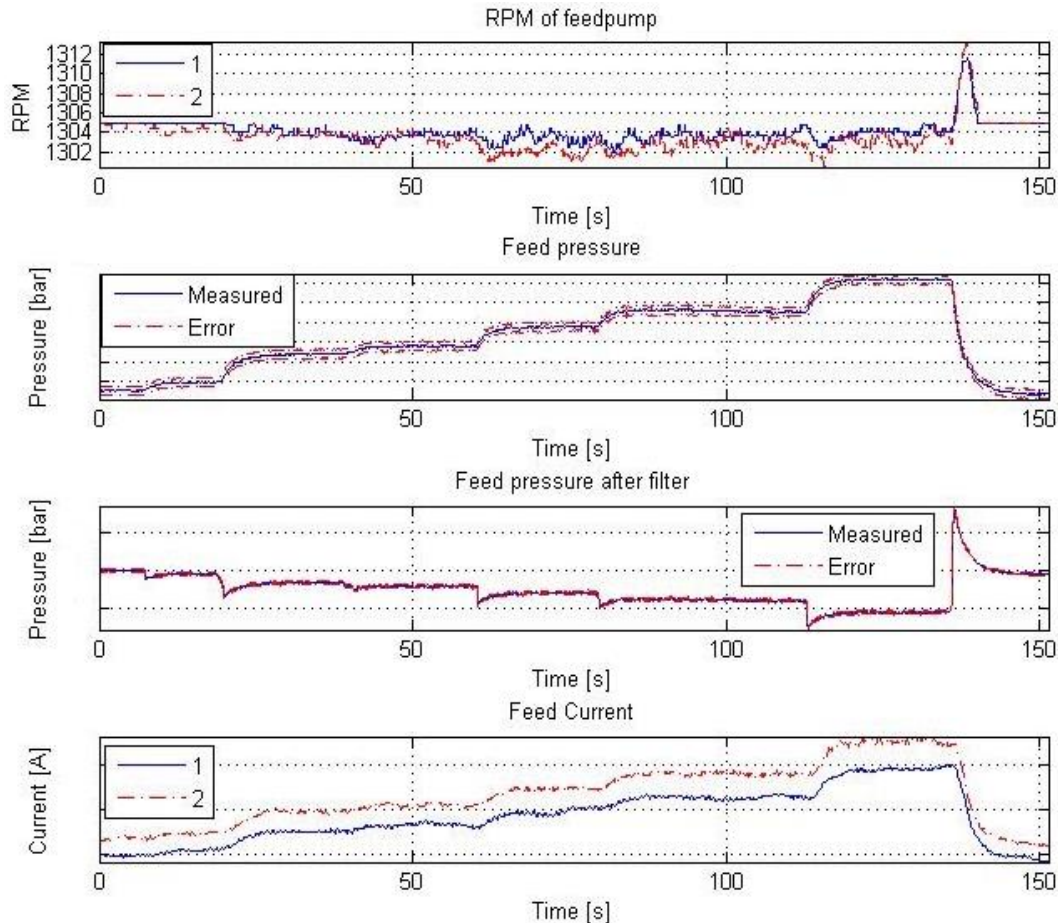


**Figure 5.25. RPM level for feed pumps, feed pressure before fuel filter, feed pressure after filter and current consumption for the feed pumps with different levels of a clogged fuel filter. For the RPM- and the current graph the blue signal is from feed pump 1 and the red signal is from feed pump 2.**

By looking at Figure 5.25, one can see that increasing the clogging, i.e. the ball valve position, the difference pressure over the filter increases. The current consumption also increases while the internal controller in the pumps struggles to regulate the demanded RPM level during pressure levels above 5-10 bar.

## **Fault detection**

A clogged fuel filter will increase the current consumption for the feed pumps but as the pressure is measured both before and after the fuel filter, the pressure difference can be used for fault detection in the system layouts that includes both sensors. To see that one of the sensors is not indicating a faulty pressure level, the first sensor must pass a separate limit check as the pressure should be higher than normal. The pseudo code for the detection test can be written as (12) presented in (Ellnefjård, 2014).

This can also be developed into steps that is depending on how clogged the filter is, which was explained for the detection test of a clogged pre-filter. This test can also be performed during an active system controller and does not require a specific mode.

As a last detection test, an increase in the current consumption must be verified. This is simply done by increasing the RPM level to the maximum when possible and compares the current consumption with what is normal for that RPM level and IMV fuel demand. The test algorithm is identical to the one presented in for a clogged pre-filter, with the exception that it is for the feed pumps. If the test is outputting false, one can however not directly confirm that one of the pressure sensors are indicating the wrong pressure in this case.

The above method does however only function with two pressure sensors on the feed pump side, which does not yield for all of the system layouts. In this case the detection test will only contain a limit check for the current consumption as the feed pressure after the filter will be constantly controlled. This test would then only be possible to execute during certain modes where the current consumption is for a normal case known, with respect to the RPM level and the IMV fuel demand.

## 5.9 STOP IN LINE BETWEEN TRANSFER PUMPS AND PRE-FILTER

A test was also performed to see how the system behaves when there is a stop in the fuel line, between the transfer pumps and the pre-filter. This was simple done by closing the ball valve completely during a normal state. The result of this was of course a pressure being built up where the speed of the pressure increase is depending on the RPM level for the transfer pumps. Due to safety reasons, the stop in line was only activated for a few seconds since the pressure increases very fast. The result of running the transfer pumps on 1300 RPM's and generating a stop in the fuel line can be seen in Figure 5.26. Another test with a higher RPM level can be found in APPENDIX B.

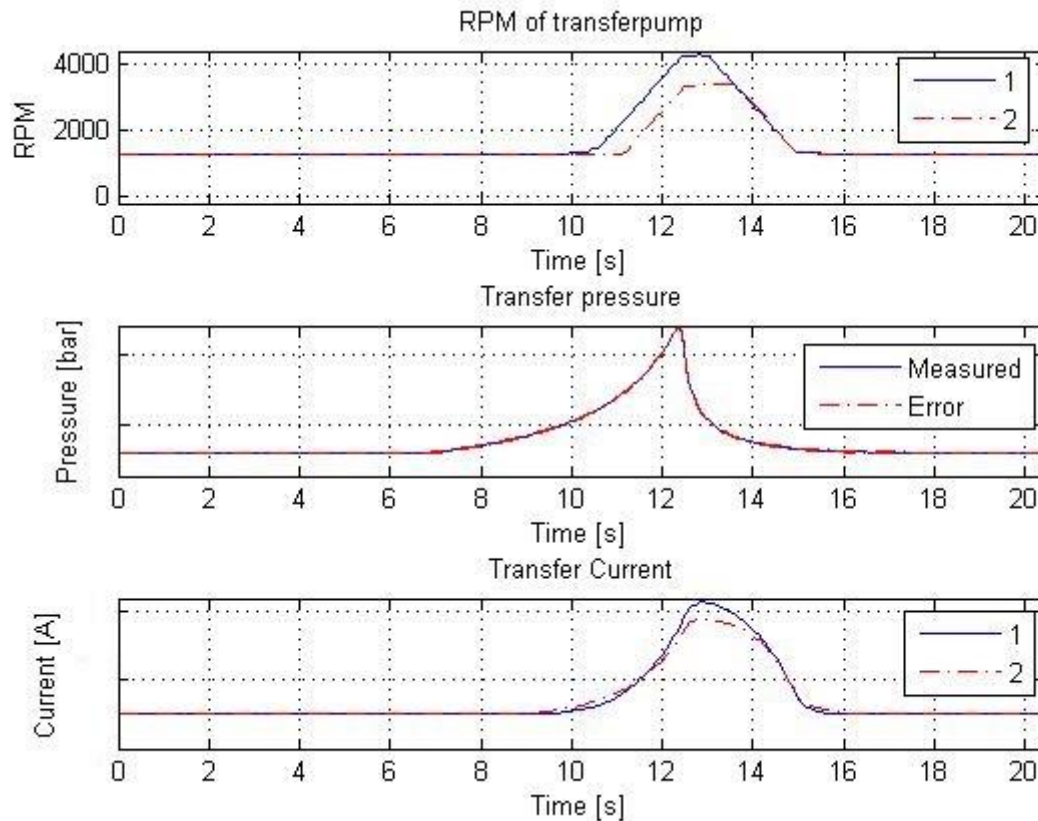


**Figure 5.26. RPM level for the transfer pumps, transfer pressure, and current consumption for the transfer pumps during a stop in fuel line occurring at  $t = 7$ . For the RPM- and the current graph the blue signal is from transfer pump 1 and the red signal is from transfer pump 2.**

The pressure and the current consumption increases rapidly as no fuel pass the stop in the line. These two will increase until the internal current limit is reached inside the pumps and they are shut off. If no current limit is set, the line will probably break from the high pressure if the pumps are not damaged before this moment.



## **Fault detection**

The detection of this fault is very easy since no other fault should be able to cause these high pressure and current levels. The detection test can in pseudo code be written as (13) presented in (Ellnefjård, 2014).

There is also a possibility that the stop has occurred after one of the pumps, i.e. before the pump lines meet in a Y- or a T- coupling. When the above test is outputting true, it is therefore necessary to run each pump separately to detect where the line is clogged. The following cases can then be expected.

- The above test is indicated as true for both pumps which means that the stop is after the Y- or T-coupling.
- Pump 1 indicates a stop in line but pump 2 does not which means that the stop is located after pump 1.
- Pump 2 indicates a stop in line but pump 2 does not which means that the stop is located after pump 2.

In the first case, there is a need of notifying the driver that only the fuel left in the tech-tank can be used for reaching a workshop.

In a case where the pressure sensor is not included in the system layout, the fault needs to be detected by only using the current consumption.

## 5.10 STOP IN LINE BETWEEN FUEL FILTER AND HIGH PRESSURE CIRCUIT

The same test was also performed for the line in between fuel filter and the high pressure circuit. As can be seen Figure 5.27, when a stop in the line occurs the pressure before and after the fuel filter increases along with the current consumption for the feed pumps. Due to safety reasons, the stop in the line was executed on a low starting pressure since the pressure increases very fast.

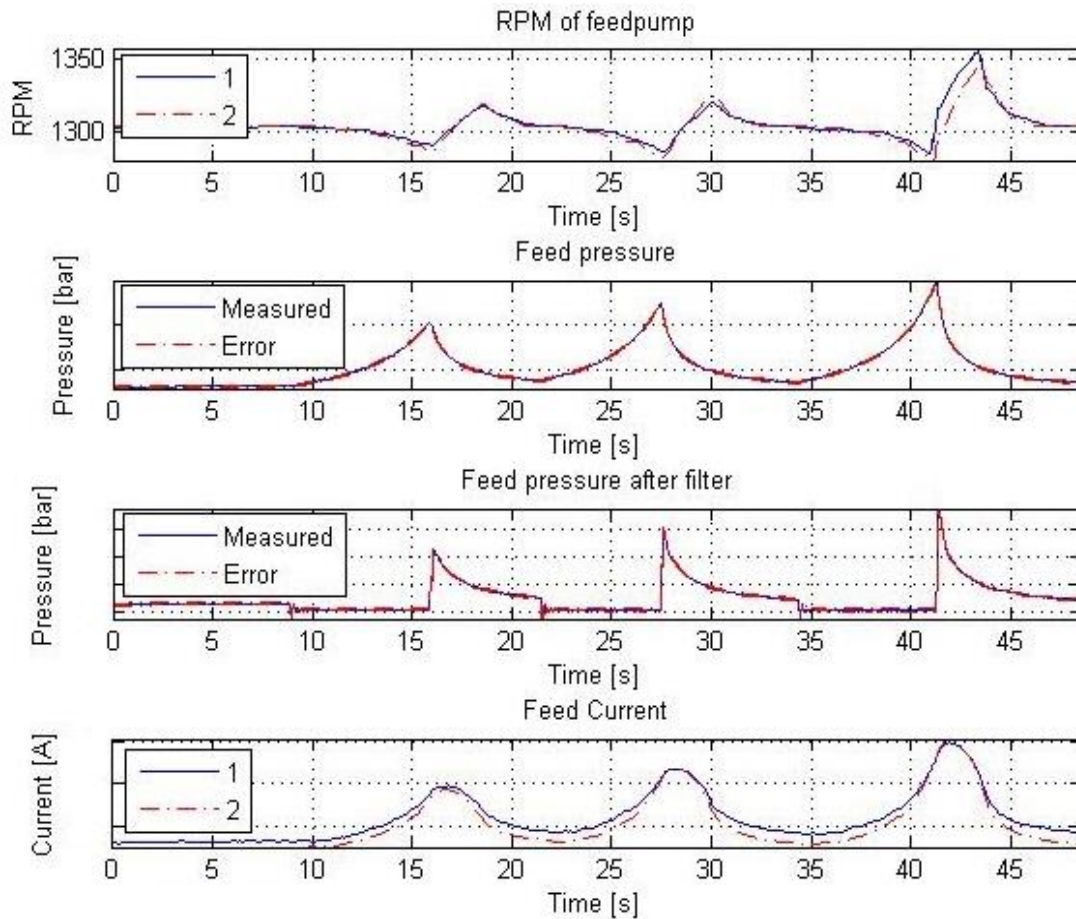


**Figure 5.27.** RPM level for the feed pumps, feed pressure before and after the fuel filter and current consumption for the feed pumps during a stop in fuel line occurring at  $t = 9$ ,  $t = 22$  and  $t = 34$ . For the RPM- and the current graph the blue signal is from feed pump 1 and the red signal is from feed pump 2.

## **Fault detection**

A stop in the line after the fuel filter will cause an increased pressure both before and after the fuel filter. The current consumption will also increase quickly until the internal current limit is reached and the pumps are shut off. As no fuel is reaching the high pressure circuit, this will cause a low pressure being indicated there. The detection test can be written as (14) presented in (Ellnefjård, 2014).

As has been mentioned, for some of the suggested system layouts the sensor before the fuel filter is not present. In these cases the second row in the pseudo code has to be removed.

## 5.11 STOP IN LINE BETWEEN FEED PUMPS AND FUEL FILTER

The difference from previous fault is that the pressure will drop completely since the line is clogged before the pressure sensors. The only indication of the faulty behavior would be the large increased current consumption for the feed pumps as the pressure levels drops and no fuel reaches the high pressure circuit.

### **Fault detection**

As the stop in the fuel line is now occurring before the fuel filter and the sensors, the measured feed pressure signals will drop and the current consumption for the feed pumps increases. The high pressure circuit will in this case also indicate a low pressure which can be utilized in the detection test. The detection test can be written as (15) presented in (Ellnefjård, 2014).

As was mentioned for the other stop in line fault one must consider that if the pressure sensor before the fuel filter is removed the second detection test in the pseudo code is removed. If this is the case the pressure sensor after the fuel filter will have the final vote of where the stop is located. If the above described test is true there is also a need of investigating if the stop is located directly after a feed pump. This is done in the same way as was explained in the fault detection for a stop in the transfer line, resulting in those stated cases.

It is known that the above detection test can be triggered by a non-functional pump, i.e. when the rotor is blocked, which is why the detection test and algorithm is further developed and explained in the fault detection for a blocked rotor.

## 5.12 NON-OPERATING PUMP

To investigate how the system behaves when a pump is non-functional one must first consider the different causes which are stated below.

- Pump does not respond at all
- RPM sensor broken
- Blocked/stuck rotor
- Broken motor shaft/axis

All of these causes will be derived and discussed below.

### 5.12.1 PUMP DOES NOT RESPOND

It was in the rig possible to test how the system behaves when a pump does not respond by disconnecting a feed pump. This was performed during a normal system behavior when the feed pumps were pressure controlled with a PI-regulator. The behavior can be seen in Figure 5.28.

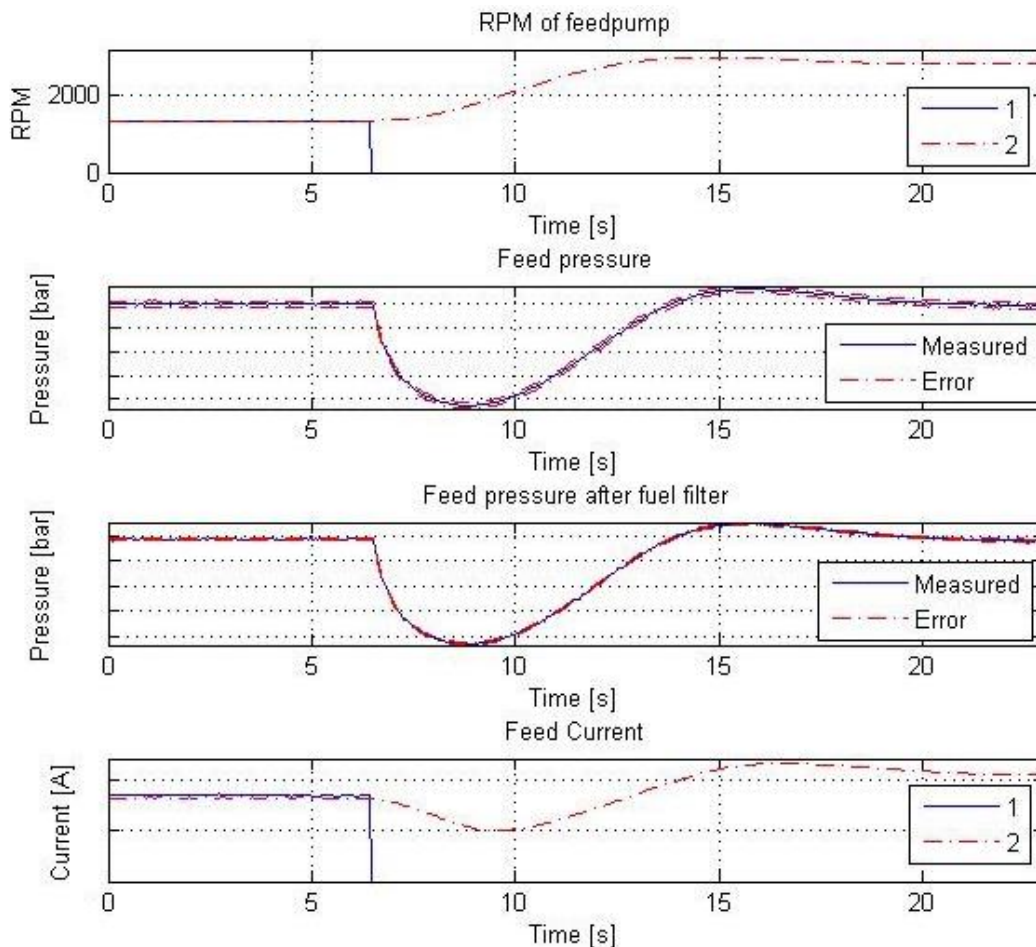


Figure 5.28. The RPM-levels for the feed pumps, the feed pressure before and after the filter and the current consumption. Feed pump 1 is disconnected at  $t=6.5$ . For the RPM- and the current- graph the blue signal is for feed pump 1 and the red signal is for feed pump 2.

When feed pump number 1 stops functioning or in this test case is disconnected, the pressure drops and the demanded RPM level is increased by the controller. The RPM level and the current consumption for pump number 1 drops to zero in this case.

#### **5.12.1.1. Transfer pumps**

This fault results in a small but sudden decrease in the transfer pressure which might be hard to detect with the current pressure sensor resolution. The controller will increase the demanded RPM level to maintain the fuel level in the tech-tank and thus the current consumption will increase for the pump that is still functional.

#### **5.12.1.2. Feed pumps**

A faulty feed pump that is not responding would cause the pressure to drop both before and after the fuel filter but will be recovered as the controller will increase the RPM level of the functional pump to maintain the demanded feed pressure.

#### **Fault detection**

As a functional pump will provide proper RPM feedback, a bigger deviation from the demanded RPM-level is an indication of a non-functional pump. To avoid a functional pump to be detected as faulty due to possible transients, the fault needs to be consistent for a certain time period to be triggered as a fault code. Each pump will have its own detection test and can in pseudo code be written as (16) presented in (Ellnefjård, 2014).

As the above also can be triggered by a faulty functioning RPM sensor inside the pump, it is necessary to investigate if the current consumption is normal or faulty as well. The following detection test, (17) presented in (Ellnefjård, 2014) shall therefore be performed if the above test is true for a pump.

#### *5.12.2 RPM SENSOR BROKEN*

If the current consumption does not change to zero in the above test, the fault is caused by a broken RPM sensor in the pump. There is a possibility that even if the RPM sensor is broken, it does not have to indicate zero as it can be constant on a non-zero level. This will cause the internal RPM controller in the pump to increase or decrease the RPM level rapidly, depending on the demand. This means that the current consumption will either increase or decrease as the RPM level is indicated as constant.

#### *5.12.3 ROTOR BLOCKED*

There is also possibility that the rotor inside the pump could be blocked or stuck which was mentioned earlier. This fault will almost cause the system to behave in the same way as if there was a stop in the line between the feed pumps and the fuel filter described earlier in 5.11. The only difference is that the RPM level will be zero if the rotor is blocked and non-zero during a stop in the line. The transfer pumps will however behave differently as the current consumption will increase and the pressure will be lower than normal as the RPM level will be zero.

### **Fault detection - Transfer pumps**

To detect a blocked rotor inside the transfer pumps, the RPM level is first checked with the test written for detecting a RPM deviation. If that test is true, i.e. there is a RPM deviation, the transfer pressure and the current consumption is tested with the pseudo code written as (18) in (Ellnefjård, 2014).

### **Fault detection - Feed pumps**

To detect if a rotor is blocked or not in the feed pumps, the pseudo code written for detecting a stop in line between the feed pumps and the fuel filter is further developed and written as (19) in (Ellnefjård, 2014).

#### *5.12.4 BROKEN MOTOR SHAFT/AXIS*

If the shaft on the motor is broken, the RPM sensor will still indicate the proper RPM level but the rotor will stand still. As the resistance for the motor is very low, the current consumption will be low as well. This cause is therefore very similar to a suction leakage with the difference that the oscillating noise is present during a suction leakage.

### **Fault detection**

To detect a broken motor shaft, the RPM deviation test has to be false since the RPM level shall be close to the demanded level. If this is the case, then the current consumption and the pressure is tested with the pseudo code written as (20) in (Ellnefjård, 2014).

The same detection test as above also yields for the feed pumps.



### 5.13 STUCK LEVEL SENSOR IN MAIN FUEL TANK

Since the level sensors uses a float, there is a risk that the float might get stuck or break during a system operation and provides faulty sensor data. This type of fault is hard to test in the used experimental setup since the resulting behavior is depending on the final chosen system controller. If the controller would be independent from this signal, the result would only be an incorrect indication of the fuel amount left in the tank and not affecting the rest of the system.

Earlier in the report, there was mentioned that there is a master thesis performed in parallel with this one, where the main focus is the control algorithms for the system. Since this master thesis student has chosen to use an implemented model, the result of this fault will then cause an error between the model and the level sensor signal, larger than usual.

#### **Fault detection**

The level sensor located in the main tank is not that essential for having a functional system but it is still important for providing information to the driver of how much fuel there is left. To detect this fault during system operation, a residual between the level from the model and the real sensor signal will be used. A bigger deviation will then trigger the fault code. The pseudo code for the detection test is presented on the corresponding page, i.e. (21) in (Ellnefjård, 2014).

As the transfer pumps are controlled for maintaining the demanded tech-tank level and temperature it is possible to test the level sensor by overriding the controller reference. By changing the demanded tech-tank level to maximum, the transfer pumps RPM level will increase. The level shall then increase in the tech-tank and decrease in the main tank. If not, the level sensor can be considered as stuck. The pseudo code for detecting a stuck level sensor in one of the tanks can also be written as (22) in (Ellnefjård, 2014).

## 5.14 STUCK LEVEL SENSOR IN TECH-TANK

As was described for the other level sensor faults, these faults are also depending on the chosen system controller and are difficult to test in the rig before implementing the model and the controller. Even though the faults are control dependent it is still possible to analyze how the system would react with and without a model. In either case, the signal from the level sensor in the tech-tank will serve as reference for the transfer pump control.

Let us consider a case where the model is not used and the transfer pumps are simply controlled with a PI-regulator.

The system behavior when the float is stuck at the top of the level sensor would be that the transfer pumps shut off (if an overfilling sequence is not demanded) since the tech-tank is indicated as full. The system would continue operating until there is no fuel left in the tech-tank, resulting in an engine stop.

If the float is stuck at the bottom of the level sensor the tech-tank would be overfilled due to the constant operating transfer pumps. The system would still function but with unnecessary pump work for the transfer pumps.

A float stuck in between the above described positions would result in a system behavior that depends whether it is stuck below or above the level reference. Above would cause the same system behavior as if it was stuck at the top and below would cause the same behavior as if it was stuck at the bottom.

Let us now consider the other case, where the system model is used and as was described for the level sensor located in the main tank, the tradeoff between trusting the model or the real signals more is affecting the outcome of the faulty behavior. If the controller relies more on the model, the system would still behave close to normal but with a larger error between the model and the level sensor signal. Trusting the real level sensor signal more would then cause a system behavior that leans towards the case without a system model that was described above.

### **Fault detection**

The fault stuck level sensor in tech-tank will be detected by generating a residual between the estimated tech-tank level from the model and the real level sensor signal. A bigger deviation will then indicate that the system is in the faulty mode. The pseudo code for this detection test can be written as (23) in (Ellnefjård, 2014).

Another test for detecting a stuck level sensor in the tech tank, without using the model, was in pseudo code suggested in the fault detection section for a stuck level sensor in the main tank.

## 5.15 TRANSFER OR FEED PUMPS ARE NOT SHUTTING OFF WHEN DEMANDED

This fault is as the above described, hard to test and even harder to design useful test cases for, since the faulty system behavior depends on how the pump is designed with software and hardware.

For the pumps that are used in this thesis, the fault could only origin from two things. Either by a fault in the internal pump controller or a fault in the system controller. The internal controller is constructed in a way that if the CAN communication is lost the pumps then run on half speed of the full RPM span and does not read the reference signal. The other cause could be a bug in the system controller that was unnoticed during the testing and implementation of the system.

The result of a transfer pump that does not shut off when demanded will act as a disturbance in the system and the tech-tank will be overfilled when not demanded. A feed pump that is not shutting off when demanded will cause the feed pressure to be higher than normal, with respect to the normal current consumption for only one running pump.

### **Fault detection - Transfer pumps**

As this fault will affect the level in the tech-tank to increase, a deviation between the model and the real level sensor signal will be noticed. The detection test will therefore be similar to the test detecting the fault mode "Tech-tank level low", but with a different detection limit. The pseudo code for the detection test can be written as (24) in (Ellnefjård, 2014).

### **Fault detection – Feed pumps**

There was earlier mentioned that this fault could have different causes and that they are depending on the chosen hardware and software inside the pumps. The cause that is assumed to trigger this fault is in this case a broken can communication.

The effect of this cause and fault will cause the feed pressure to increase and which will be faulty with respect to the total current consumption for the feed pumps, which in this case only will be for one pump. The detection test will therefore be chosen as the pseudo code written in (25) presented in (Ellnefjård, 2014).

## 5.16 TEMPERATURE SENSOR IN MAIN-TANK BROKEN

The temperature sensor in the located in the main tank does not provide any necessary information for controlling the system and might be unnecessary in the final system layout. Since it does not affect anything inside the system whether it is functional or not, it is very hard to design a suitable test case. The fault might however be worth investigating and analyzing if the sensor will exist in the final system layout.

### **Fault detection**

To determine if a temperature sensor is functional or not can be done with a test during a startup sequence of the engine. As there exists several temperature sensors inside this system but also outside, these can be used for physical redundancy. An example where

the internal temperature sensor is used for this is in pseudo code written as (26) in (Ellnefjård, 2014).

Other temperature sensors that can be used for this are stated below.

- Temperature sensor in the urea tank
- Ambient temperature sensor
- Temperature sensor in oil pan
- Temperature in tech-tank

The latter one stated, i.e. the temperature in the tech-tank can be utilized when performing an overfilling of the tech-tank during a certain time. The two temperature sensors shall then move towards each other's temperature levels. If the overfilling mode has been activated during a longer period and the temperature saturate near each other, one of the sensors is broken. If this is the case, both of the sensors shall be compared to another temperature sensor outside the system for identifying which sensor is faulty.

## 5.17 TEMPERATURE SENSOR IN TECH-TANK BROKEN

In contrast to the temperature sensor in the main tank, the temperature sensor in the tech-tank is strongly affecting the system controller decisions and is therefore necessary to be able to diagnose correctly.

If this temperature sensor is non-functional and indicates a low temperature constantly, the temperature will increase in the tech-tank, which could increase to dangerous temperature levels with respect to the fuel.

If the temperature sensor indicates a high temperature constantly, the controller will demand overfilling of the tech-tank until the tech sensor is replaced. The system will still be functional but with unnecessary energy consumption for the transfer pumps.

### **Fault detection**

Since there are temperature sensor located inside each pump, these can be used for physical redundancy during a startup sequence. The difference between the sensors will indicate if a sensor is faulty or not. The pseudo code for detecting a faulty temperature sensor in the tech tank during an engine startup sequence is written as (27) in (Ellnefjård, 2014).

This test might only be possible during the startup sequence that was mentioned earlier since the temperatures in the pumps are increasing faster. There is a possibility to switch to another temperature sensor that always indicates values closer to the tank temperature. These sensors could be one of those that were stated in the fault detection for temperature sensor in main tank broken.

## 5.18 PRESSURE INDICATING THE WRONG PRESSURE

If a pressure sensor indicates the wrong pressure the system behavior will, as for many other faults described, depend on how the system controller is reacting with or without a system model and an observer. The following analysis assumes that the sensor signals are more trusted than the model parameters. If it is the opposite, the system behavior would still be acceptable, but with errors between the model and the real sensor signals.

### *5.18.1 PRESSURE SENSOR AFTER FUEL FILTER*

If the pressure sensor indicates a too high pressure, the feed pump will decrease in speed and current consumption. This will then cause the pumps to not providing enough fuel to the high pressure circuit.

An indication of a too low pressure would cause the system to behave in the opposite way, the RPM level would increase along with the current consumption as the system would struggle to maintain the demanded pressure level.

Also, this is of course depending on the control strategy, whether the feed pumps are flow controlled or pressure controlled. The above described cases assume pressure control since a flow controlled system would not need to use the pressure sensors.

### *5.18.2 PRESSURE SENSORS BEFORE FUEL FILTER AND BEFORE PRE-FILTER*

Since these pressure sensors does not have any effect on the controller and is only for diagnostic purposes, a wrongly indicated pressure would only affect the diagnostic system which will be discussed later.

## **Fault detection**

The two pressure sensors located before and after the fuel filter should always indicate pressure levels relatively near each other, depending on how clogged the filter is and the current fuel flow, i.e. the RPM level for the feed pumps. Physical redundancy can therefore be used for these sensors and the detection test can in pseudo code be written as (28) in (Ellnefjård, 2014).

To establish which sensor is broken it should be possible to utilize the pressure sensor located in the high pressure circuit. If no indication of a too low pressure in the high pressure circuit is given, the pressure sensor after the fuel filter is functional and the pressure sensor before the filter is faulty. The limit that is used must either be fixed for a certain RPM level, where the then test is performed, or change as a function of the RPM level. One must also consider that a clogged fuel filter will affect the chosen detection limit.

As was mentioned earlier, some detection tests can be performed during an engine startup sequence and as no pressure has been built up in the system. All of the pressure sensors should then indicate pressure levels relatively near each other, i.e. the atmospheric pressure.

As the different system layouts utilize different amounts of pressure sensors it will not be possible to utilize physical redundancy in all of them. It would therefore be a good idea to instead install T-couplings in these locations such that a sensor can be attached inside the workshop. The exact location for the T-couplings should be a tradeoff between being able to provide physical redundancy and be a part of other workshop tests needed for diagnosis.

## 5.19 COMPARISON BETWEEN STEP RESPONSES

In the above analysis of the faults, step responses was performed and compared to the normal behavior. It might however be useful to see how these step responses acts in comparison to each since it can provide further useful information for fault detection tests.

A comparison between the step responses that is affecting the feed pump side of the system can be seen in Figure 5.29. The ball valve, representing the IMV, was for these steps put in a position that gives a pressure around 3 bar during normal conditions.

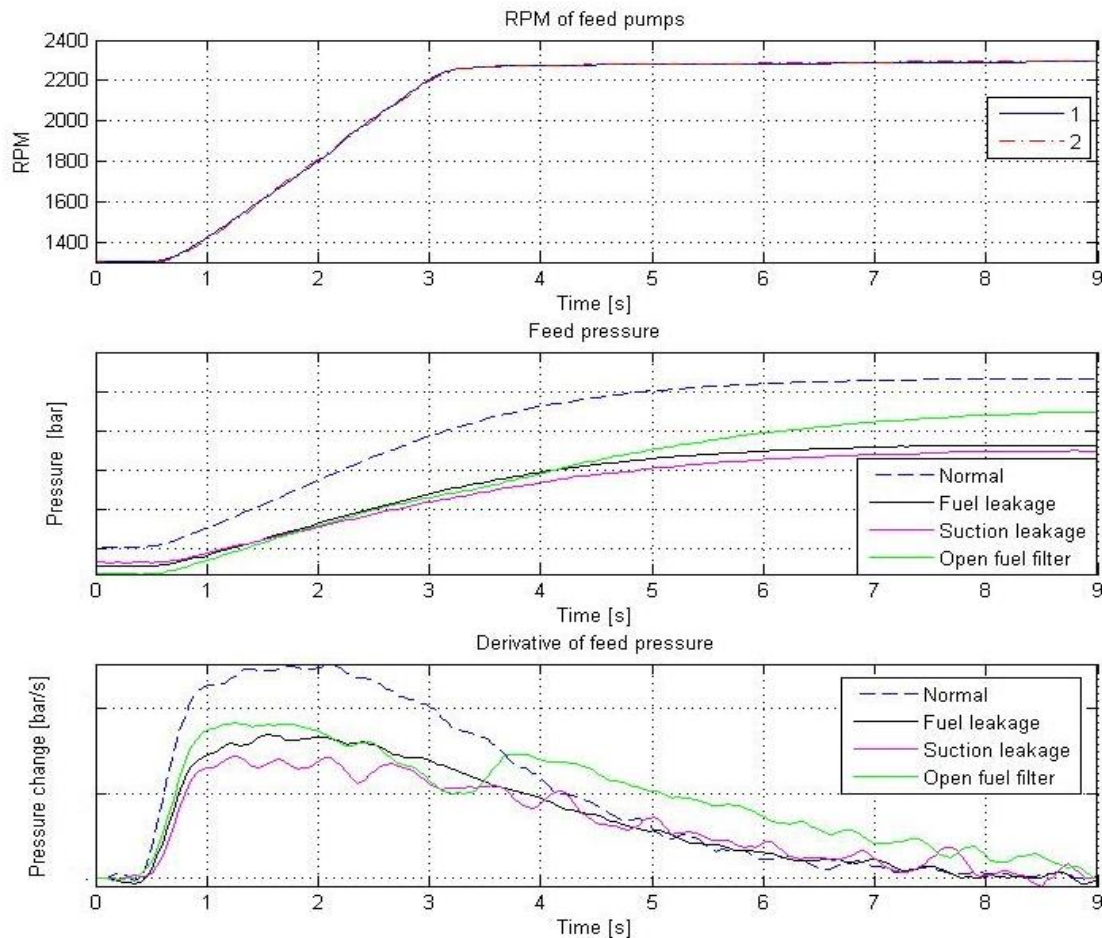


**Figure 5.29.** The top graphs shows the RPM level step from 1300 to 2300 RPM's and the middle graph shows the different behaviors of the feed pressure during normal conditions, a fuel leakage, a suction leakage and during an open fuel filter. The lower graph shows the derivative of the pressure graph.

In the derivative graph, one can see that the green line representing an open fuel filter suddenly increases at  $t = 3,4$ . This is most likely a depending on a defect from the test, i.e. the filter is less open than before  $t = 3,4$ . From the comparison it is safe to say that the rise time is clearly affected by the different faults but that they are hard to distinguish from each other since it also depends on the how large a leakage is and the current fuel demand.



Comparing the pressure level before and after the step, i.e. when the pressure has settled, gives the pressure difference that occurs for each fault. This can be done in several ways, e.g. by taking the integral before and after the step or by utilizing simple means. In this case, the pressure is integrated between  $t = 0$  to  $t = 0,8$  and  $t = 8$  to  $t = 8,8$ . The differences can be seen in a table on the corresponding page in (Ellnefjård, 2014).

Since this result is for a certain leakage size, with respect to each fault, a second test was performed with other leakage sizes. The result can be seen in Figure 5.30.

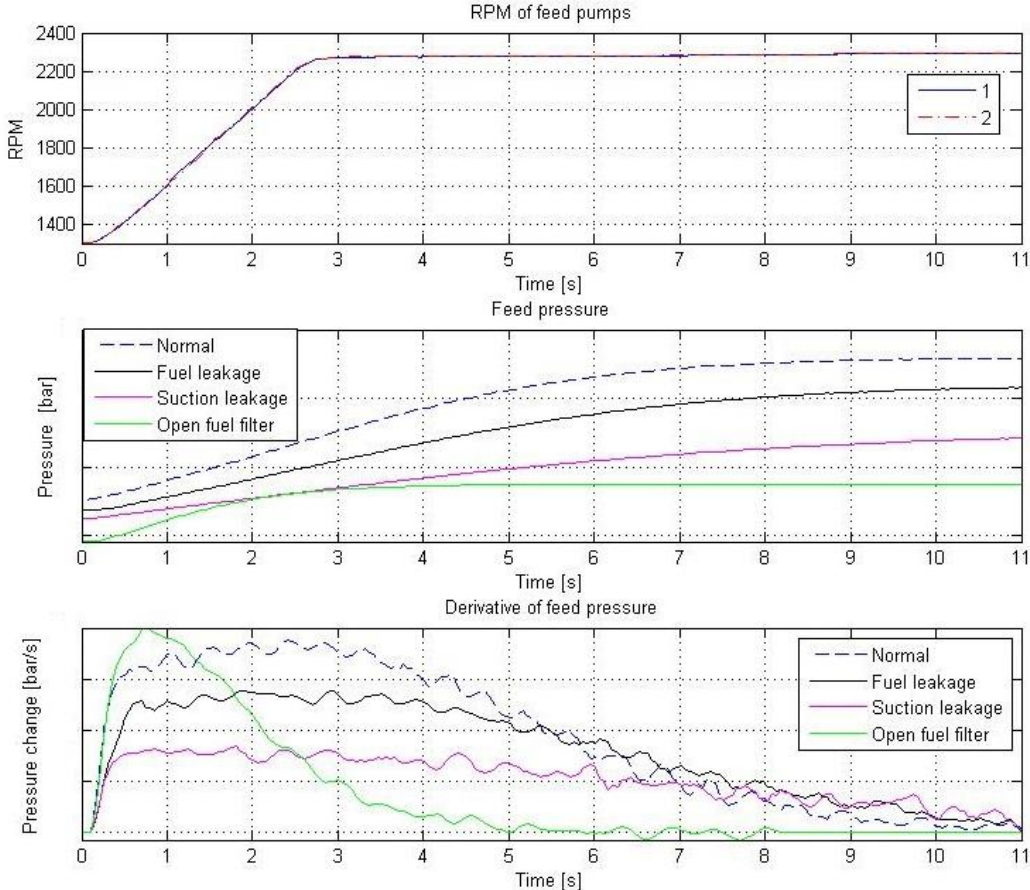


**Figure 5.30. Results from the second step response tests The top graphs shows the RPM level step from 1300 to 2300 RPM's and the middle graph shows the different behaviors of the feed pressure during normal conditions, a fuel leakage, a suction leakage and during an open fuel filter. The lower graph shows the derivative of the pressure graph.**

In the above figure, one can see that when changing the leakage sizes the rise time and the derivatives are different from before. It is however safe to say that a suction leakage and a fuel leakage is affecting the feed pressure the most as the open fuel filter is located after the feed pressure sensor in this case. The static differences are depending on a combination of the RPM of the feed pumps and the leakage size. As can be seen for the open fuel filter in Figure 5.30, the amount of fuel that is leaking out from the filter is in this case very large which gives a large static difference from the normal behavior.

A comparison between the pressures differences retrieved in the above two tests can be seen in the corresponding page in (Ellnefjård, 2014).

The pressure difference for a fuel leakage and a suction leakage are relatively similar in both tests. An open fuel filter does however not show the same consistency. This type of

comparison could be used for identifying the faults but requires more testing for different leakage sizes.

An attempt of estimating the transfer functions for each fault was performed for the two tests. There was however no consistency between the transfer functions describing the faulty behavior in each test.

There is however another interesting information that can be found in Figure 5.29 and Figure 5.30. As was mentioned, the static difference from the pressure curve during the normal behavior is depending on how big the leakage is. This means that it is possible to diagnose how critical the leakage is and what measure to take from that conclusion.

### **Leakage size detection test**

This is detected by either measuring the settling time for the pressure or the decay in the derivative. To accomplish this with an ECU or a computer, one must integrate the pressure or the derivative of the pressure in small steps and compare the differential. This is in pseudo code written as (29) in (Ellnefjård, 2014) and starts after the RPM step has been acknowledged by the pumps.

Moving over the analysis to the transfer pump side of the system, step response tests was performed for a leakage in between the transfer pumps and the pre-filter, a suction line leakage and an open pre-filter. A comparison between the transfer pressure behaviors can be seen in Figure 5.31.

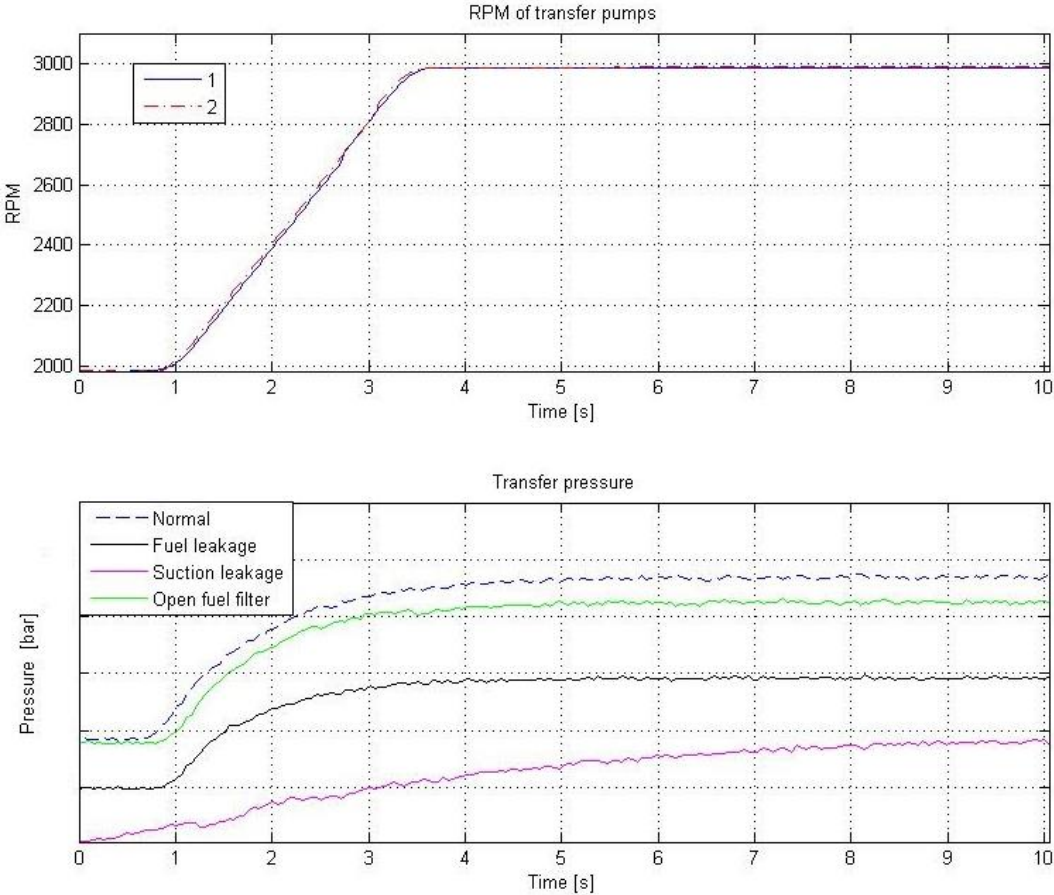


**Figure 5.31. The top graphs shows the RPM level step from 2000 to 3000 RPM's and the lower graph shows the different behaviors of the feed pressure during normal conditions, a fuel leakage, a suction leakage and during an open fuel filter.**

As can be seen, the shape of the pressure increase for an open pre-filter and a fuel leakage are very similar to each other. The suction leakage is in this case completely different since the leakage was relatively large. This also explains the non-static behavior before  $t = 1$ .

The information gained from the above two analyses is that it is possible to use step responses for detecting that there is a fault present in the system. It is however more difficult to establish which fault that is present. The integral comparison that was in pseudo code shown in (29) in (Ellnefjård, 2014) can definitely be used for identifying how critical a leakage is.



## 6. RESULTING DIAGNOSTIC SYSTEMS

*In this chapter, diagnostic algorithms including fault detection and isolation methods will be presented and discussed for the different system layouts that were suggested earlier in the report. Detectable leakage sizes and required sampling frequency will also be presented and discussed.*

### 6.1 EXPLANATION PROCEDURE OF THE DIAGNOSTIC SYSTEMS

From the analysis performed in the previous chapters it was realized that it is not possible to run the same fault detection tests for all of the different system layouts. To simplify the explanation of how the diagnostic is affected when removing pressure sensors, algorithms for the layout that includes all pressure sensors, i.e. system layout C will be presented first.

As the diagnostic system is relatively large it is difficult to show the complete algorithm in one big flowchart. The algorithm has therefore been divided into detection tests that are being performed in different modes which are stated below.

- System startup
  - Occurs when the driver unlocks the truck or when turning the ignition.
- System operating with normal controller
  - The engine is operating in driving modes and system is controlled according to the normal control algorithms.
- System controller overridden
  - Occurs when an isolation test is demanded from the detection tests running in the mode described above.
- Time scheduled tests with and without a system controller override
  - Detection tests that are performed less frequently.

## 6.2 ALGORITHMS FOR SYSTEM LAYOUT C

As was mentioned earlier, this layout includes all of the pressure sensors that was used in the experimental rig and is therefore the most expensive system layout. This means that all of the suggested detection and isolation methods that were suggested in the previous chapter is fully applicable in this case.

### 6.2.1 *SYSTEM STARTUP*

When the system starts, pressure sensors and temperature sensors are tested with the aid of physical redundancy. The pressure sensors are compared against each other as they shall all indicate pressure levels near each other, i.e. the atmospheric pressure. The same principal yields for the temperature sensors. The level sensors shall indicate a level that is within the normal range to be considered as non-faulty. A flowchart for the startup diagnosis can be found in the corresponding section in (Ellnefjård, 2014). If a fault already is present from an earlier test, there is no need for testing that particular fault before maintenance has been performed.

### *6.2.2 DETECTION TESTS DURING A NORMAL CONTROLLER MODE*

There is several detection tests that can be performed when the system is operating with the normal controller, i.e. these tests occurs in every loop iteration. To simplify the algorithm visualization for the reader, it has chosen chosen to divide the algorithm into components located on the transfer pump side of the system and the feed pump side of the system. The faults that can be detected with an active normal controller on the transfer pump side are stated and summarized in the corresponding section in (Ellnefjård, 2014).

The algorithm for the transfer pump side- and feed pump side- of the system can be found in two figures located in the corresponding section in (Ellnefjård, 2014).

As was described, some of these detection tests are not enough for being able to isolate all of the faults and is in the need of a specific isolation test. These tests require an override of the system controller and are shown and described in the next section.

### 6.2.3 DEMANDED ISOLATION TESTS WITH AN OVERRIDDEN SYSTEM CONTROLLER

The amount of tests placed in this category is highly dependent on the system layouts and as system layout C is able to isolate most of the faults, these tests are very straight forward. The faults that needs to be further isolated from each other are stated below.

- Clogged pre-filter and faulty transfer pressure sensor
  - A faulty transfer pressure sensor could indicate a clogged pre-filter which is why a current consumption test is needed for full fault isolation.
  
- Open fuel filter and suction leakage for feed pumps
  - Both faults affect the system in the same way and are detected by an abnormal amplitude change in the noise. These are isolated from each other with a current consumption test on the highest RPM level. To establish how critical the leakage or the fault is, the earlier mentioned step response test is performed; see the pseudo code written as (29) in (Ellnefjård, 2014) for details.

The isolation algorithms are shown in a figure located in the corresponding section in (Ellnefjård, 2014).



### **6.2.3.1. Level sensors and temperature sensors**

As some processes are slower than others in this system, e.g. the temperature level and fuel level changes slower than the pressure level, they are therefore not equally critical to test with the same frequency. With this in consideration, the level sensors and the temperature sensors shall be tested once every 15 minutes with the algorithm shown in the corresponding section in (Ellnefjård, 2014). The 15 minutes is an approximated time in which noticeable changes should have occurred for the level sensors. This time is depending on the size of the tank, the current fuel consumption and the length of the steps between the internal switches inside the level sensor.

### **6.2.3.2. Leakage tests**

As the leakage detection tests requires a separate controller it also has to consider the mode of the engine, i.e. how much fuel that is demanded. The starting RPM level in the test has to provide enough fuel in that particular mode, e.g. when the truck is on the freeway. It is therefore suggested to request a leakage test with a certain time span but with the constraint that it only starts when entering the suggested mode. The algorithm is shown in the corresponding section of (Ellnefjård, 2014). If a leakage is detected, the size of the leakage is determined with a step response test, where the settling time is the measurement of the leakage size.

## 6.3 ALGORITHMS FOR SYSTEM LAYOUT B

The difference between system layout C and B is that the pressure sensor located before the pre-filter has been removed. This means that every detection and isolation test that utilizes the transfer pressure sensor signal has to be changed.

### 6.3.1 *SYSTEM STARTUP*

The diagnostic algorithm that was presented for the startup sequence in system layout C is still applicable to this layout with the exception that no test has to be performed for the transfer pressure sensor. This does however affect the possibility to tell which of the two feed pressure sensors that is faulty. To compensate for this flaw, an external sensor, e.g. the pressure sensor in the high pressure circuit can instead be used for achieving full fault isolation.

As there are no bigger differences in the startup sequence algorithm, the reader is together with the above text piece referred to the same algorithm as for system layout C during a startup sequence.

### 6.3.2 *DETECTION TESTS DURING A NORMAL CONTROLLER MODE*

As no change has been done in the feed pump side of the system, there is no need of changing the algorithm that covers these faults. This means that the algorithm presented for system layout C, during a normal mode, is valid for system layout B as well.

When it comes to the algorithm for the fault detection on the transfer pump side, there is a big difference for system layout B as most of the test used the transfer pressure sensor signal. This new algorithm is instead utilizing the relationship between the current consumption and the RPM level, i.e. an accurate look-up table or a polynomial function. This does however increase the requirements on the current consumption resolution which is discussed later.

The new suggested algorithm can be found in a figure located in the corresponding section in (Ellnefjård, 2014).

### 6.3.3 DEMANDED ISOLATION TESTS WITH AN OVERRIDDEN SYSTEM CONTROLLER

As there were no changes made on the feed pump side of the system, the same isolation test is required for separating a suction leakage for the feed pumps and an open fuel filter. This means that the algorithm covering the feed pump side of the system for system layout C is still valid.

For the transfer pump side, there was however several changes made in the diagnostic algorithm which is why there is now a need of separating the following faults from each other.

- Broken/stuck tech-tank level sensor, open pre-filter and a fuel leakage.
  - If an error exists between the fuel level in the model and the measured level meanwhile the current consumption is indicated as normal, the faults above are possible causes.
- Suction leakage for transfer pumps and shaft/axis broken inside pumps.
  - These faults also causes an error for the tech-tank level but is separated from the above faults as they will cause the current consumption to be low.

At this point, it was realized that isolation with confidence for the faults above is very difficult to achieve out in the field. It is however possible to determine if the level sensor is broken or stuck by running both of the transfer pumps on their maximum RPM level. If the level sensor in the tech-tank does not increase, it can be assumed to be stuck or broken. The algorithm for this test can be seen in the corresponding section in (Ellnefjård, 2014).

If the test shows that the level sensor is functional, it means that there is fuel leakage or an open pre-filter. The easiest and most confident way of separating these faults from each other is by performing a workshop test. This also yields for the faults; suction leakage and a broken shaft/axis.

### **6.3.3.1. Workshop tests**

As was mentioned in analysis in the previous chapter, there is a possibility to attach a T-coupling in between the transfer pumps and the pre-filter. The purpose of this is to be able to attach a pressure sensor inside the workshop, such that the isolation methods for system layout C can be used inside the workshop.

When the transfer pressure sensor has been attached inside the workshop the isolation algorithms can be executed. These can be found in the corresponding section in (Ellnefjård, 2014). This is only one of many ways to isolate these faults in the workshop as it is also possible to utilize the whole algorithm that was suggested for system layout C. There is however no need for this if the faults are visible, e.g. if there is a larger fuel leakage.

### *6.3.4 TIME SCHEDULED TESTS*

The time scheduled tests are for this system layout the same as for system layout C. The exception is that a leakage test on the transfer pump side is not possible and is instead isolated inside the workshop as explained in the subsection above.

## 6.4 ALGORITHMS FOR SYSTEM LAYOUT D

In system layout D, the transfer pressure sensor is reintroduced and the feed pressure sensor before the fuel filter is removed. This means that there is now one feed pressure sensor located after the fuel filter and one transfer pressure sensor before the pre-filter.

### 6.4.1 SYSTEM STARTUP

The algorithm that shall run during the startup sequence is still the same, with the exception that the pressure sensor in the high pressure circuit is used in the redundancy test instead of the feed pressure sensor before the fuel filter. The reader is therefore still referred to the algorithm used for system layout C during a startup sequence.

### 6.4.2 DETECTION TESTS DURING A NORMAL CONTROLLER MODE

As this system layout is similar to system layout C, it is possible to utilize the same algorithms with smaller modifications. The only tests that utilize the pressure sensor before the fuel filter is the tests for detecting a faulty feed pressure sensor and also a clogged fuel filter. It will therefore only be explained how these can be detected differently for this system layout.

A clogged fuel filter will cause the system controller to increase the current consumption for maintaining the demanded pressure level but as this is also depending on how much fuel that is demanded it becomes more difficult. It is therefore suggested that a clogged fuel filter is detected with a time scheduled test that takes place in pre-determined engine mode, where the system controller is overridden. It is also possible to verify that the pressure sensor is properly functioning with this test as well. This will be explained and shown in the subsection Time scheduled tests.

Besides the fault detection tests above, the algorithms is identical with the two suggested for system layout C, see corresponding section in (Ellnefjård, 2014) for more details.

### *6.4.3 DEMANDED ISOLATION TESTS WITH AN OVERRIDDEN SYSTEM CONTROLLER*

As there were not many changes from system layout C, in the diagnostic algorithm running with the normal controller, the demanded isolation tests are the same with the exception that it is only needed for separating a suction leakage from an open fuel filter. With the above information, the reader is referred to the algorithm shown for system layout C in (Ellnefjård, 2014).

### *6.4.4 TIME SCHEDULED TESTS*

The level sensor test, the temperature test and the leakage tests that were suggested for system layout C is still valid for this system layout as well. Besides these tests, a test for a clogged fuel filter and a faulty feed pressure sensor needs to be added.

To test if the filter is clogged or not one needs to know the relationship between the RPM level, the pressure and the current consumption for a known fuel demand, e.g. the IDLE mode. In this mode, the pumps can be set to the maximum RPM level for a short time period as the current consumption and the pressure level is measured and compared to pre measure values in the case of non-clogged filter. If the pressure level is lower than normal and the current consumption is larger than normal, it is certain that the fuel filter is clogged. If the current consumption is within normal range and the pressure level is lower or higher than normal, with respect to the pressure sensor error boundaries, the pressure sensor is faulty. The algorithm can be seen in the corresponding section in (Ellnefjård, 2014).

## 6.5 ALGORITHMS FOR SYSTEM LAYOUT A

This system layout only includes the feed pressure sensor located after the fuel filter as the other pressure sensor has been removed. The diagnostic algorithms will for this system layout therefore be a combination of the algorithms that was presented for system layout D and B.

### 6.5.1 SYSTEM STARTUP

The detection tests that were suggested for system layout C, during a startup sequence, are still valid with the exception that the feed pressure sensor needs be controlled against the pressure sensor in the high pressure circuit or another system external pressure sensor.

### 6.5.2 DETECTION TESTS DURING A NORMAL CONTROLLER MODE

As this system layout does not include the transfer pressure sensor, the algorithm presented for system layout B, will be used for detecting and isolating the faults on the transfer pump side of the system.

The feed pump side is for this system layout identical with system layout D and will therefore use the same algorithms. This means that the algorithm for the feed pump side will be used with the same exception that was explained for system layout D. A clogged fuel filter or a faulty pressure sensor is detected with a time scheduled test.

### 6.5.3 DEMANDED ISOLATION TESTS WITH AN OVERRIDDEN SYSTEM CONTROLLER

Since the detection test algorithms running with a normal controller is a combination of system layout B and D, the demanded isolation tests will be a combination as well.

For the feed pump side of the system, there is only a need for separating an open fuel filter from a suction leakage and the algorithm is presented on the left side in the figure describing the algorithm demanded isolation tests for system layout C.

For the transfer pump side of the system the demanded isolation tests are identical with those that was suggested for system layout B. See corresponding section in (Ellnefjård, 2014) for more details.

#### *6.5.4 TIME SCHEDULED TESTS*

The level sensors and the temperature sensors will still be tested according to the algorithm presented for system layout C which will be executed once every 15 minutes as mentioned for the other layouts.

The other time scheduled tests that are needed for this system layout are the leakage test for the feed pump side which was shown in the fuel leakage detection algorithm for system layout C and the test for detecting a clogged fuel filter or a faulty pressure sensor shown for system layout D.

The leakage test and the clogged fuel filter/faulty pressure sensor test will run when entering the correct engine mode i.e. high fuel demand and low fuel demand respectively. If a test has been performed the latest hour, there is however no need for performing the same tests again. This is however discussable and the time span must be chosen as functions of the probabilities of the faults and this is not considered in this thesis.



## 6.6 COMPARISON OF SYSTEM LAYOUTS

All of the developed diagnostic systems for the different layouts can be categorized according to cost, complexity and the ability to detect and isolate faults. Each diagnostic system will be analyzed and discussed below. One of these layouts will then be chosen as the most suitable with respect to diagnostic performance and system cost.

### 6.6.1 *SYSTEM LAYOUT A*

This system layout corresponds to the lowest possible cost since it only utilizes one pressure. As the amount of pressure sensors is reduced to the minimum, the fault detection methods are more separated into different modes. There are also some faults that cannot be isolated from each other since they affect the signals in the same way. These are therefore in the need of being isolated with a test inside the workshop. As the test has to be executed in different modes the complexity increases for the complete diagnostic system.

### 6.6.2 *SYSTEM LAYOUT B*

System layout B is considered to have a medium cost as an extra pressure sensor is added to the system. Workshop tests are however still needed as some faults are not possible to isolate from each other.

### 6.6.3 *SYSTEM LAYOUT C*

This system layout is the most expensive as uses all of the possible pressure sensors. It is with this system layout theoretical possible to detect and isolate all faults from each other out in the field. There is therefore no need for workshop tests and the amount of detection tests performed in other modes has reduced.

### 6.6.4 *SYSTEM LAYOUT D*

In system layout D, the pressure sensor before the fuel filter is removed. The ability to detect and isolate faults is for this layout still very efficient. The cost is for this layout also considered as medium as only two pressure sensors is utilized.

### 6.6.5 CHOOSING THE FINAL SYSTEM LAYOUT

From the above analysis it is clear that system layout A and B provides the lowest ability to detect and isolate faults. As there is no transfer pressure sensor in either of these two layouts the detection tests for the transfer pump side are less robust as they are mostly depending on the signals from the pump. The same algorithm for system layout C and D is completely different as it is utilizing the signals from the pump along with the pressure sensor signal which makes the fault detection and isolation easier and more robust.

As system layout B does not provide any large improvements for the diagnostic performance and doubles the pressure sensor cost in comparison with system layout A, this system layout can be neglected.

The biggest difference between system layout C and D is that the most expensive layout, i.e. C, has the ability to test two more faults during the normal mode than with system layout D. With this in mind, system layout C is neglected.

After the above analysis it comes down to either system layout A or D which have different pros and cons. System layout A has the lowest cost with a diagnostic system spread out into different modes that also requires workshop tests for full isolation. System layout D doubles the pressure sensor cost but provides a more robust and efficient diagnostic system.

The improvement in the diagnostic performance when adding that extra pressure sensor is more valuable than the cost for pressure sensor. System layout D is therefore chosen as the most suitable system layout with respect to cost and diagnostic performance.

## 6.7 DETECTABLE LEAKAGE SIZES

In the performed experiments, it was quickly realized that the size of the faults influenced the signal deviations tremendously. Some of the analyzed faults has either occurred or not occurred in a system and is therefore easier to detect, e.g. a stuck rotor in a pump or a stuck level sensor meanwhile the presence of a leakage fault is more dependent on the size of the leakage and the chosen limits. This section will therefore try to provide the reader with the necessary information for gaining the knowledge in what leakage sizes that can be detected or not.

### 6.7.1 LEAKAGES AFTER THE FEED PUMPS

Let us first consider leakages that occur on the feed pump side of the system, i.e. after the feed pumps. Since the operating pressure is relatively high in this part of the system, a leakage is easier to detect. The smallest generated leakage on the feed pump side was measured to  $\omega$  ml/min and gave a deviation of  $\theta$  bar when a feed pump was operating with 2000 RPM and provided around  $\beta$  l/min. This means that it is possible to detect even smaller leakages on the feed pump side with respect to the error of the pressure sensor. As the leakage increases with the RPM level, there exists a smallest detectable leakage size for each level. This size is corresponding to the error of the pressure sensor, i.e. the lowest pressure deviation that is larger than the error boundary. One must also consider that the error is temperature dependent and thus the lowest detectable leakage size increases. From the performed tests one can be certain that with the used pressure sensor, it is possible to detect a leakage of approximately  $\lambda$  ml/min without considering the temperature level. This is corresponding to leakage size that is approximately 10% of the flow.

### 6.7.2 LEAKAGES AFTER THE TRANSFER PUMPS

Since the operating pressure is lower on the transfer pump side it becomes more difficult to detect a leakage on the lower RPM levels. In the static leakage tests that was performed, the pressure deviations was less than  $\varepsilon$  bar for a leakage size around  $\xi$  l/min when both transfer pumps operated at 1300 RPM's providing around  $\Omega$  l/min. When increasing the RPM level and thus also the leakage size, the pressure deviation increases. The deviation is however not larger than the pressure sensor error before reaching above 3400 RPMs. With this in mind, one can say that it is possible to detect a leakage of  $\alpha$  l/min at 1300 RPM's but that the designed leakage test is only detecting this on the higher RPM levels which also causes the leakage to be larger. The result would however be better if the transfer pressure sensor was intended for a smaller pressure range and a better sensitivity. The current detectable leakage size corresponds to a leakage size that is approximately 15 % of the provided flow.

## 6.8 SAMPLING FREQUENCY

In all of the performed experiments the sensor and actuator signals have been sampled with a sampling frequency of  $\Omega$  Hz. This frequency is more than enough for detecting the different faults. As there are some faults that are utilizing the noise in the signals the final sampling frequency must be chosen such that these faults are still detectable. To be able to detect a suction leakage with the oscillating noise of  $\mu$  Hz the sampling frequency must be at least twice as fast, i.e.  $\zeta$  Hz. To be able to detect the amplitude changes, the sampling frequency must be twice as fast as the frequency of the noise which is around  $\nu$  Hz. This means that the lowest sampling frequency must at least  $\epsilon$  Hz in order to be able to detect amplitude changes and noise oscillations.

## 7. DISCUSSION AND CONCLUSIONS

*In this chapter, a discussion regarding the experiments and the results will be presented followed by the thesis conclusions.*

### 7.1 DISCUSSION

In the previous chapter, the resulting diagnostic systems were presented and evaluated. Since the diagnostic systems are depending on the results retrieved in the rig, there are several factors that have influenced the result and will be further discussed in this section.

#### 7.1.1 SENSOR RESOLUTIONS

As the sensors are a big part of the diagnostic system, the sensor resolutions, sensor errors and sensor sensitivities have had a huge impact on the chosen fault detection methods and in turn the final diagnostic systems.

##### 7.1.1.1. Pressure sensors

From the data retrieved in the performed experiments it was realized that the pressure sensor sensitivity had a big influence on what leakage size that could be detected or not.

As the feed pressure was relatively large, around 5-10 bar during the tests, the used pressure sensor with the range of  $\varepsilon$ - $\psi$  bar was enough for identifying differences between faults. It would however be preferred to use a higher sensitivity in order to improve the detection of leakages lower than  $\lambda$  ml/min.

The transfer pressure sensor that was used in the rig were of the same kind as the above mentioned feed pressure sensor. As the pressure was lower in this side of the system, the pressure sensor range was too large. This led to unnoticeable signal changes when smaller leakages were generated. A transfer pressure sensor with a better sensitivity and a lower pressure range is therefore strongly suggested. The transfer pressure sensor does not need to be able to indicate pressures higher than  $\beta$  bar as the diagnostic system shall indicate a faulty system before that.

The error for the pressure sensors are temperature dependent which makes all of the chosen detection limits to be temperature dependent as well if not considering the worst possible error at all times. As the pressure range is lowered it is implied that the error is lowered as well. The overall diagnostic performance would benefit the most from a different transfer pressure sensor with the above information in consideration.

##### 7.1.1.2. Current sensors

It was in the results for the normal system behavior explained why the current consumption levels differed from each other on the lower RPM and pressure levels. The cause was the low resolution due to the choice of how to round the value and transfer it with the CAN communication. This resulted in current consumption levels that are not reliable at all times and is in the current diagnostic system detected as high or low. It is therefore suggested that an external current consumption sensor is used or that the manufacturer changes the internal software such that the resolution is higher for the lower current consumption levels. This would increase the reliability in the current

signal and can therefore be utilized more in the diagnostic system, e.g. detection limits that considers more than normal, high or low.

In two of the system layouts, i.e. system layout A and B, the diagnostics for the transfer pump side of the system depends a lot on the current consumption with respect to the RPM level. It is for these system layouts therefore more essential that the current consumption has a better resolution.

### *7.1.2 UTILIZING THE REDUNDANCY*

As the system layouts in this thesis includes two feed pumps and two transfer pumps, many faults are verified and isolated with the aid of the redundancy. This has been described in the fault detection methods and the diagnostic algorithms in the previous chapters. The redundancy could however be utilized more for the robustness of the diagnostic system. Every time a non-pump related fault is indicated, one can simply switch to the other pump for verifying that the same fault is present. If the system functions properly when switching to the other pump, the diagnostics has most likely been wrongly diagnosed.

### *7.1.3 EXPERIMENTS*

All of the performed experiments took place in the developed experimental rig which was developed in an early stage of the thesis project. Since the system components and their performance were unknown, this became an iterative process. When it was assumed that all the faults had been defined and began the test phase, it was realized that more faults was of importance. This led to the need of adding further hardware and software which was extremely time-consuming and delayed the experiments. In turn, this resulted in quick fixes and mistakes which were realized in the post analysis, where the data sometimes differed from equally performed tests. Instead of using ball valves it would have been a lot easier to use electrical valves with respect to experiment repeatability. This would have reduced unnecessary uncertainties and more focus could have been used for the actual fault detection methods.

Another issue that was realized was the measurement of the leakages. As these were measured manually it was hard to both control the system and measure at the same time. With this in consideration, it would have been better to use longer hoses and a portable flow meter that could have been attached and removed from the different leakage positions.

### *7.1.4 RESULTING DIAGNOSTIC SYSTEMS*

Four diagnostic systems were developed and presented in the results, one for each system layout. One of these was also suggested as the most useful system layout with respect to the diagnostic performance and system price.

The diagnostic systems were all developed from the differences that were discovered between the normal and the faulty system behavior. The diagnostic systems utilizes physical redundancy, filters, FFT, combinations of detection limits, settling time/rise time and residual generation between the model and the real system signals. As the system model was developed in parallel with this thesis, it was difficult to know how useful it would be for the diagnosis before determining its accuracy. The aim was therefore to develop the fault detection methods without the dependency on the model

as far as possible. This was achieved for all of the faults but as the model became more finished and thus more reliable it was realized that some faults are more easily detectable with the aid of the model, e.g. a stuck level sensor.

The most questionable detection method that has been suggested is the FFT performed on the pressure sensor signal which might consume too much computational power with respect to the loop time. Instead of using a FFT, a simple band pass filter could be utilized. This requires that the noise frequency founding is present in the real installed system as well. This will reduce the information gain a lot and can therefore be questionable the other way around as the available computation power increases rapidly with the ongoing research and development.

The most important assumption that has been made in this thesis is that the feed pumps are pressure and flow controlled meanwhile the transfer pumps are controlled by the level and the temperature inside the tech-tank. The faults would be possible to detect with the same principals but for some, it would require a different test mode.

The idea was from the beginning to implement the whole diagnostic system in the developed rig and try to verify as many detection tests as possible. As there were a lot of unforeseen obstacles during the thesis, there was simply not enough time for this. The diagnostic performance mentioned in the report is therefore referring to the robustness of the fault detection with respect to the data retrieved from the faulty behavior. This means that the diagnostic algorithms have not yet been verified in the system in real time. Implementing the diagnostic algorithms alone would not provide any new information as the success of the diagnostic system is depending on whether the faulty behaviors detectable in normal mode has the same characteristics with the final chosen controller.

This is also why numerical detection limits not been suggested as it also requires implementation of both the diagnostic algorithms and the final system controller. The detection limits may also change completely if the resolution for the transfer pressure sensor is increased.

## 7.2 CONCLUSIONS

The main objective of this thesis was to design the system layout and diagnostic algorithms, for the low pressure fuel circuit, that can detect faulty functioning system levels and isolate the faulty components. In order to accomplish this, the following sub objectives must be fulfilled.

- Identify multiple system layouts with respect to the system price, diagnostic- and control – performance.
- Identify and develop methods for detecting and isolating faults that can occur in the system.
- Decide the necessary sensor resolution.
- Develop the diagnostic algorithms for each system layout.

### *7.2.1 SYSTEM LAYOUTS AND DIAGNOSTIC ALGORITHMS*

Four possible system layouts were identified where one of them was given by the company. This is the minimum required set up from a control perspective. The difference between the suggested layouts is the amount of pressure sensors, their placements and the resulting diagnostic algorithms.

Multiple fault detection and isolation methods were developed from the experimental results. It was discovered that some faults can be detected with multiple methods. It was further realized that it was difficult to develop one big algorithm for the complete diagnostic system. As the different detection test and isolation methods require different system modes, the diagnosis was therefore divided accordingly. The amount of detection tests in each mode differs for each system layout. It was also shown that a removed sensor reduces the diagnostic possibilities.

When comparing the system layouts and the diagnostic performance it was shown that a system layout that includes all three pressure sensors, could perform more detection and isolation tests in a normal mode. For a system layout with a reduced amount of sensors, it was still possible to isolate the faults when overriding the system controller in different modes. This does however increase the complexity of the algorithm implementation and also the time before a present fault can be detected. In the system layout and algorithm evaluation it was stated that system layout D has the best diagnostic possibilities with respect to the system price. As all of the defined faults can be theoretical detected and isolated, it can be said that a successful system layout with corresponding diagnostic algorithm has been identified and developed. The diagnostic system is however in the need of implementation and verification to be considered validated.

### *7.2.2 FAULT DETECTION AND ISOLATION*

The fault detection and isolation tests that were developed for the feed pump side of the system are similar for all system layouts except for detecting a clogged fuel filter and a faulty feed pressure sensor. The diagnostic performance for the feed side of the system is therefore not that dependent on whether one or two feed pressure sensors are used.



The detection test for the transfer side of the system is on the other hand very dependent on whether there exists a transfer pressure sensor or not. It was shown that the transfer pressure sensor simplifies the fault detection and isolation for the transfer pump side of the system and is essential if one want to achieve complete fault isolation without the need of workshop tests.

All of the developed fault detection and isolation methods are in the need of numerical detection limits which have to be determined from further testing whit the final system controller. It can however be said that the fault detection test have been successfully developed and should theoretically achieve complete fault isolation.

### *7.2.3 SENSOR RESOLUTIONS*

It has been verified that the feed pressure sensor after the fuel filter can with the current resolution detect leakages down to 10 % of the provided flow. With respect to all of the developed detection tests, this sensor and its range is applicable and enough for the final system.

The transfer pressure has an oversized pressure range but can still detect leakages down to approximately 15 % of the provided flow. With respect to the developed detection tests, it would be enough with an absolute pressure range of  $\beta$  bar with a better resolution.

The current consumption sensor resolution is enough for two of the system layouts, i.e. C and D, with corresponding diagnostic algorithms as the current consumption is only detected as high, low and normal. For the two other layouts, the current consumption is a big part of the fault detection methods and therefore requires a higher resolution, i.e. at least two times better. It would however be preferable for all layouts to have a better current consumption resolution, especially for the lower current consumption levels. It is also suggested that the current consumption measurement is performed pump externally such that the rounding and current range can be modified.

### *7.2.4 OVERALL CONCLUSION*

With respect to the purpose and delimitations of this thesis, diagnostic algorithms have successfully been developed where all of the defined faults theoretically can be detected and isolated from each other. Workshop tests have been proposed for the layouts that cannot isolate all of the faults out in the field. System layouts has been compared against each other with respect to system cost and diagnostic performance where one layout has been suggest as the most suitable. The sensor resolutions for the different sensors have been evaluated with respect to the sizes of the faults and diagnostic robustness.

The objectives of this thesis has therefore been successfully accomplished with the exception that the diagnostic algorithms is in the need of being implemented and verified to determine whether the theoretical fault detection and isolation methods, that has been developed from rig data, are valid in reality.



## 8. RECOMMENDATIONS AND FUTURE WORK

*In this chapter, recommendations are stated followed by future work to be carried out.*

### 8.1 RECOMMENDATIONS

It is recommended that the following stated below is taken into consideration before carrying out future work.

- That the pump internal current consumption sensor is changed to an external sensor with at least a resolution two times better than the existing.
- That another transfer pressure sensor is used, with a lower absolute pressure range and a better resolution.
- If further tests are to be performed in the rig, the ball valves should be replaced with electrical valves, e.g. proportional valves or electrical switch valves and also a modular flow meter that can be attached and removed for measuring leakages easier.
- That the sampling frequency for all sensor signals is set to a minimum of 1 Hz.
- That the model is further investigated for the purpose of being utilized more in the diagnostics in order to accomplish an even more robust diagnosis.

### 8.2 FUTURE WORK

When the recommendations in the previous section have been considered there are some future work that has to be performed before proceeding with the final system layout and respective diagnostic algorithm.

As the time did not allow for implementation and verification of the diagnostic system, it is strongly suggested that this is performed as soon as possible.

Before running longer verification tests of the whole diagnostic system, the suggested detection limits has to be given numerical values. These values depend on the system behavior when the final system controller has been implemented. This has to be tested with trial and error when implementing the diagnostic algorithm with the aid of the resulting faulty behaviors shown earlier in this thesis. The order of the detection limit calibration/testing is preferable performed in the same order as the detection tests are executed in the resulting algorithm. The simple suggested procedure and needed detection limits for system layout D can be seen in a flowchart and a table in APPENDIX C. By tuning the detection limits with this procedure, one does automatically confirm that a specific fault detection method only triggers by the corresponding fault. This will also function as a first verification for each separate detection test.

When the fault detection limits has been determined, it is possible to test the complete diagnostic system in a test cell and verify that each fault is detected correctly and is suitable in the suggested mode. If deviations and unknown problems occur at this stage, it might be necessary to reduce the diagnostic system and put more focus on workshop tests. The time that has been given to the above implementation, testing and verification is approximately estimated to 3-4 weeks.

## 9. REFERENCES

- Antory, D., 2007. Application of a data-driven monitoring technique to diagnose air leaks in an automotive diesel engine: A case study. *Mechanica Systems and Signal Processing*, Volym 21.
- Bartys, M., 2013. Generalized Reasoning about Faults based on the diagnostic matrix. *Int. J. Appl. Math. Comput. Sci.*, 23(2), pp. 407-417.
- Chiang, L., Russell, E. & Braatz, R., 2002. *Fault detection and Diagnosis in Industrial Sytems*. London: Springer-Verlag.
- Chow, E. Y. & Wilsky, A. S., 1984. Analytical Redundancy and the Design of Robust Failure Detection Systems. *IEEE transactions on automatic control Vol. AC-29 No7*.
- Ding, S. X., 2008. *Model-based Fault Diagnosis Techniques*. London: Springer-Verlag.
- Ellnefjård, A., 2014. *Diagnostic of sensors, transfer pipes, filters, transfer- and feed- pumps: Diarienummer/ Reference number:7026887*, Södertälje: Scania.
- Gertler, J. J., 1988. Survey of Model-based Failure Detection and Isolation in Complex Plants. *IEEE Control Systems Magazine*, pp. 3-4.
- Gertler, J. J., 1998. *Fault Detection and Diagnosis in engineering Systems*. Basel: Narcel Dekker Inc.
- Hess, A. o.a., 2006. Chapter 5, Fault diagnosis. i: *Intelligent Fault Diagnosis and Prognosis for Engineering Systems*. u.o.:John Wiley & Sons Inc.
- Hosseini Sobhani, M. & Pshtan, J., 2011. *Observer-based Fault Detection and Isolation of Three-tank Benchmark System*. Shiraz, Iran, u.n.
- Huh, k. o.a., 2008. *A Model-Based Fault Diagnosis System for Electro-Hydraulic Brake*, Detroit, Michigan: SAE Technical paper Series.
- Höfling, T. & Iserman, R., 1996. Fault detection based on adaptive parity equations and single-parameter tracking. *Control eng. Practice*, 4(10), pp. 1361-1369.
- Iri, M., Aoki, K., O'Shima, E. & Matsuyama, H., 1979. An algorithms for diagnosis of system failures in the chemical process. *Computers & Chemical Engineering*, Volym 3, pp. 489-493.
- Iserman, R., 2006. *Fault Diagnosis Systems*. Berlin: Springer-Verlag.
- Katipamula, S. & Brambley, M. R., 2005. Methods for fault detection, diagnostics and Prognostics for building systems - A review, part I. *HVAC&R Reasearch*, 11(1).
- Mattone, R. & De Luca, A., 2006. Nonlinear Fault Detection and Isolation in a three-Tank Heating System. *IEEE Transactions on Control Systems technology*, 14(6), pp. 1158-1166.
- McDowell, N. o.a., 2007. *Fault Diagnostics for Internal Combustion Engines - Current and Future Techniques*, Detroit, Michigan: SAE International.

- Milne, R., 1987. Strategies for Diagnosis. *IEEE Transactions on Systems, Man and Cybernetics*, SMC-17(3).
- Pernestål, A., 2007. *A Bayesian Approach to Fault Isolation with Application to Diesel Engine Diagnosis*, Stockholm: u.n.
- Potter, J. & Suman, M., 1977. Threshold redundancy management with arrays of skewed instruments. *AGARD*, pp. 213-236.
- Salvador, d. L., Puig, V., Quevedo, J. & Husar, A., 2010. *LPV Model-Based Fault Diagnosis Using Relative Fault Sensitivity Signature Approach in a PEM Fuel Cell*. Marrakech, u.n.
- Sun, Y., Wang, Y.-Y., Chang, C. & Levijoki, S., 2012. *Detection of Urea injection System Faults for SCR systems*, Detroit, Michigan: SAE Technical Paper Series.
- Svärd, C., 2012. *Methods for Automated Design of Fault Detection and Isolation Systems with Automotive Applications*. Linköping: s.n.
- Venkatasubramanian, V., Rengaswamy, R. & Kavuri, S. N., 2003. A review of process fault detection and diagnosis Part II: Qualitative models and search strategies. *Computers & Chemical Engineering*, Volym 27.
- Venkatasubramanian, V., Rengaswamy, R., Yin, K. & Kavuri, S. N., 2003. A review of process fault detection and diagnosis Part I: Quantitative model-based methods. *Computers and Chemical Engineering*, Volym 27.
- Willsky, A. S., 1976. A survey of design methods for Failure Detection in Dynamic Systems. *Automatica*, Volym 12.
- Witczak, M., 2007. *Modelling and Estimation Strategies for Fault Diagnosis of Non-linear Systems*. Berlin: Springer-Verlag.
- Zhang, K., Jiang, B. & Shi, P., 2010. Observer-based integrated robust fault estimation and accommodation design for discrete-time systems. *International journal of control*, 83(6).

# APPENDIX A

## CAN communication for pumps

The speed on the can bus is set to 250 kb/s and uses 29-bit identifiers. The identifier used for sending messages from Labview to the pumps can be seen in Table A.1.

**Table A.1. Identifiers for sending messages to the pumps.**

Pump	Identifier (hex)
Transfer pumps	0x10EF9xxx
Feed pumps	0x10EF1xxx

The message frame for the transferred data (Labview to pumps) can be seen in table A.2.

**Table A.2. Message frame from Labview to the pumps.**

<b>Byte 0</b>	Message TAG (MSB)
<b>Byte 1</b>	Message Tag (LSB)
<b>Byte 2</b>	Speed Command
<b>Byte 3</b>	Command (version request)
<b>Byte 4</b>	Set current limit
<b>Byte 5</b>	Unused
<b>Byte 6</b>	Unused
<b>Byte 7</b>	Unused

The identifier used for sending messages from the pumps to Labview can be seen in Table A.3.

**Table A.3. identifiers for sending messages from the pumps to Labview.**

Pump	Identifier (hex)
Transfer pumps	0x10Exxx92
Feed pumps	0x10Exxx12

The message frame for the transferred data (pumps to Labview) can be seen in Table A.4.

**Table A.4. Message frame from pumps to Labview.**

<b>Byte 0</b>	Message TAG (MSB)
<b>Byte 1</b>	Message Tag (LSB)
<b>Byte 2</b>	Speed feedback
<b>Byte 3</b>	Current feedback
<b>Byte 4</b>	Temperature
<b>Byte 5</b>	Supply voltage
<b>Byte 6</b>	Unused
<b>Byte 7</b>	Unused

# APPENDIX B

## Determining the flow as a function of the RPM level

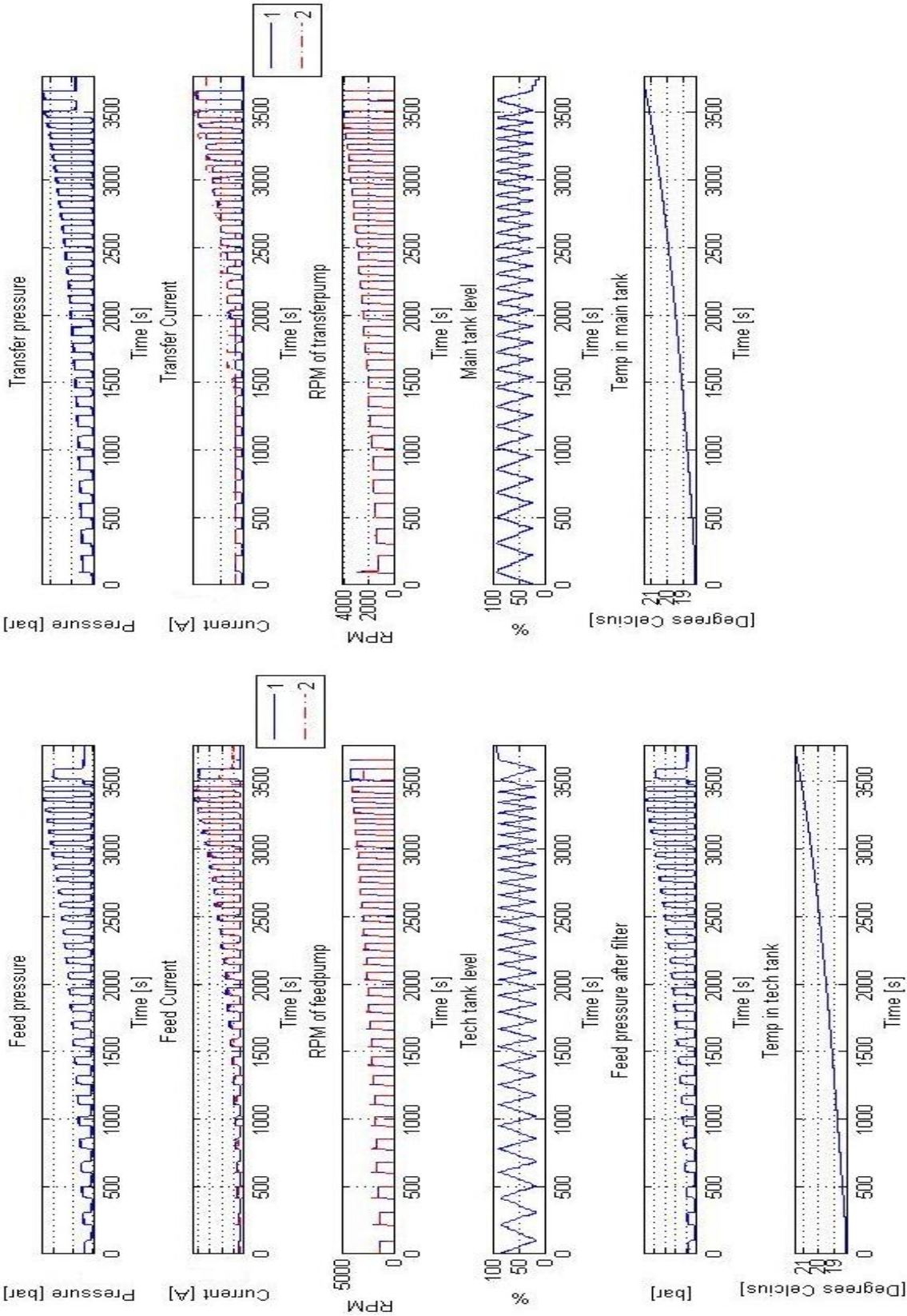
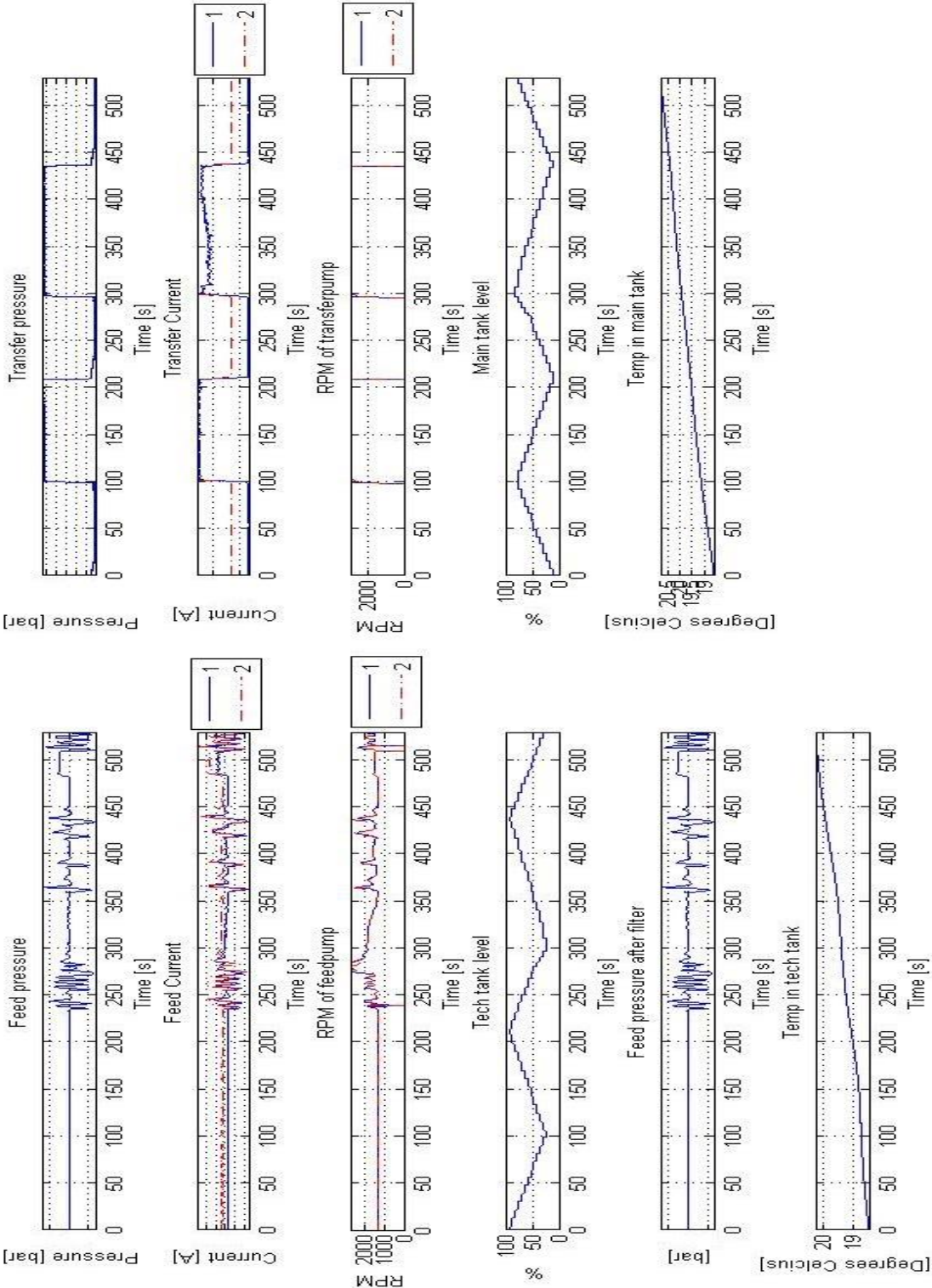


Figure B.1. Data from all sensors and actuator during the flow as function of RPM test.

**Normal behavior with PI regulated feed pumps and tech-tank level hysteresis**



**Figure.B.2. Data from all sensors and actuators during normal behavior with PI-regulator for feed pumps and hysteresis control for transfer pumps.**



**Normal behavior with constant RPM for feed pumps and tech-tank level hysteresis**

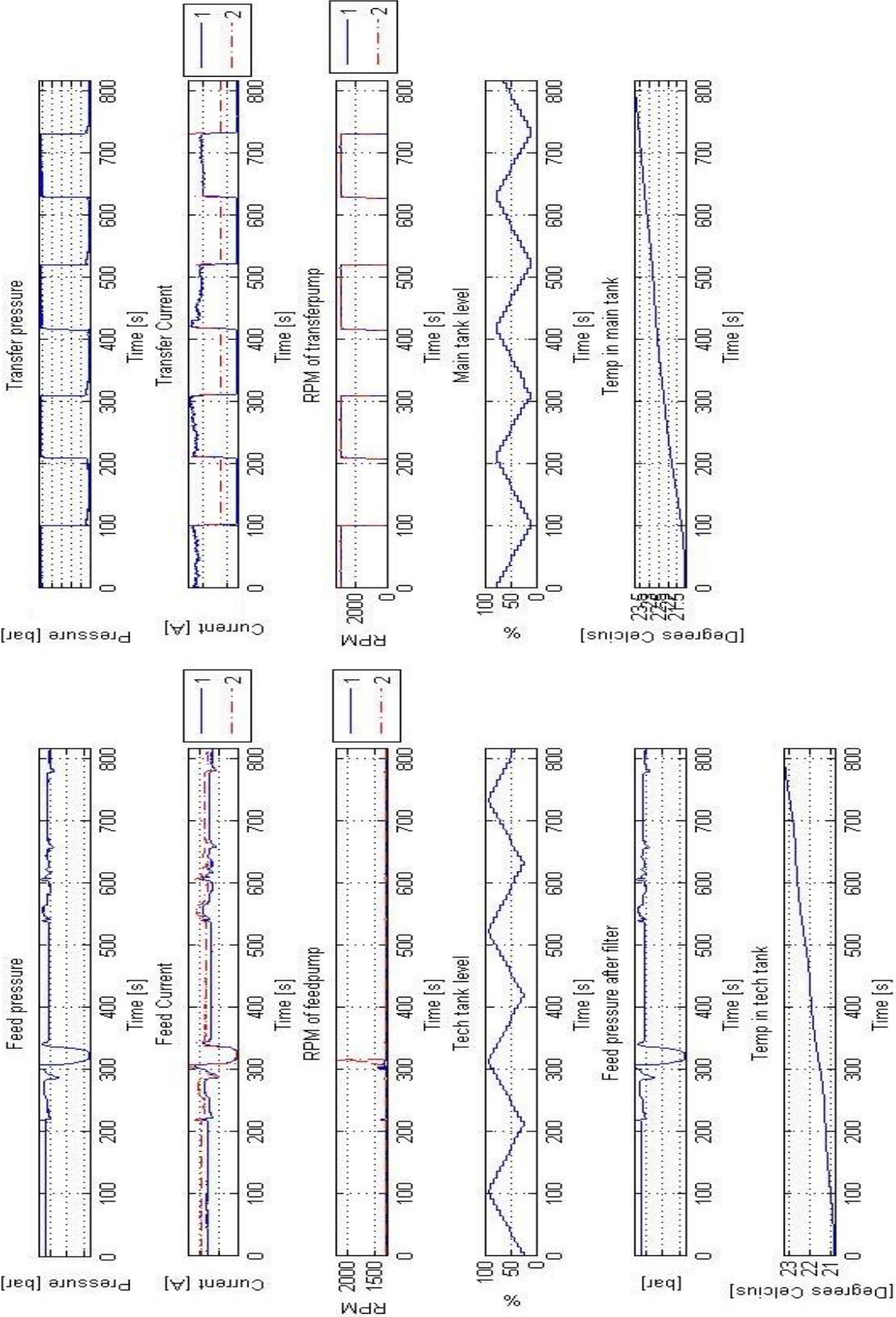


**Figure B.3. Data from all sensors and actuators during normal behavior with constant RPM level for the feed pumps and hysteresis control for transfer pumps.**

## **APPENDIX C**

See Appendix C in (Ellnefjård, 2014).

**Figure C.1. Procedure for determining detection limits for the different fault detection methods applied in the diagnostic system.**

**Table C.1. A table describing what detection limits and constants that needs to be determined for each fault detection test with layout D. Note that each detection test is depending on other variables as well and that these are test specific.**

<b>Mode</b>	<b>Fault detection test</b>	<b>Detection limits and constants to be determined.</b>
<b>Startup</b>	Physical redundancy between pressure sensors.	Maximum allowed absolute difference between pressure sensors when no RPM level is set.
<b>Startup</b>	Level sensor signals in range (tech-tank and main tank).	Max and min level for sensors.
<b>Startup</b>	Physical redundancy between temperature sensors ( for both tech-tank and main tank).	Maximum allowed absolute temperature difference between pump temperature and tank temperature.
<b>Normal</b>	Noise amplitude test for transfer side.	Maximum allowed absolute noise level and during which time span.
<b>Normal</b>	Open pre-filter and suction leakage for transfer pumps.	Maximum amplitude for frequency spectrum or amplitude level with band pass filter.
<b>Normal</b>	Stop in transfer line or rotor in transfer pump blocked.	Current consumption max limit and transfer pressure max and min limit.
<b>Normal</b>	Non responding pump or faulty RPM sensor (transfer).	Absolute RPM deviation limit and during which time sequence.
<b>Normal</b>	Pump/motor shaft broken (transfer)	Low limit for transfer pressure and current consumption.
<b>Normal</b>	Noise amplitude test for feed side	Maximum allowed absolute noise level and during which time span.
<b>Normal</b>	Stop in feed line or rotor in feed pump blocked.	Higher limit for current consumption, lower limit for pressure sensor in high pressure circuit and maximum limit for feed pressure.
<b>Normal</b>	Non responding pump, motor shaft broken or faulty RPM sensor (feed pumps).	Absolute allowed RPM deviation limit and during what time span. Current consumption and feed pressure low limit.
<b>Demanded (Controller override)</b>	Open fuel filter or suction leakage for feed pumps.	Maximum error between normal and measured current consumption on max RPM level.
<b>Demanded (Controller override)</b>	Leakage size test (when a fuel leakage, suction leakage or an open fuel filter has occurred).	Settling time for large, medium and small leakages. The difference limit that indicates that the pressure has settled.
<b>Demanded (Controller override)</b>	Clogged pre-filter or faulty transfer pressure sensor.	Max error between normal and measured current consumption on max RPM level.
<b>Time scheduled</b>	Physical redundancy between temperature in pumps and tanks.	Maximum allowed error between pump temperature and respective tank temperature.
<b>Time scheduled</b>	Residual for level sensors.	Max allowed error between level sensor signal and model.
<b>Time scheduled (Controller override)</b>	Fuel leakage tests.	Normal transfer and feed pressure vector during RPM steps. Starting RPM level for test.
<b>Time scheduled (Controller override)</b>	Clogged fuel filter.	Absolute pressure error limit between measured and normal behavior with max RPM level. Current consumption limit for clogged fuel filter.